ADVANCED MATERIALS TECHNOLOGIES
www.advmattechnol.de

Advancements in Electronic Materials and Devices for Stretchable Displays

Yeongjun Lee, Hyeon Cho, Hyungsoo Yoon, Hyunbum Kang, Hyunjun Yoo, Huanyu Zhou, Sujin Jeong, Gae Hwang Lee, Geonhee Kim, Gyeong-Tak Go, Jiseok Seo, Tae-Woo Lee, Yongtaek Hong,* and Youngjun Yun**

A stretchable display would be the ultimate form factor for the next generation of displays beyond the curved and foldable configurations that have enabled the commercialization of deformable electronic applications. However, because conventional active devices are very brittle and vulnerable to mechanical deformation, appropriate strategies must be developed from the material and structural points of view to achieve the desired mechanical stretchability without compromising electrical properties. In this regard, remarkable findings and achievements in stretchable active materials, geometrical designs, and integration enabling technologies for various types of stretchable electronic elements have been actively reported. This review covers the recent developments in advanced materials and feasible strategies for the realization of stretchable electronic devices for stretchable displays. In particular, representative strain-engineering technologies for stretchable substrates, electrodes, and active devices are introduced. Various state-of-the-art stretchable active devices such as thin-film transistors and electroluminescent devices that consist of stretchable matrix displays are also presented. Finally, the future perspectives and challenges for stretchable active displays are discussed.

1. Introduction

Information and communication technology (ICT) has evolved toward higher speed, density, and resolution, with lower power consumption, and has ushered in an era of mobile devices such as laptops, smart phones, and tablets. Interactions between mobile devices have proliferated with advances in device performance, and various services have been provided to connect and exchange data with other devices and systems over the internet. Furthermore, going beyond the connection of devices, the "Internet of Things" (IoT) has emerged, where everything around us is connected.[1] Devices will evolve into human-centric devices that require more user-convenience, portability, and better connectivity with their surroundings, and people will demand wearable devices that are easier to carry around.[2]

In recent years, there has been a proliferation of wearable electronics such as smart watches, clothes, and patches, and even implantable devices to detect physiological signals for healthcare monitoring. With the advent of wearable technology, the medical system is shifting from managing a few patients in hospitals to remotely monitoring several people who have potential risks to their health during daily activities. Although commercial wristwatches are useful and widely used, some people still do not want to wear them because they can be uncomfortable and inaccurate. In particular, during a high level of physical activity, they cannot obtain accurate data because of losing skin contact or motion artifacts.[3–5] This is leading to the development of stretchable and skin-like electronics, in which electronic functions are introduced to the surface of the skin to maximize a user's comfort during daily life and ensure secure contact with the skin to detect physiological signals.[6]

Y. Lee
Department of Chemical Engineering
Stanford University
Stanford, CA 94305, USA
E-mail: yeongjunlee@gmail.com

H. Cho, H. Yoon, H. Yoo, S. Jeong, G. Kim, J. Seo, Y. Hong
Department of Electrical and Computer Engineering
Inter University Semiconductor Research Center (ISRC)
Seoul National University
Seoul 08826, Republic of Korea
E-mail: yongtaek@snu.ac.kr

The ORCID identification number(s) for the author(s) of this article can be found under https://doi.org/10.1002/admt.202201067.

DOI: 10.1002/admt.202201067

H. Kang, G. H. Lee, Y. Yun
Organic Material Lab.
Samsung Advanced Institute of Technology (SAIT)
Samsung Electronics
Suwon 16678, Republic of Korea
E-mail: youngjun.yun@samsung.com

H. Zhou, G.-T. Go, T.-W. Lee
Department of Materials Science and Engineering
Seoul National University
Seoul 08826, Republic of Korea

T.-W. Lee
School of Chemical and Biological Engineering
Institute of Engineering Research
Research Institute of Advanced Materials, Soft Foundry
Seoul National University
Seoul 08826, Republic of Korea

Figure 1. Conceptual image of stretchable displays in the potable electronics and skin-like wearables.

The display is the most important front-end interface for communication between users and devices, and thus occupies a fairly large area in the appearance of the device. This makes a stretchable display essential for skin-like electronics (**Figure 1**). Although the research on stretchable displays is still in the early stage, much research is being actively reported. Display form factor innovation is accelerating. Thus, stretchable displays are expected to be commercialized in the near future.[7]

In the mid-2010s, flat-panel displays, which are usually less than 10 cm thick, completely replaced cathode ray tube (CRT) displays, which were introduced in 1939 by the Radio Corporation of America (RCA). It took almost 70 years to change the form from heavy and cumbersome to a thin, light, and flat screen. Flexible displays, which are designed to withstand being folded, bent, and twisted, as opposed to the traditional flat-panel displays used in most devices, allow innovative smartphone designs with various forms.[8] In the late 2010s, interest in various form factors such as multi-foldable, rollable, and stretchable displays began to increase with the release of foldable phones in the consumer market. Although this market is still in an early adopter phase, it is expected to be a mainstream in the near future. A foldable display is a type of flexible display that can be folded and unfolded like paper. This includes not only a single fold but also multiple folds such as G-folding, in which it is folded inward twice in a "G" shape, and Z-folding, in which it is folded in a "Z" shape, with only a third of the screen exposed to the outside. A rollable display is also a type of flexible display with the ability to expand the display area by pulling on it vertically or horizontally so that the screen behaves like paper on a scroll.

Stretchable displays, which can be stretched in all directions to change their shape, will be the next generation of displays with a new form factor a step beyond that of flexible displays. They can be deformed in any direction, freely folded, and fit on any surface. Based on numerous studies of stretchable electronic materials, strain releasing geometries, stretchable backplanes, and stretchable light-emitting diodes (LEDs), a few prototypes of stretchable displays have been demonstrated. For example, Samsung demonstrated a 9.1-inch stretchable active-matrix organic light-emitting diode (AMOLED) display with 5% stretchability at the Society for Information Display (SID) in 2017.[9] Someya et al. reported a highly elastic, 1 mm thick skin display, which consisted of a 16 × 24 array of micro-light emitting diodes (μ-LEDs) with 45% stretchability, at the American Association for the Advancement of Science (AAAS) Annual Meeting in Austin, Texas in 2018. In 2020, Beijing Oriental Electronics (BOE) reported a stretchable AMOLED with a 10% stretch ratio.[10] In 2021, Lee et al. showed the feasibility of a skin-like display patch with a passive-matrix (PM) OLED array,[11] and Royole demonstrated a 2.7 in. 96 × 60 pixel (42 pixels per inch, ppi) μ-LED display with 120% stretchability at SID.[12] Based on such interest and the research conducted in academia and industry, it is expected that stretchable displays and skin-like electronic devices will be realized in the near future and will provide unprecedented types and shapes of electronic devices.

This review outlines the recent progress made in the development of deformable and stretchable displays. First, it discusses the current technical approaches and prospects for strain engineering, including pre-strained structures, island-bridge structures, and intrinsically stretchable materials that could be implemented for stretchable display arrays. Second, stretchable electrodes for the interconnections are discussed, including intrinsically stretchable conductors (e.g., conductive nanomaterial composites, liquid metals (LMs), and conductive polymers) and structural designs. Third, the stretchable thin film transistors (TFTs) made from various semiconducting materials that are capable of being used for a stretchable backplane are summarized. In particular, the results of strain-engineered inorganic stretchable TFTs and intrinsically stretchable TFTs that exploit semiconducting carbon nanotubes (CNTs) and polymer semiconductors are discussed. Following this, stretchable light-emitting devices such as inorganic, organic, and metal-halide perovskites LEDs, along with alternating current electroluminescence (ACEL) devices, are discussed. Finally, we report the recent progress on stretchable display arrays and future perspectives on high-density stretchable displays.

2. Structural Strategies for Stretchable Display

Most electronic materials such as semiconductors and conductors are brittle; however, they can be made more flexible by decreasing their thickness. Downscaled materials can withstand significantly larger strains and stresses than their bulk states. However, they cannot afford a tensile strain that is greater than the bending strain. To apply these electronic materials to stretchable devices, there have been several approaches to make electronic materials and devices stretchable at the macro-scale level (extrinsically stretchable geometries) or at the micro-scale level (intrinsically stretchable materials).

This section describes representative strategies for structural designs that are viable for stretchable displays, including geometrical engineering approaches to produce 1) wrinkled structures using a pre-strain method, 2) island-bridge structures, and 3) approaches that use intrinsically stretchable materials that exploit nanomaterial composites, molecular blending, and molecular chemistry.

2.1. Prestrained Structures

The prestrain method is a prevalent method for forming a wrinkled structure for a flexible device using a pre-stretched elastomer substrate. Wrinkled structures are flattened after restretching, which allows the flexible devices to be stretched without

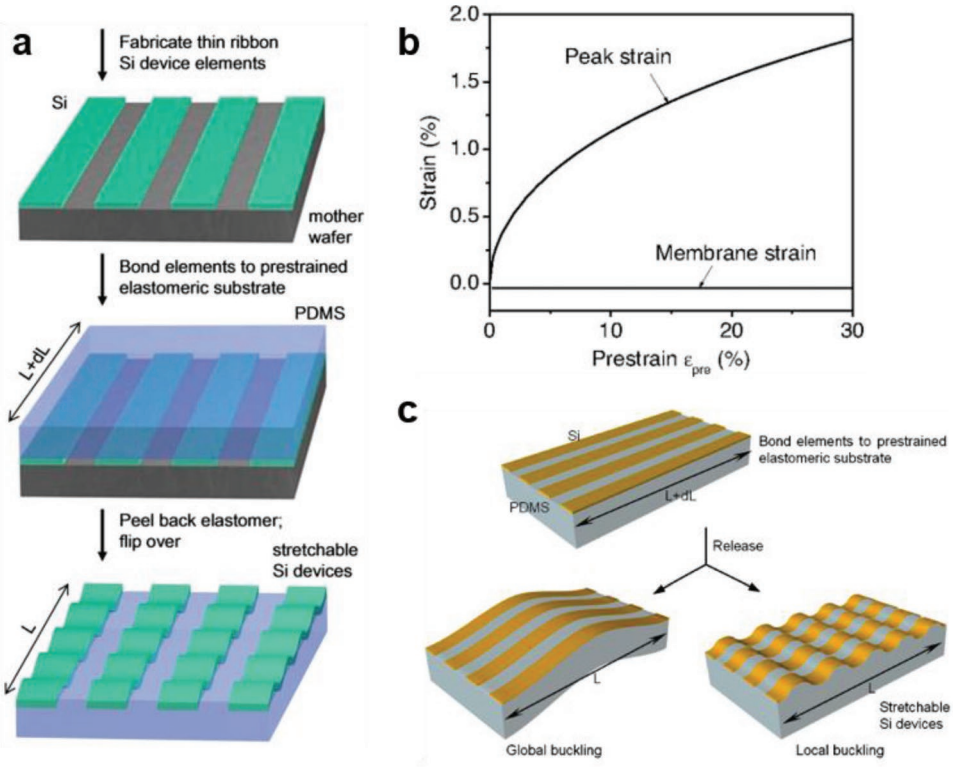

Figure 2. Prestrain-induced wrinkled stretchable structure. a) Schematic process diagram of prestrain method. Reproduced with permission.[16] Copyright 2006, American Association for the Advancement of Science. b) Peak strain and membrane as a function of the pre-strain in Si ribbon/PDMS substrate system. Reproduced with permission.[25] Copyright 2007, PNAS. c) Schematic diagrams of global and local buckling and local buckling. Reproduced with permission.[27] Copyright 2008, AIP Publishing.

mechanical failure.[13,14] The wrinkled structure is fabricated by the deposition or lamination of a flexible film on a pre-stretched elastomeric substrate.[15] The first pre-strain-induced stretchable wrinkled structure was developed by the transfer of thin silicon ribbons to a pre-strained elastomeric substrate (poly(dimethylsiloxane), PDMS). After peeling off the silicon ribbons from the elastomeric substrate, they had a periodic wavy structure (**Figure 2**a).[16] Because the prestrain method achieves reliable and stable stretchable properties, various materials and devices have been researched to make stretchable devices and systems.[17–22]

The theoretical model of a buckled structure has been suggested to design the materials and geometries for stretchable devices with the pre-strain method. The wavy configuration can be determined by various factors such as the thickness, elastic modulus, adhesion, Poisson ratio of the materials, and geometry of the structure.[15] First, the wavelength (λ_0) and amplitude (A_0) of the buckling are calculated by the model with a well-defined sinusoidal wavy structure with a buckled geometry.[23,24] In this model, the elastomeric substrate is assumed to be a very thick film (semi-infinite solid), which was widely researched for early wearable electronics:

$$\lambda_0 = \frac{\pi h}{\sqrt{\varepsilon_c}}, A_0 = h\sqrt{\frac{\varepsilon_{pre}}{\varepsilon_c} - 1} \tag{1}$$

where h is the thickness of the stiff material, ε_c is the critical buckling strain, and ε_{pre} is the strain of the prestrained elastomeric substrate. However, this buckled geometry can be formed only when ε_{pre} is larger than the critical buckling strain. The critical buckling strain, ε_c, is determined by the elastic modulus values of the elastomeric substrate, E_s, and stiff film, E_f:

$$\varepsilon_c = \frac{1}{4}\left(\frac{3E_s}{E_f}\right)^{2/3} \tag{2}$$

However, delamination can occur between stiff materials and soft elastomeric substrates. In this case, the model cannot predict the buckling behavior. Therefore, a new model has been suggested to explain the finite deformation and non-linear strain displacement relation.[15,25,26] Using this model, wavelength λ and amplitude A of the buckling are calculated as follows:

$$\lambda = \frac{\lambda_0}{(1+\varepsilon_{pre})(1+\xi)^{1/3}}, A = \frac{A_0}{(1+\varepsilon_{pre})^{1/2}(1+\xi)^{1/3}} \tag{3}$$

where $\xi = \frac{5\varepsilon_{pre}(1+\varepsilon_{pre})}{32}$. In addition, the maximum strain of the film, which is called the peak strain, can be calculated as the sum of the membrane strain and bending strain in the buckling structure. Peak strain ε_{peak} is calculated as follows:

$$\varepsilon_{peak} = 2(\varepsilon_c\varepsilon_{pre})^{1/2}\frac{(1+\xi)^{1/3}}{(1+\varepsilon_{pre})^{1/2}} \tag{4}$$

The value of ε_{pre} is much larger than that of ε_{peak}. Therefore, a pre-strained structure can be effectively used for a stretchable

device (Figure 2b).[25] In addition, the maximum pre-strain before fracture, $\varepsilon_{pre,max}$, can also be calculated by this model:

$$\varepsilon_{pre,max} = \frac{\varepsilon_{fracture}^2}{4\varepsilon_c}\left(1+\frac{43\varepsilon_{fracture}^2}{144\varepsilon_c}\right) \quad (5)$$

where $\varepsilon_{fracture}$ is the fracture strain of the stiff material. Therefore, the maximum prestrain is limited by the mechanical properties of the materials.

This well-defined wavy structure can only be formed on a thick elastomeric substrate, which is considered a semi-infinite solid. However, global buckling occurs instead of periodical local buckling when the elastomeric substrate is thin. The mode of buckling is illustrated in Figure 2c.[27] To predict the buckling mode, a pre-strained structure can be modeled with rigidity. The critical global buckling strain can be calculated as follows:

$$\varepsilon_{c,global} = \frac{1}{1+\frac{1.2F_c^\circ}{\overline{G}(h_s+h_f)}}\frac{F_c^\circ}{\overline{EA}} \quad (6)$$

where $F_c^\circ = 4\pi^2\overline{EI}/L^2$ is the critical buckling load, $\overline{G}$ is the effective shear modulus of a composite beam, h_s is the thickness of the substrate, h_f is the thickness of a stiff film, L is the length of the composite beam, $\overline{EA} = E_s h_s + E_f h_f$ is the effective tensile rigidity, and $\overline{EI} = \frac{(E_f h_f^2 - E_s h_s^2)^2 + 4E_f h_f E_s h_s (h_s+h_f)^2}{12\overline{EA}}$ is the effective bending rigidity.[27] When $\varepsilon_{c,global}$ is larger than ε_c, local buckling occurs. However, if $\varepsilon_{c,global}$ is smaller than ε_c, global buckling occurs. To avoid this global buckling, the materials and geometrical structure must be designed appropriately according to the model. Moreover, the adoption of a thin layer between the film and substrate can eliminate global buckling.[17] Using these theoretical models, the geometrical parameters and mechanical properties of the materials are the keys to designing a stretchable system using pre-strain methods.[23,28]

2.2. Island-Bridge Structures

The structure engineering method of implementing a stretchable display is to divide it into a soft area and hard area on a plane. The rigid electronic devices (e.g., inorganic/organic LEDs and TFTs) are placed in island-shaped rigid pixelated areas and connected through interconnects that are intrinsically or externally (geometrically) stretchable (**Figure 3**a). In this structure, the devices in the rigid pixels are hardly affected by external strain. Thus, this structure can impart mechanical stretchability to well-developed rigid devices, including LEDs and TFTs, which has the advantage of using the mature manufacturing process that has been established for rigid displays over previous decades. Thus, the island–bridge structure has been the most widely adopted method to implement stretchable displays.[10,12,29,30]

One method of connecting rigid/flexible islands is to use metallic bridges.[31] A serpentine-shaped bridge is mainly used with metal thin film electrodes, where the stretching motion is performed by 3D torsions of the flexible bridges.[32] Because the local strain distribution and resultant distortion stress under stretching are dependent on the geometry of the island–bridge structures, the global strain range of the stretchable display is modulated by geometrical factors such as the ratio between island and bridge regions, design of the bridge interconnects, in-plane/out-of-plane distortion, and buckling.[33–36]

The island and serpentine bridge structures can be fabricated on one plane by patterning a silicon on insulator (SOI) wafer[37,38] or plastic substrate such as polyimide (PI).[34,39] A low island/bridge ratio can increase the elongation with a wide deformation area, but there is a limit to the increase in resolution due to a small pixel area ratio. It is possible to improve the elongation at a high island/bridge area ratio by applying bridges with various curvatures, horseshoes, and fractal patterns (Figure 3b).[40–43] In the serpentine structures, because the strain is mainly concentrated on the inner and outer edges of the curves,[44,45] it is necessary to limit the elongation, which can minimize fatigue failure due to repeated stretching.

The rigid island and bridge interconnect regions can be separately fabricated on the elastomeric substrate, and it is also possible to apply not only serpentine flexible metal films but also intrinsic stretchable conductors (e.g., LMs, conductive nanocomposites, and conducting polymers).[11,46–48] The intrinsically stretchable interconnect can be fabricated in a straight shape that minimizes the area occupied by the wavy flexible interconnect, thereby improving the resolution. Furthermore, intrinsically stretchable interconnects can be patterned in a wavy shape to further improve the elongation and mechanical stability.[49,50] In addition, the rigid island region can be located above or below the elastomer or embedded therein to modulate the strain distribution and provide more options in terms of device structures and fabrication processes.[9,51]

The disconnection of interconnects near the edge of the island pixel area due to localized strain can limit the stretchability of the island-bridge structures.[52–54] To improve the stretchability of the stretchable display array, various strain engineering approaches that have applied lower Young's modulus materials (Figure 3c),[55] stiff materials with a gradient modulus (Figure 3d),[56–61] or pillar structures (Figure 3e)[62] have been reported. In addition, a kirigami-based design for a stretchable display without image distortion was suggested.[63] The μ-LEDs were transferred onto an electrical circuit board with kirigami cutting patterns (Figure 3f). The meta-atom expanded in the perpendicular direction to the loading with a strain identical to the loading strain, resulting in a Poisson's ratio of –1 (Figure 3g,h).

2.3. Intrinsically Stretchable Structures

Unlike the aforementioned structural methods for fabricating stretchable electronics, intrinsically stretchable devices would not require geometry-based strain engineering. Thus, they would sufficiently increase the device stretchability while avoiding the reduction of both the overall device density and complexity of the device processes.[64–66] Therefore, introducing inherently stretchable materials (e.g., conductors and semiconductors) into stretchable electronic devices is an important method to develop stretchable displays. Intrinsically stretchable electronic materials are mostly based on polymeric materials as elastic matrices or substrates that incorporate conducting

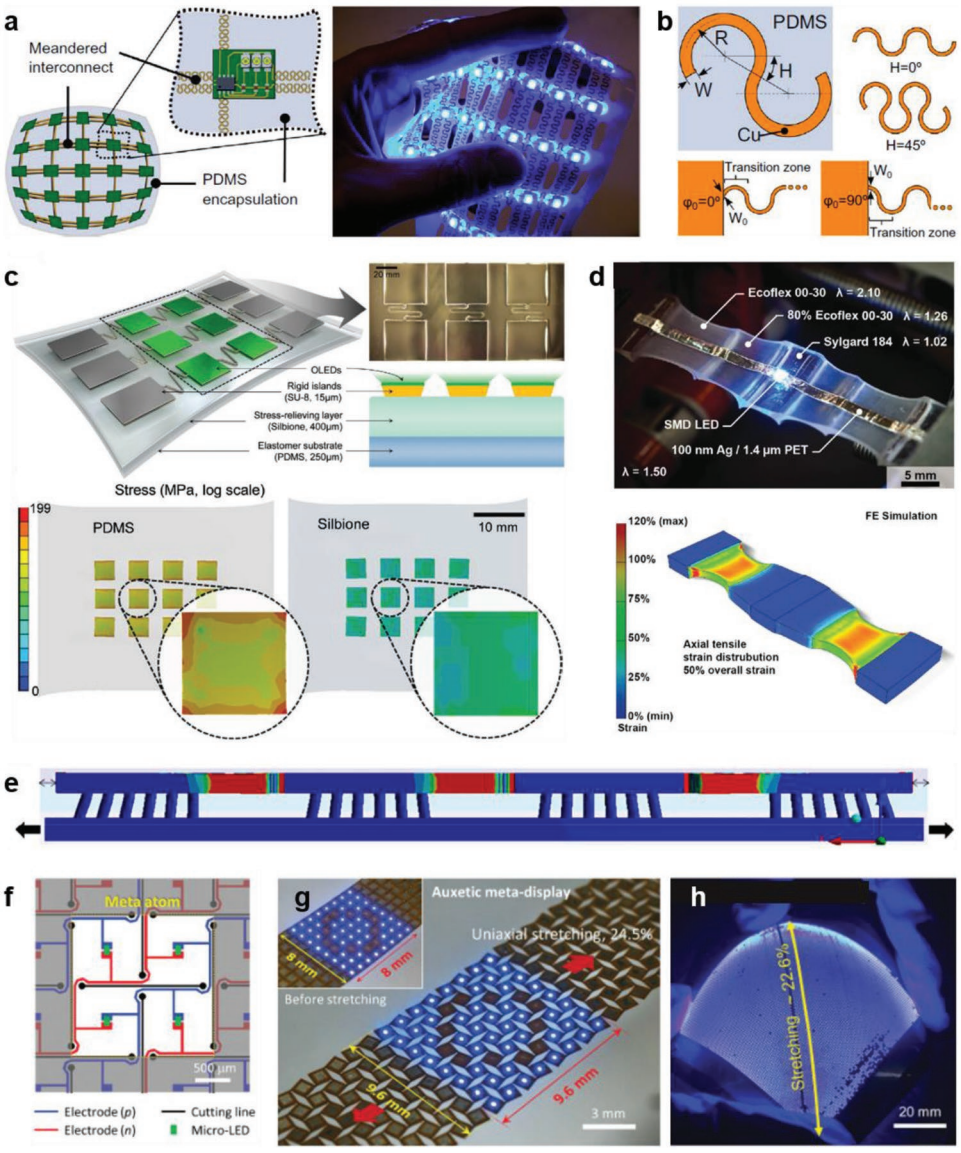

Figure 3. Representative island-bridge structure. a) Stretchable LEDs with rigid islands and serpentine interconnects, along with b) their geometric parameters. Reproduced with permission.[40] Copyright 2015, Elsevier. Various strain engineering approaches with c) lower Young's modulus materials,[55] d) gradient Young's modulus materials,[60] and e) pillar structures.[62] Reproduced with permission.[55] Copyright 2020, Wiley-VCH. Reproduced with permission.[60] Copyright 2016, Wiley-VCH. Reproduced with permission.[62] Copyright 2020, American Chemical Society. f) Stretchable micro-LED display designed with auxetic metamaterials. Digital images of g) a stretchable micro-LED meta-display with Poisson's ratio of -1 and h) display attached to a hemisphere. Reproduced with permission.[63] Copyright 2022, Wiley-VCH.

or semiconducting materials. Because polymer materials can be functionalized with additional unique properties such as self-healing, biocompatibility, and antioxidation properties, intrinsically stretchable electronic materials could broaden the functionality of skin-like electronics, including the development of damage-resilient and biocompatible biometric devices beyond those used for conventional applications.[67,68] This section discusses recent representative approaches and their electronic device applications in terms of both inherent material designs and physical blending approaches for improving the stretchability while maintaining the electrical/optical properties.

Intrinsically stretchable conductors have been intensively developed and utilized in stretchable electrodes and current collectors to demonstrate intrinsically stretchable TFTs,[66,69,70] LEDs,[64,71,72] photovoltaics (PVs),[73] and high-frequency diodes.[74] Furthermore, intrinsically stretchable conductors are used as the mechanically robust interconnects of stretchable device arrays. Various kinds of conducting materials such as LMs, conducting polymers, and conductive nanomaterials (e.g., Ag nanowires (AgNWs), Ag flakes, and CNTs) have been widely used as intrinsically stretchable conductors. For examples, Matsuhisa et al. recently demonstrated the intrinsically stretchable display and sensor systems (**Figure 4**a) by integrating high-frequency (HF) diodes (Figure 4b), current collectors, stretchable antennas, and strain sensors.[74] The conducting polymer poly(3,4-ethylenedioxythiophene):polystyrene

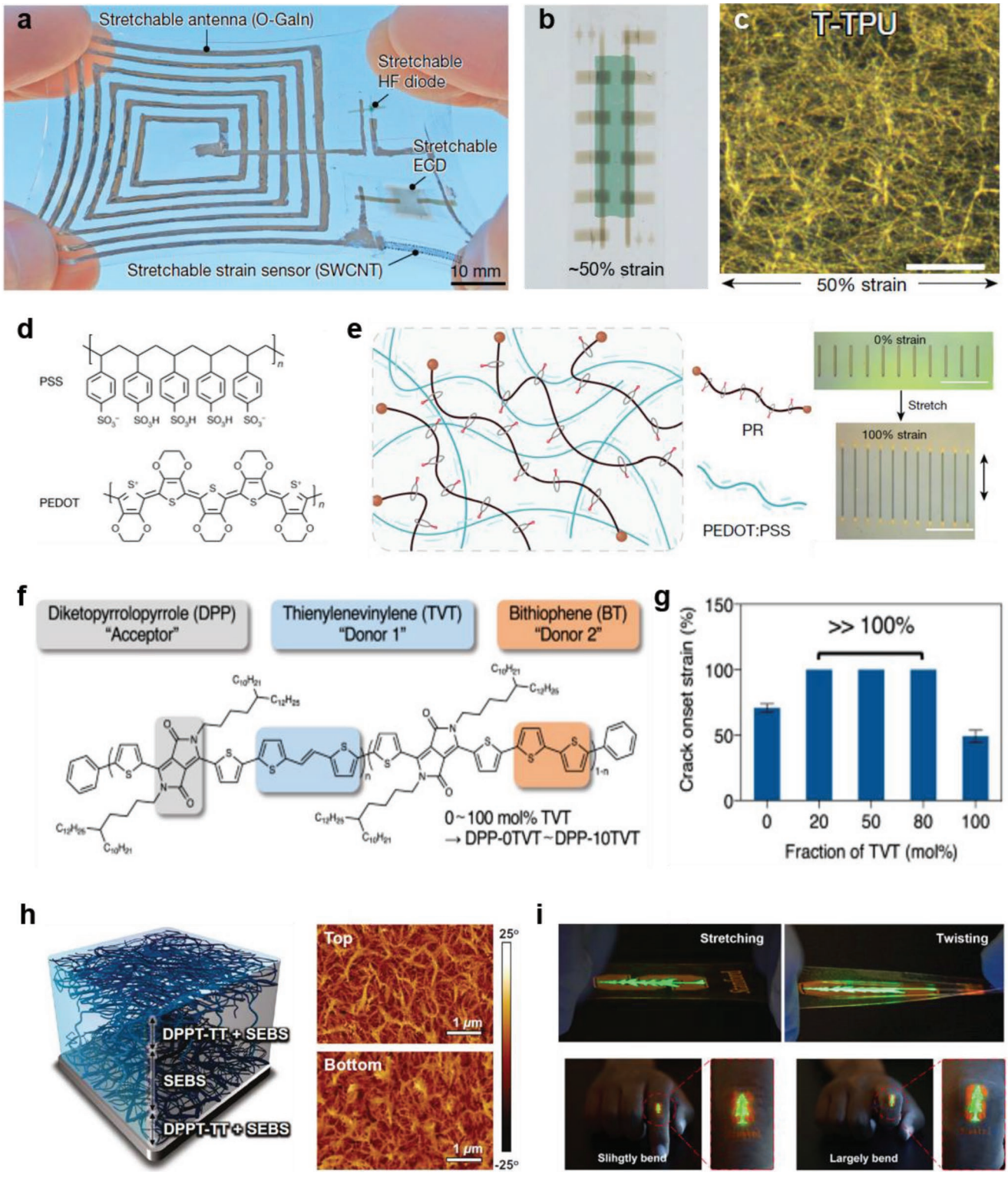

Figure 4. Representative material candidates and their applications to intrinsically stretchable electronics. Digital images of a) oxidized eGaIn-based interconnects for stretchable wireless sensor and display system and b) high-frequency and intrinsically stretchable diodes. c) Optical microscope image of AgNW-elastomer composite for stretchable current collectors. Reproduced with permission.[74] Copyright 2021, Springer Nature. d) Molecular structure of PEDOT:PSS. Reproduced with permission.[64] Copyright 2022, Springer Nature. e) Schematic and optical microscope image of PR-PEDOT:PSS-based conducting polymer for stretchable electrodes. Reproduced with permission.[64] Copyright 2022, Springer Nature. f) Schematic and g) crack onset strain with terpolymer approaches for modulating the mechanical properties of CPs. Reproduced with permission.[65] Copyright 2021, Springer Nature. h) CP/SEBS elastomer blends for intrinsically stretchable TFTs. Reproduced with permission.[69] Copyright 2017, American Association for the Advancement of Science. i) Digital images of intrinsically stretchable polymer light-emitting layers composed of CP/PU elastomer blends. Reproduced with permission.[64] Copyright 2022, Springer Nature.

sulfonate (PEDOT:PSS) with ionic additives, AgNWs/tough thermoplastic polyurethane (T-TPU)-based elastomeric composites (Figure 4c), oxidized eutectic gallium-indium (oxidized eGaIn) printed on a stretchable substrate (Figure 4a), and single wall CNTs (SWCNTs) were used for high-frequency diodes, current collectors, stretchable antennas, and strain sensors, respectively. In addition, Zhang et al. reported highly efficient and intrinsically stretchable polymer LEDs (PLEDs) that showed stable operation with up to 100% strain by developing highly stretchable PEDOT:PSS electrodes with a polyrotaxane (PR)-based photopatternable crosslinker (PR-PEDOT:PSS) (Figure 4d,e).[64] Furthermore, Jiang et al. successfully demonstrated intrinsically stretchable and biophysical sensor arrays based on the aforementioned PR-PEDOT:PSS systems.[75]

Intrinsically stretchable semiconductors have also been actively developed and utilized as the active layer for intrinsically stretchable devices. Among the several material candidates for stretchable semiconductors, conjugated polymers (CPs) have emerged as key materials because of their excellent optical and electrical properties, with inherently lower Young's moduli compared to those of silicon and inorganic semiconductors. However, the major challenge faced in developing CPs lies in maintaining good electrical, optical, and mechanical properties simultaneously. Because of the extended π-conjugation of the CP backbone, which is vital for electronic properties, they often have rigid and semicrystalline properties. To lower the rigidity and enhance the stretchability of CPs, a significant structural modification process for CPs has been developed by incorporating dynamic bonding units, conjugation breakers, and several flexible chemical structures.[67,76–78] A random terpolymer approach was also effectively used to simultaneously control the backbone rigidity and thin-film morphology. For example, Mun et al. developed high mobility (>1 cm^2 V^{-1} s^{-1}) and stretchable (>100% strain) diketopyrrolopyrrole (DPP)-based CPs by incorporating two different types of randomly distributed co-monomer units, which reduced the overall crystallinity and long-range orders while maintaining short-range ordered aggregates (Figure 4f).[65] As a result, the resulting CPs showed improved electrical and mechanical properties compared to those of a control system (polymer/polymer blend) (≈75% strain) (Figure 4g).

Similar to the approach for an elastomeric composite system for stretchable conductors, CPs/elastomer (e.g., styrene-ethylene-butylene-styrene [SEBS], PDMS, or TPU) blend systems have also been widely used. In particular, the similar surface energies of the CPs and SEBS elastomer ensure a nanoscale intimated morphology, which is crucial for efficient charge transport in electronic devices. For examples, Xu et al. reported intrinsically stretchable TFTs based on a DPP-based CPs/SEBS active layer (Figure 4h).[69] In these blended systems, the increased polymer chain dynamics from nanoconfinement significantly reduces the Young's modulus of the CPs and largely delays the crack formation under strain. Zheng et al. also improved the chemical resistance of stretchable polymer semiconductors by selectively crosslinking the backbones of the elastomer (polybutadiene) and alkyl chains of DPP-based CPs to make it feasible to photopattern stretchable polymer semiconductors.[79] The fabricated TFTs showed a stable performance up to 100% strain without affecting the charge carrier field-effect mobility. In addition, stretchable polymer light emitting layers with a nanoconfined light emitting polymer nanofiber network in a polyurethane (PU) elastomer matrix showed stable photoluminescent characteristics on the skin during various deformations (Figure 4i).[64]

3. Stretchable Electrodes

Stretchable electrodes have been intensively investigated in response to the rising demand for stretchable displays with new form-factors such as foldable, rollable, and stretchable architectures. These displays must be able to operate reliably even in unexpected deformations. Under such perspectives, many researchers have developed stretchable electrodes to achieve robust electrical interconnection between active devices such as light-emitting devices and TFTs, since the active materials are generally vulnerable to external stresses. To achieve mechanical reliability and electrical conductivity simultaneously, various methods with material-based and structural-based engineering for stretchable electrodes have been developed, which can maintain their interconnection under mechanical deformations such as folding, stretching, and twisting circumstances.

In this regard, this section begins with a discussion of representative approaches and fabrication technologies for stretchable electrodes, focusing on interconnection of active devices on stretchable substrate, classifying them into 1) intrinsically stretchable electrodes, 2) structurally designed stretchable electrodes, and 3) vertical interconnection access (VIA) for highly integrated stretchable system with advanced functionalities.

3.1. Intrinsically Stretchable Conductors

Stretchable electrodes with intrinsic elasticity are regarded as one of the most promising candidates for realization of stretchable electronic systems. By maintaining conductive percolation paths under mechanical deformation, the electrode with superior elasticity can endure localized strain from external stress, and then successfully interconnect functional devices. As a representative methods, elastomeric composites of an elastomer and conductive fillers,[57,80–86] LMs,[87–93] and conductive polymers[48,94–97] have been commonly used for intrinsically stretchable electrodes.

3.1.1. Conductive Nanomaterials Composites

As intrinsically stretchable electrodes, electrically conductive composites with combining an elastomer and conductive fillers are commonly used. Depending on target stretchability of desired applications, various types of elastomers such as PDMS, PU, and fluorinated rubber can be used, and conductive fillers such as metal NWs,[80–83] metal particles,[57] and CNT[84–86] can be mixed with the elastomer.

By using 1D metallic fillers, Lee et al. suggested AgNW-PDMS nanocomposites as intrinsically stretchable electrodes.[80] Since AgNW has 1D structure with high aspect ratio as well as high electrical conductivity, the electrodes could

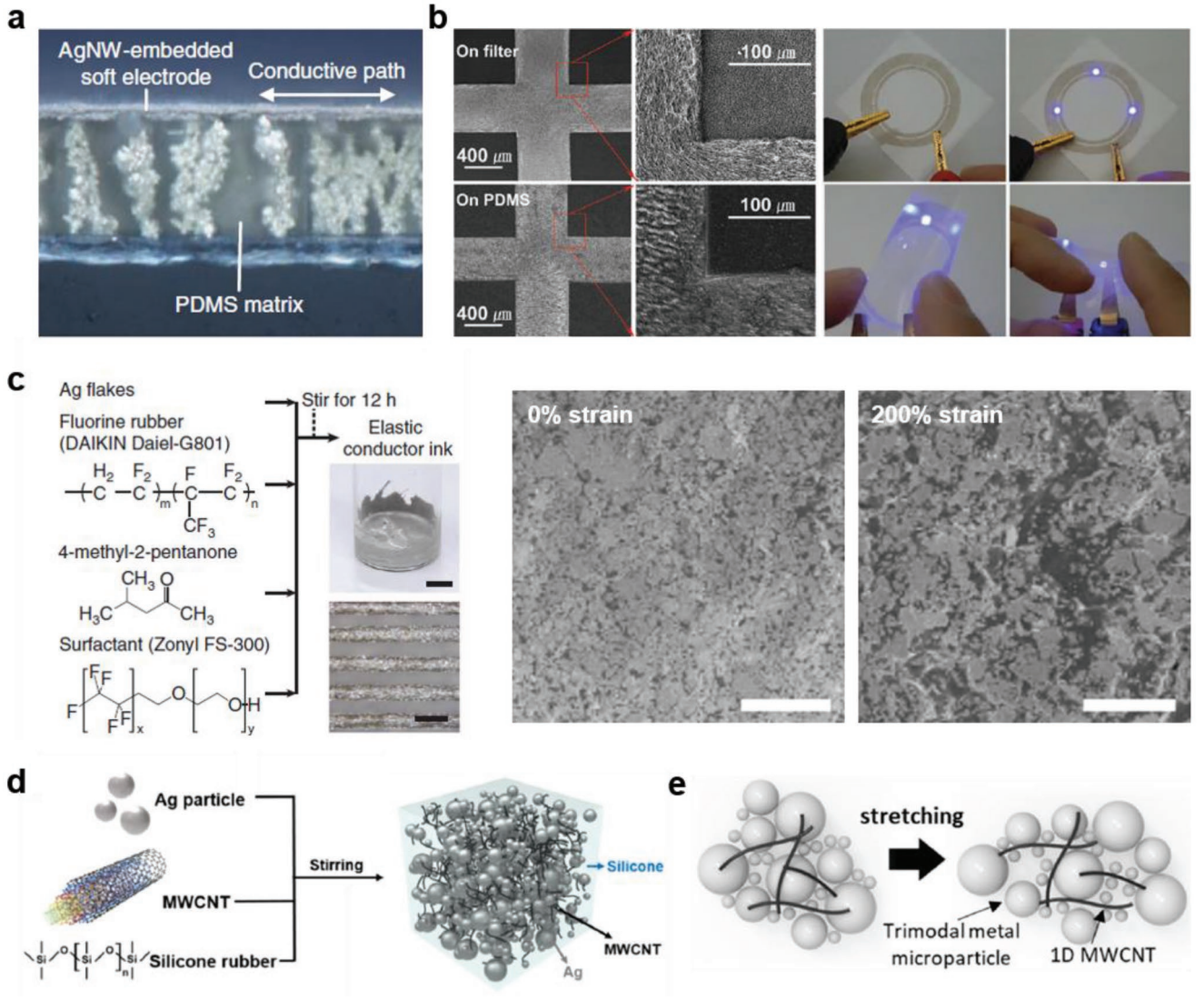

Figure 5. Stretchable composite electrodes. a) AgNW-embedded stretchable electrodes. Reproduced with permission.[80] Copyright 2020, Springer Nature. b) AgNW–elastomer composite electrodes fabricated using vacuum filtration method. Reproduced with permission.[81] Copyright 2018, Royal Society of Chemistry. c) Printable elastic electrodes with Ag flakes, fluorine rubber, and fluorine surfactant. Reproduced with permission.[57] Copyright 2015, Springer Nature. d) AgNW-embedded stretchable electrodes. Reproduced with permission.[84] Copyright 2019, American Chemical Society. e) AgNW-elastomer composite electrodes fabricated using vacuum filtration method. Reproduced with permission.[85] Copyright 2022, American Chemical Society.

maintain electrical percolation paths by forming entangled structure in an elastomer. To fabricate AgNW-embedded PDMS structures, as-coated AgNWs on a carrier substrate were transferred to uncured PDMS, and then the intrinsically stretchable electrodes were formed by simultaneous embedding and curing processes. The electrodes exhibited mechanical softness due to the fact that the AgNW layer was formed just on the surface of the PDMS substrate (**Figure 5**a), which has a negligible influence on elasticity of the substrate. When a tensile strain of 20% was applied, the AgNW electrodes could absorb the external strain and maintain their resistance under various mechanical deformations such as bending and stretching. There are several strategies for fabricating AgNW-based electrodes, including direct patterning method such as inkjet printing and bar coating as well as indirect fabrication techniques such as shadow masking and dry transfer patterning. Considering pros and cons of each fabrication methods, Yang et al. reported facile and highly efficient fabrication methods for robust AgNW–elastomer composite electrodes, combining a vacuum filtration system with an improved 3D PDMS mask.[81] The AgNW solution was successfully deposited on the target region of membrane filter via the channels within the 3D mask. As a result, clear edges could be achieved in both the AgNWs deposited on the filter and transferred to the PDMS (Figure 5b). The resultant electrodes showed electrical conductivity of ≈3000 S cm^{-1} at high deposition density of 10 g m^{-2}. By varying the AgNW deposition density and the PDMS peel-off direction, the stretchable electrodes could be stretched up to strain of

80%, exhibiting mechanical robustness with the LEDs turning on even under bending conditions.

Furthermore, since the composite mixed with elastomeric matrix is generally in fluidic state before curing, various solution processes can be utilized to form stretchable electrodes depending on target applications. In this regard, Matsuhisa et al. reported a printable elastic electrode comprised of Ag flakes, a fluorine rubber and a fluorine surfactant.[57] By modifying the Ag flake surface from a water-based fluorine surfactant, which is main component for formation of conductive networks, the electrical conductivity and mechanical stretchability of the printed electrodes could be enhanced, showing 738 S cm^{-1} at strain of 0% and 182 S cm^{-1} at strain of 215%. Although the electrical conductivity was relatively low, the electrode with superior elasticity can be stretched over strain of 200%, maintaining percolation paths of the composites by adding the surfactant (Figure 5c).

Metal nanomaterials have high electrical conductivity because of their metallic nature but it also brings low mechanical flexibility compared to carbon nanomaterials. By combining those metal and carbon nanomaterials, they can have synergetic effect on conductivity and stretchability. In this regard, Ko et al. reported stretchable conductive interconnects with superior electrical stability by forming composites that consist of Ag particles with different sizes as 0D conductive fillers, multi-walled CNTs (MWCNTs) as 1D conductive fillers and silicone rubber matrix (Figure 5d).[84] The micro-sized Ag particles could enhance electrical conductivity of the composites, while the nano-sized Ag particles could allow dense conductive network to be formed. Generally, the composite mixed with only MWCNT networks has not enough electrical conductivity compared to counterparts with other metallic conductive fillers. However, the MWCNTs used as auxiliary fillers could enhance interactive attraction between Ag particles, enabling to achieve high electrical conductivity and mechanical robustness of the composites. The different-sized Ag particles in the silicone matrix formed percolation paths and the MWCNTs were positioned around the Ag particles. The subsequently achieved stretchable electrodes exhibited high electrical conductivity of 6450 S cm^{-1} with little change under 3000 tensile cycle tests at strain of 50%. By utilizing aforementioned methods, Hong et al. demonstrated intrinsically stretchable and printable lithium-ion battery by using nanostructure-controlled multimodal conductive fillers (Figure 5e).[85] As the conductive fillers, various multimodal micro-particles such as Ag particles for the anode and Ni particles for the cathode were used. As an auxiliary fillers, MWCNTs were also employed to form a networked structure with conductive metal fillers. The composites with Ag particles and Ni particles shows high electrical conductivity of 3912 and 2105 S cm^{-1}, respectively, which exhibited stable operation until tensile strain of 130%.

Conductive composites are widely used in apposite ways with various conductive fillers and elastomeric substrates according to the target application. However, the electrical conductivity remains low in compared to other metal film, since the majority of components are nonconductive elastomer matrix. In addition, the strain-sensitive electrical conductivity based on percolation of conductive fillers is still limitation for cycling stability. Therefore, it is important to enhance mechanical stability as well as electrical conductivity for implementation of practical applications.

3.1.2. LMs

LM is a representatively used material for an intrinsically stretchable electrode, because it can maintain high electrical conductivity under strain by changing its shape from fluidic property. Especially, since LM exists as liquid phase at room temperature with ultralow Young's modulus, an LM electrode is capable of easily deformed to any direction with negligible resistance change unlike other solid-phase stretchable electrodes.

Taking advantage of fluidic property, Yang et al. used a eutectic alloy of LM (Galinstan) that consists of Ga, In, and tin (Sn) for intrinsically stretchable electrodes.[87] The LM could flow in a liquid form, congregating together with high surface tension (**Figure 6**a). Since the electrical conductivity can be maintained due to self-healing property as long as the interconnection is not completely damaged, the stretchability of LM electrodes can be directly affected by the material properties of an elastomeric substrate such as Young's modulus, yield strength, and maximum yield point strain. To achieve high stretchability over 300%, the Ecoflex silicone rubber was used as an elastomeric substrate, and then the LM was injected into empty channel in the rubber to form electrical interconnection. The subsequently achieved LM electrodes showed superior stretchability over 300% of strain.

Similarly, Bartlett et al. also reported LM-embedded elastomers. Mixing the LM eutectic alloy that consists of Ga and In with Ecoflex or PU elastomer, the intrinsically stretchable electrodes were fabricated (Figure 6b).[88] Various types of solution fabrication processes including dispensing, screen printing, stencil printing, and spray coating can be utilized for patterning of the LM-elastomer composites. Especially, the LM electrodes patterned by stencil printing exhibited superior stretchability from 0% to 500% strain. To further enhance mechanical reliability, Pan et al. suggested a LM-elastomer composite with various sizes of LM droplets in an elastomeric substrate (Figure 6c).[89] The effect of LM droplet sizes to stiffness of the composites was investigated. The LM-elastomer composites with small fillers could maintain mechanical stretchability, but counterpart composites with large fillers showed a degradation of stretchability in the strain at break. Therefore, the sizes of LM droplets must be carefully considered depending on target stretchability.

As another characteristic of LM electrodes, a thin oxide layer can be naturally and rapidly formed around the LM electrodes, enabling various architectures to be easily designed with maintaining mechanical stability. However, there are challenges in high resolution patterning due to its rapid oxidation with high surface tension in air environment. To overcome this issue and exhibit feasibility of the LM electrodes for stretchable electronic systems with various designs, Silva et al. reported high-resolution stretchable circuits with finely patterned LM electrodes by controlling the oxide layer of LM (Figure 6d).[90] Polyvinyl alcohol (PVA) was coated on an elastomeric substrate, which enables inkjet printing of conductive materials on an

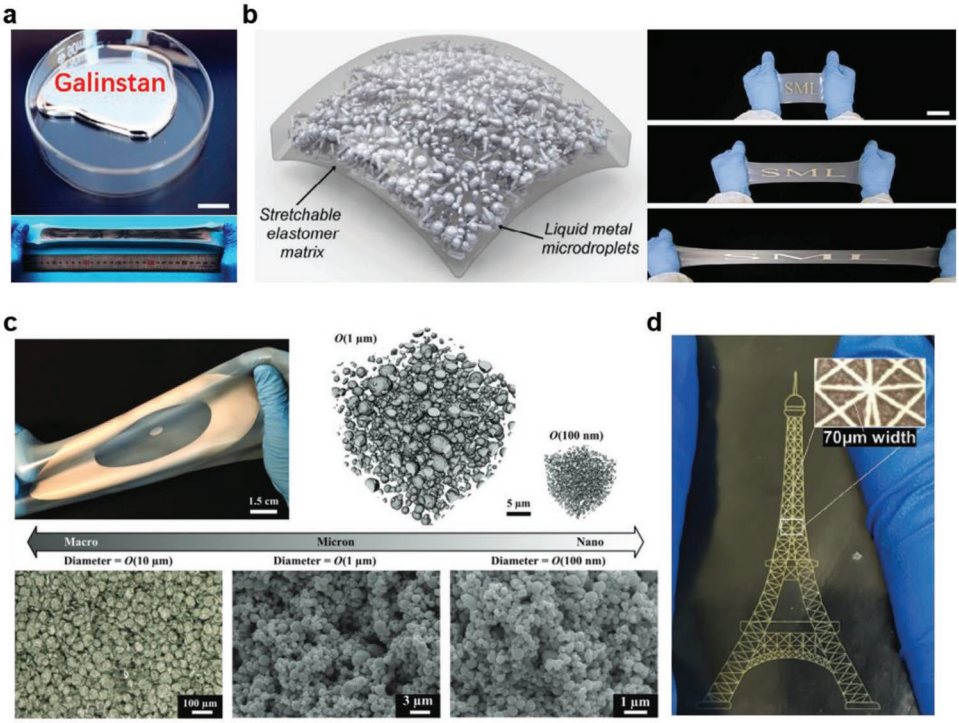

Figure 6. LM stretchable electrodes. a) A eutectic alloy of LM that consists of Ga, In, and Sn for intrinsically stretchable electrodes. Reproduced with permission.[87] Copyright 2018, American Chemical Society. b) LM microdroplet-embedded stretchable electrodes. Reproduced with permission.[88] Copyright 2016, Wiley-VCH. c) LM–elastomer composites with various sizes of LM droplets. Reproduced with permission.[89] Copyright 2019, Wiley-VCH. d) Finely patterned LM stretchable electrodes for high-resolution applications. Reproduced with permission.[90] Copyright 2020, Wiley-VCH.

elastomeric substrate, followed by printing of Ag nanoparticles (AgNPs). By removing oxide layer of LM through dissolving in acetic acid solution, the LM could be selectively patterned on the printed AgNP traces due to its dewetting property from the PVA layer. Taking advantages of the self-patterning characteristics, complicated patterns and circuits with different fine lines could be achieved, exhibiting outstanding electrical conductivity and stretchability over 100% of strain.

Although LM electrode can exhibit superior elasticity with high electrical conductivity, there are still critical issues to use it together with other conductive metal, since Ga easily penetrates other metals along to grain boundaries, resulting in irreversible performance degradation such as swelling and cracking. Therefore, specific integration methods including pattering, deposition, and encapsulation technologies must be considered together.

3.1.3. Conductive Polymers

Conductive polymers have advantages in direct processability and tunability of the molecular structures to determine electrical and mechanical properties. Since they are capable of being soluble in proper solvents, various solution processes such as inkjet printing, spray coating, and screen printing can be utilized. Among a lot of conductive polymers, PEDOT:PSS has been intensively utilized as transparent stretchable electrode for stretchable electroluminescent devices due to its high electrical conductivity, transparency, and easy work function modification compared to other conductive polymers.

Oh et al. reported modification of nanostructure and viscoelastic property of PEDOT:PSS by using plasticizer (Triton X-100).[94] By optimizing weight fraction of the surfactant, electrical conductivity and mechanical stretchability could be enhanced simultaneously. Due to the viscoelasticity from the addition of Triton X-100, the conductive polymer could be molded into micro-patterns which enable implementation of high resolution OLEDs array (**Figure 7**a). PEDOT:PSS electrodes are generally incorporated with such plasticizers to enhance its stretchability, but the electrical conductivity is still low to be used for realization of high performance stretchable devices. To further improve stretchability and electrical conductivity, Wang et al. reported the highly stretchable, transparent and conductive PEDOT:PSS electrodes, which were incorporated with ionic additives-based stretchability and electrical conductivity (STEC) enhancers (Figure 7b).[48] The STEC enhancers with ionic additives enabled formation of soft domains, better connectivity between PEDOT-rich domains, and higher crystallinity in PEDOT regions, resulting in implementation of highly conductive and stretchable PEDOT:PSS electrodes which exhibited 4100 S cm^{-1} under 100% of strain.

Similarly, Park et al. suggested transfer-printed conductive polymer electrodes for highly customizable PLEDs.[95] To achieve better wettability on an elastomeric substrate, surface treatments such as ultraviolet (UV) light exposure and oxygen plasma treatment have been widely used, but these treatments could degrade performance of organic layers. To overcome this issue, they suggested dry transfer printing methods for

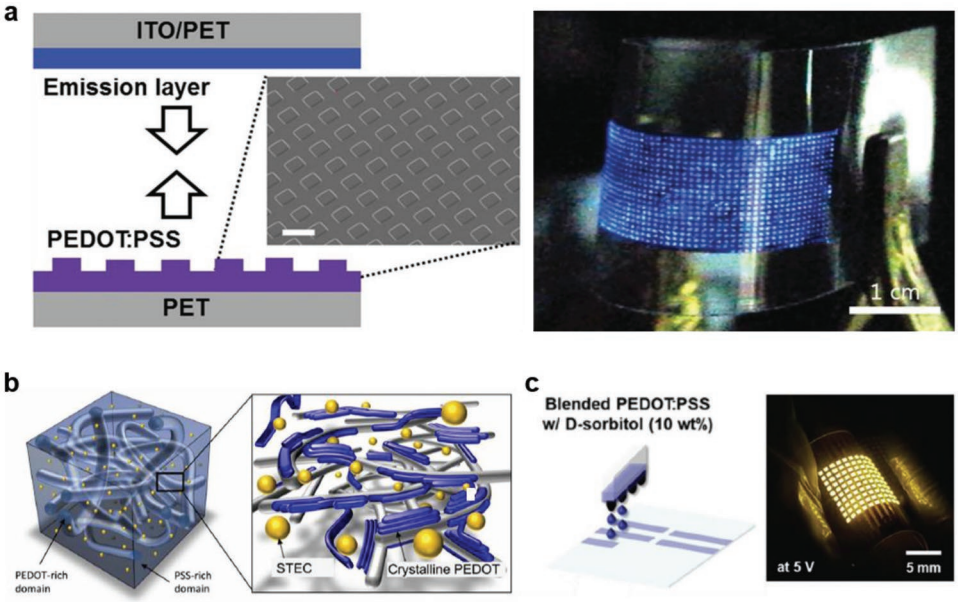

Figure 7. Conductive polymer-based stretchable electrodes. a) Micropatterned PEDOT:PSS electrodes blended with Triton X-100 to control viscoelasticity. Reproduced with permission.[94] Copyright 2016, Wiley-VCH. b) PEDOT:PSS-based stretchable interconnects with ionic additives and STEC enhancers. Reproduced with permission.[48] Copyright 2017, American Association for the Advancement of Science. c) PEDOT:PSS electrodes incorporated with D-sorbitol to enhance bonding force during lamination processes. Reproduced with permission.[95] Copyright 2019, Wiley-VCH.

PEDOT:PSS patterning to minimize degradation of organic layers during whole fabrication processes. The PEDOT:PSS electrodes incorporated with D-sorbitol, which was used to enhance bonding force in a lamination processes, were successfully transferred to a PDMS substrate. The transferred electrodes exhibited outstanding transparency compared to conventional ITO (Figure 7c). As a proof of concept, the matrix display were demonstrated which maintains its brightness under bending state when the PEDOT:PSS electrodes were used as anodes of PLEDs.

Despite its transparency and intrinsic elasticity, since PEDOT:PSS has relatively low electrical conductivity compared to metal film, it is difficult to use it alone as an stretchable electrode. Therefore, multidisciplinary research should be conducted to improve electrical and mechanical performance through material synthesis or hybrid with other electrodes.

3.2. Structurally Designed Stretchable Interconnects

Structurally designed stretchable electrodes with various geometrical patterns are one of the most promising candidates for interconnection component of high-performance stretchable display, taking advantages originated from well-established fabrication processes and material properties of metal films with high electrical conductivity.[98] However, since the metal films such as Cu, Au, and Ag have much lower tensile limit than intrinsically stretchable electrodes, specific structural designs to dissipate localized strain should be employed. Therefore, many researchers have developed representative structural designs such as serpentine[99–102] and wrinkled electrodes,[98,103–105] which can maintain electrical conductivity by changing their geometrical shapes.

3.2.1. Serpentine Electrodes

Serpentine electrodes are commonly used as metallic stretchable electrodes due to their superior electrical conductivity. The metal electrodes are capable of being easily patterned by well-established conventional photolithographic processes. Due to unique structural designs with horseshoe shapes, the electrodes could endure localized strain by changing their geometrical shapes under various mechanical deformations (**Figure 8**a).[99] Considering this characteristic, Biswas et al. reported stretchable active matrix display with multilayered serpentine electrodes.[100] By using photolithography process, 10 μm thick Cu electrode was deposited on carrier substrate where sacrificial layers of poly(methyl-methacrylate) (PMMA) and PI were coated, and then insulation layer composed of photopatternable PI was used to secure separation of row and column electrodes (Figure 8b). Even though there were thick parts of coated films, the electrodes could be stretched due to its structural design. To demonstrate their stretchability, commercially available surface mount LEDs were integrated with the electrodes, followed by encapsulation process with Ecoflex elastomer with very low Young's modulus to achieve softness. The subsequently fabricated stretchable active matrix display exhibited no significant performance changes under stretching at 220% of strain.

By further developing the serpentine structure designs, Li et al. suggested 2D fractal-inspired shapes for advanced interconnect configurations.[101] The unique shapes could render metal electrodes enhanced stretchability compared to conventional serpentine electrodes, but the stretchability is still as low as 11% when the electrodes were just stretched along to in-plane direction. Therefore, two-stage solid encapsulation methods were further suggested for formation of 3D configurations, resulting in four times improved stretchability up to 46% strain

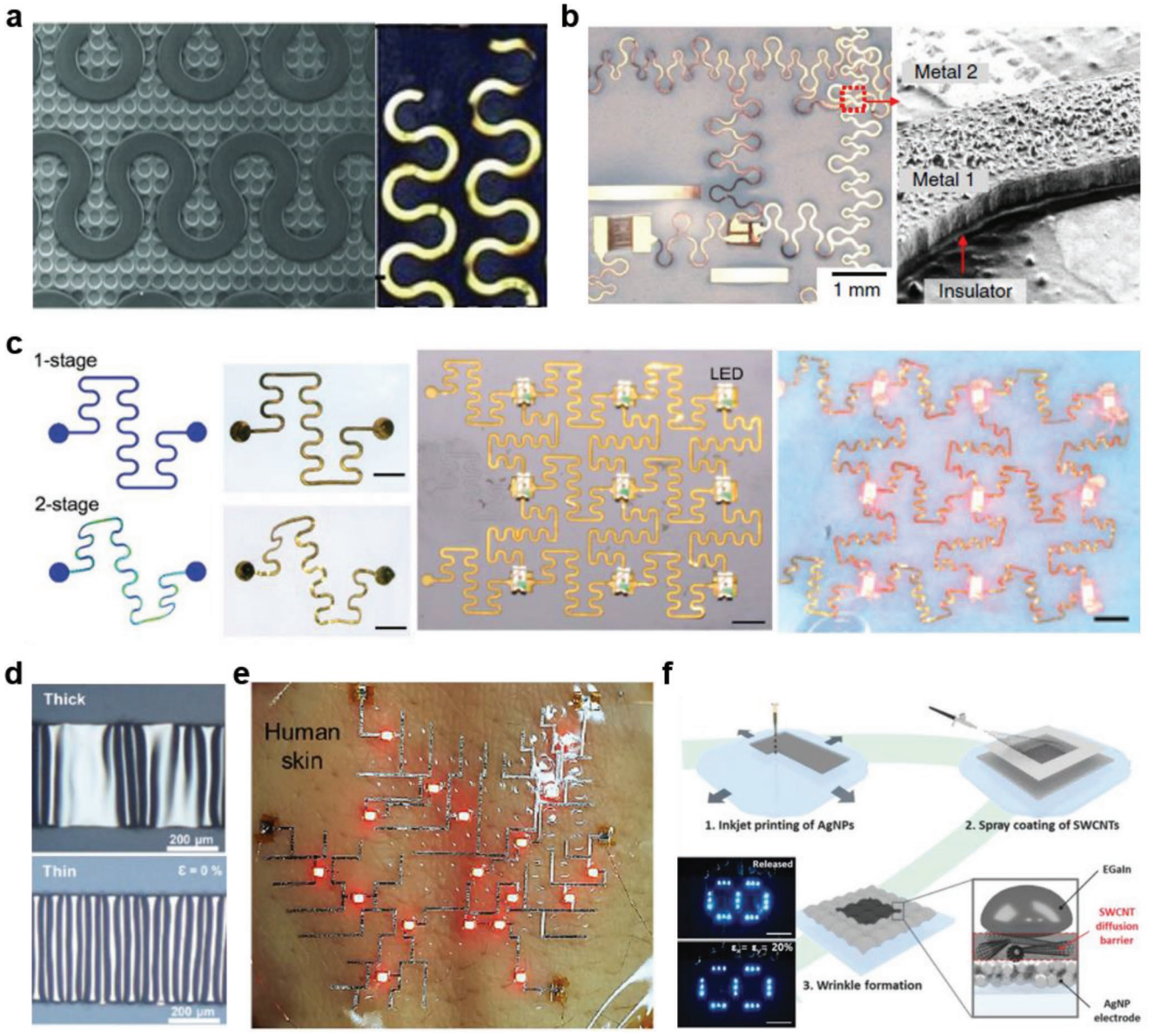

Figure 8. Structurally designed serpentine and wrinkled stretchable electrodes. a) Horseshoe-shaped serpentine structural designs to endure localized strain. Reproduced with permission.[99] Copyright 2014, Wiley-VCH. b) Serpentine stretchable electrodes fabricated using well-established conventional photolithographic processes. Reproduced with permission.[100] Copyright 2019, Springer Nature. c) Fractal-inspired serpentine electrodes for advanced interconnect configurations. Reproduced with permission.[101] Copyright 2019, Wiley-VCH. d) Strain-tolerant wrinkled electrodes. Reproduced with permission.[103] Copyright 2019, Taylor & Francis. e) Wrinkled electrodes with integrated LEDs fabricated by customizable inkjet printing methods. Reproduced with permission.[104] Copyright 2017, Springer Nature. f) Corrugated SWCNT diffusion barrier with wrinkled electrodes. Reproduced with permission.[105] Copyright 2018, Wiley-VCH.

(Figure 8c). By using these configurations, stretchable LED systems could be successfully achieved, maintaining electrical performance even under 40% of biaxial strain.

3.2.2. Wrinkled Electrodes

Wrinkled electrodes can be directly formed on elastomeric substrates using not only vacuum evaporation but also various solution processes such as inkjet printing, screen printing, spray coating, and electroless deposition. Among various methods, inkjet printing is commonly used for patterning of the metal films due to its facile customizability and low temperature processability. Cho et al. reported strain-tolerant wrinkled electrodes for stretchable electrodes.[103] The wrinkled structure could be introduced by releasing a pre-stretched elastomeric substrate where conductive inks were printed by inkjet printing method. Especially, they pointed out that the stretchability was dominantly affected by the regularity of wrinkles since mechanical strain could be concentrated at the thicker regions of the electrode. By optimizing inkjet printing processes for implementation of thin and flat metal films, well-defined wrinkles

on the films could be obtained (Figure 8d), and showed a little resistance changes of 10% even under 10 000 stretching cycles at 25% tensile strain. Similarly, Byun et al. fabricated various types of stretchable display by using customizable inkjet printing methods with integrating LEDs on wrinkled electrodes.[104] By forming gradual wrinkles on metal films with embedded strain modulators, the mounted LEDs could maintain their electrical performance on human skin (Figure 8e).

To further improve mechanical reliability, Oh et al. suggested a corrugated SWCNT diffusion barrier for the wrinkled electrodes.[105] LM was used as contact materials, which could dissipate concentrated mechanical strain at the boundary between LEDs and wrinkled electrodes. However, the LM could react with the wrinkled electrodes by penetrating grain boundaries in metals. Considering this issue, corrugated SWCNT was introduced to diffusion barrier for wrinkled electrodes. Based on the corrugated and wrinkled configurations, stretchable display with wrinkled electrodes was demonstrated, which showed no noticeable change in the luminance of the LEDs under 20% of biaxial strain (Figure 8f).

As described in previous examples, stretchable electrodes with serpentine and wrinkled structure could be variously designed depending on target stretchability of desired applications, and exhibited outstanding performance with high electrical conductivity under various mechanical deformations. However, the fabrication processes for serpentine electrodes such as photolithography and etching are still challenging for direct fabrication onto elastomeric substrates, and prestretching process for wrinkled structures is critical bottleneck for mass production of stretchable display. Therefore, it is important to further establish suitable fabrication technologies considering compatibility, processability, customizability, and feasibility.

3.3. VIAs with Stretchable Electrodes

To implement a stretchable matrix display integrated with multifunctional layers, formation of VIAs in stretchable substrate has been vigorously investigated in multidisciplinary research fields. By interconnecting various active layers in stretchable systems with high integration density, versatile operations can be achieved. To form VIAs in stretchable substrate, materials and fabrication technologies should be carefully selected since conductive paths along to vertical direction must be reliably maintained when the systems are stretched along to horizontal direction. In addition, the VIAs are generally filled in perforated regions in an elastomeric substrate, which can lead electrical failure and mechanical tear at the regions. Therefore, many research groups have considered various methods to make VIAs strain-insensitive without degrading mechanical reliability and stretchability of stretchable substrates.

To form VIAs with serpentine electrodes, Huang et al. reported a framework for 3D integrated stretchable systems with VIAs, which were formed by laser ablation and filling conductive materials in predefined region.[106] Elastomer matrix were selectively perforated by laser ablation with careful optimizations of fabrication parameters such as laser wavelength, pulse, and absorption rate. The geometries of VIAs such as depth and width were controlled to secure electrical contacts between VIA and other layer. By increasing diameter from 300 to 600 μm up to the fourth layer, enough contact in through VIA could be ensured by filling conductive solder pastes in the region (**Figure 9**a). Although the VIA was nonstretchable due to rigid nature of filling material, it was stably interconnected by serpentine electrodes with island-bridge configurations. Based on this approach, highly conductive and strain-insensitive VIAs could be achieved, and the VIAs exhibited ultralow

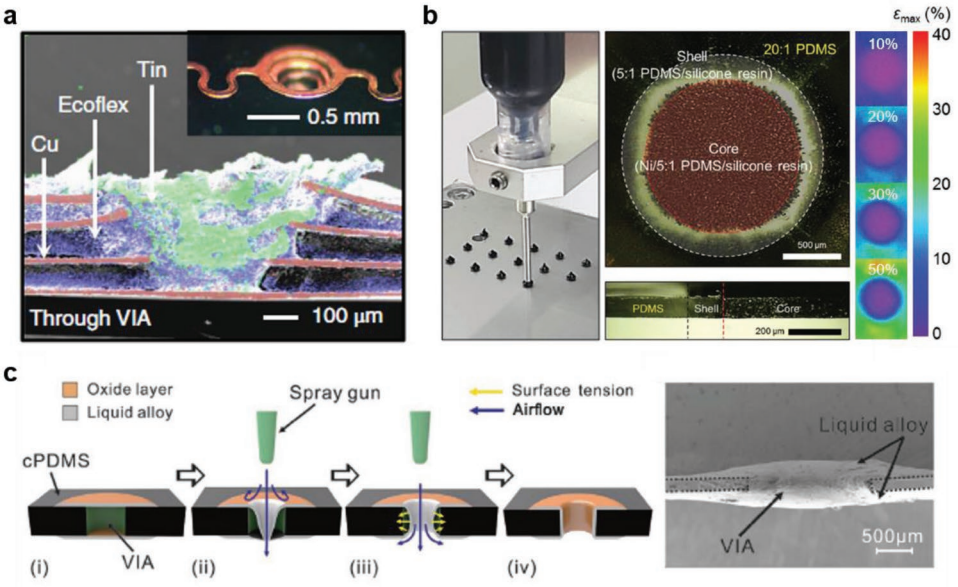

Figure 9. VIAs with stretchable electrodes. a) 3D integrated stretchable systems with VIAs formed by laser ablation and filling conductive materials with serpentine electrodes. Reproduced with permission.[106] Copyright 2018, Springer Nature. b) Modulus-gradient stretchable VIAs fabricated by printing-based methods with wrinkled electrodes. Reproduced with permission.[107] Copyright 2017, Wiley-VCH. c) Liquid alloy stretchable VIAs fabricated by spray coating methods with LM stretchable electrodes. Reproduced with permission.[108] Copyright 2021, Wiley-VCH.

resistance about 68.7 mΩ, which enables implementation of high-performance stretchable systems with increased integration density.

In case of VIA with wrinkled electrodes, Byun et al. suggested double-side soft electronic platform with core–shell VIA.[107] By using printing-based method, the conductive VIA was patterned on an elastomeric substrate. To resolve discontinuity in elastic modulus between the VIA and substrate, which could lead unexpected delamination, geometrical design and compositions of the VIA were carefully optimized. The conductive composites that consist of Ni particles, PDMS, and silicone resin were printed on desired position, and then magnetic alignment of the composites was conducted to form gradual stiffness in a single VIA (Figure 9b). Due to the focused magnetic alignment, Ni particles were converged into center of VIA and aligned along to vertical direction, simultaneously. The subsequently stiffness-gradient shell, being relatively high Young's modulus than the substrate, could stably protect the conductive vertical paths. Based on this approach, double-side stretchable platform with wrinkled electrodes was successfully demonstrated, which showed high-speed operation of stretchable computing circuits.

To implement LM-based VIA, Jiang et al. reported LM alloy VIAs for fabricating multilayered stretchable systems.[108] To generate microholes in an elastomeric substrate, UV laser for ablation was used to implement vertical profile with microstructures, and then the liquid alloy was deposited in the holes by spray coating. Taking advantages in unique properties such as liquid phase and rapid oxidation in air environment, the liquid alloy could be coated on both sides of holes (Figure 9c). After selectively pinning at both sides, the oxide layer surrounding the coated liquid alloy was rapidly formed, which enable that the liquid alloy could maintain its shape against high surface tension and gravity. The subsequently formed VIA exhibited a resistance variation ($\Delta R/R_0$ <300%) under stretching test with tensile strain >90%, which is average strain of elongation at break for elastomer substrate.

As aforementioned examples of VIA for stretchable system, there are various fabrication methods and material candidates to achieve robust interlayer interconnection and high integration in the stretchable system with multilayered structure. To further improve integration density with maintaining electrical performance and mechanical stability simultaneously, apposite strategies must be selected depending on target applications with careful consideration of the pros and cons in each method.

4. Stretchable TFTs

Stretchable TFT is a fundamental component in the backplane of stretchable display, driving the electroluminescent devices as well as performing signal switching and amplification. To implement advanced stretchable systems, there are significant efforts to fabricate mechanically reliable stretchable TFTs, which can maintain their performances in various mechanical deformations. Along with stretchable electrodes that introduced in the previous chapter, the development of stretchable semiconducting active materials is critical for stretchable TFTs. Therefore, it is important to develop apposite strategies for implementation of stretchable TFTs depending on active channel materials. In this regard, we discuss the various methodology of forming stretchable TFTs in terms of active channel materials, classifying into 1) inorganic, 2) CNT, and 3) organic semiconductors.

4.1. Inorganic TFTs

Despite the inherent brittleness of inorganic active channel materials including conventional silicon-based materials and oxide semiconducting materials, there are various attempts to implement stretchable inorganic TFTs for practical applications. Kim et al. suggested wrinkled structured TFTs for silicon-based CMOS integrated circuits.[17] Although the inorganic materials are generally vulnerable to external stress, the wrinkled structures can render the fragile materials stretchable by minimizing the deformation energy. Since inorganic TFTs could be hardly fabricated onto the elastomeric substrate due to the high temperature process, the TFTs were transferred from the carrier substrate to prestretched PDMS substrate, and then released them to initial state to achieve desired stretchability. As proof of concept, stretchable CMOS integrated circuits were demonstrated, which could maintain their electrical performances under deformations (**Figure 10**a). Although the wrinkled inorganic TFTs has excellent electrical properties due to well-defined crystallinity of inorganic semiconductors, they require specialized manufacturing procedures such as prestretching and transferring. In addition, cracks are also likely to occur when external strain applied to the device exceed limit of prestrain, which can cause irreversible damage of electrical behavior. Moreover, since TFTs consist of multiple layers with electrodes, dielectric, and active channels, it is difficult to form regular wrinkles on whole layers due to variation of their thickness and Young's moduli.

A strain-modulating structures such as an island-bridge structure can be an efficient way to facilitate fabrication process and to modulate strain distribution.[109–112] Since the inorganic semiconducting materials have higher Young's moduli compared to elastomeric substrate, they can be located on the strain-free region where the rigid parts are formed in the soft substrate. When TFTs are fabricated on the strain-free areas with stretchable interconnects, the deformation of TFTs can be minimized. From this perspectives, Park et al. demonstrated an array of stretchable oxide TFTs by transferring ZnO TFTs onto the strain-modulated substrate with rigid island structure (Figure 10b).[109] The stretchable interconnects with wrinkled structures could endure bidirectional strain, reducing the mechanical stress on brittle oxide TFTs formed on strain free regions.

By further developing material and structural designs, Park et al. used LM for stretchable electrodes and fabricated TFTs at the cross-point rigid island (Figure 10c).[110] The LM-based stretchable electrodes can improve maximum strain limitations due to its fluidic properties with maintaining electrical conductivity under various deformations. Moreover, LM can be easily patterned in submicrometer feature size.[113] Also, to improve scalability of stretchable TFTs, Cantarella et al. suggested structurally engineered substrate where pillar structures

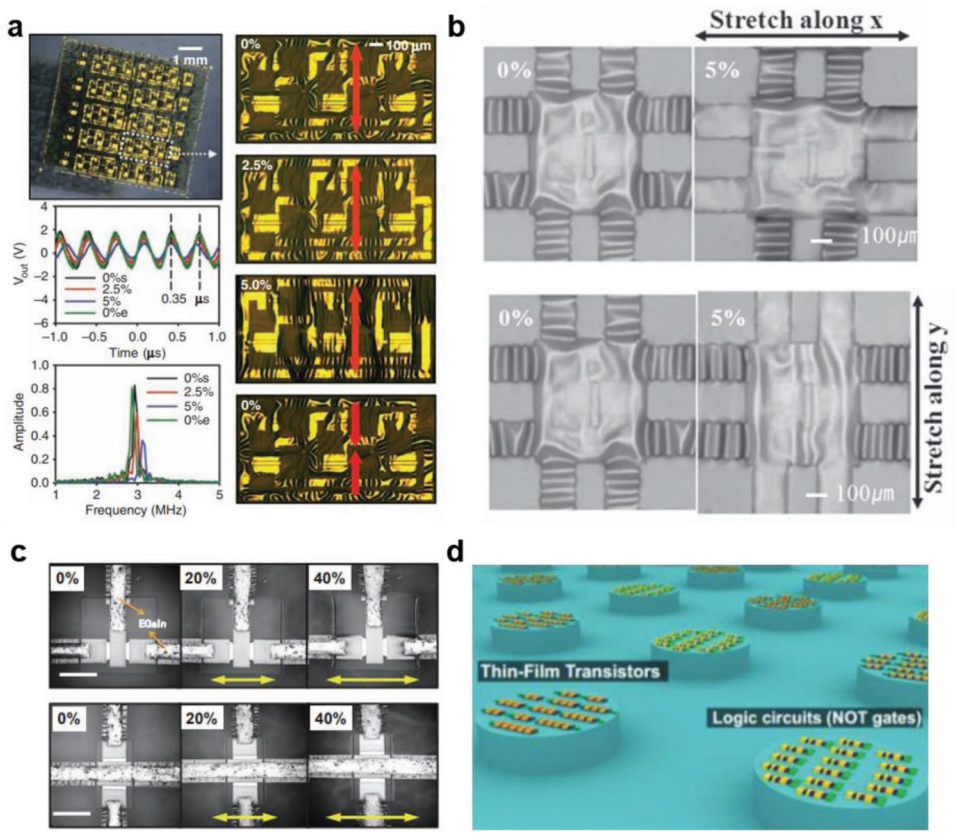

Figure 10. Stretchable inorganic transistors. a) Wrinkled structured CMOS circuit based on silicon active channel and its output characteristics with external strain Reproduced with permission.[17] Copyright 2008, American Association for the Advancement of Science. b) Image of island structure used for stretchable oxide transistor array, with 5% of *x*- and *y*-axis strain. Interconnections are formed with a wrinkle to withstand the external strain. Reproduced with permission.[109] Copyright 2010, Wiley-VCH. c) Image of island-structured oxide transistors with 40% external strain. Interconnections are LM-based electrodes. Reproduced with permission.[110] Copyright 2018, The Japan Society of Applied Physics. d) Schematic of large pillar islands used to fabricate a transistor array or logic circuits. Reproduced with permission.[111] Copyright 2018, Wiley-VCH.

were formed to obtain strain-free regions (Figure 10d).[111] Since the pillar structures could be freely designed according to the geometries of designed TFTs, it could be applied to large-scale logic circuits which consists of various types of TFTs.

Likewise, most of researches about stretchable inorganic TFTs have generally focused on structural designs to achieve mechanical stretchability and robustness. However, structural improvement alone cannot overcome the intrinsic brittleness fundamentally. In addition, conventional fabrication methods such as photolithography and etching are not fully compatible with elastomeric substrates, resulting in further increasing the difficulty of the whole processes. For these reasons, additional integration techniques should be developed for realization of more advanced stretchable systems.

4.2. CNT TFTs

CNT is one of the promising materials for implementation of stretchable TFTs due to its superior electrical and mechanical properties.[114–118] The 1D nanostructured CNTs can maintain their electrical percolation paths with formation of entangled networks.

In this regard, Chae et al. demonstrated stretchable CNT TFTs by combining semiconducting CNT networks, graphene electrodes, and wrinkled Al_2O_3 dielectric layer.[117] In contrast to conventional inorganic materials, since the CNT networks and graphene layers are extremely thin, well-defined wrinkles could be easily formed. By combining CNTs with corrugated structure design of dielectric layer, the mechanical stability could be further improved without compromising electrical characteristics up to 20% strain in channel width direction, which showed on/off ratio of 10^5 and high mobility of 40 cm^2 V^{-1} s^{-1}. This approach not only showed the structural design applicability of carbon-based materials but also exhibited their stretchability and feasibility for intrinsically stretchable TFTs. In addition, CNTs can be used for both electrodes and active channel materials simultaneously depending on their metallic and semiconducting properties, respectively. In this regard, Cai et al. demonstrated fully printed stretchable TFTs and integrated logic circuits by using CNTs as both electrode and active channel materials (**Figure 11**a).[119] To implement fully stretchable TFTs, they fabricated stretchable dielectric composite that consist of barium titanate ($BaTiO_3$) NPs and PDMS matrix, which exhibited high dielectric constant and stretchability. Due to the intrinsic stretchability of electrodes, dielectric, and active

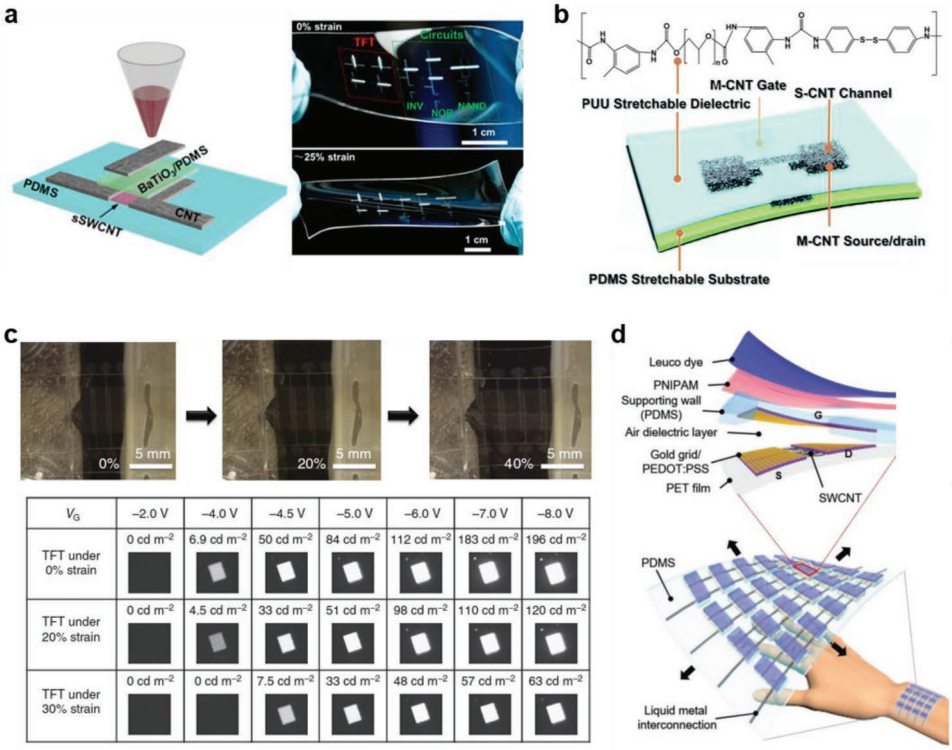

V_G	−2.0 V	−4.0 V	−4.5 V	−5.0 V	−6.0 V	−7.0 V	−8.0 V
TFT under 0% strain	0 cd m^{-2}	6.9 cd m^{-2}	50 cd m^{-2}	84 cd m^{-2}	112 cd m^{-2}	183 cd m^{-2}	196 cd m^{-2}
TFT under 20% strain	0 cd m^{-2}	4.5 cd m^{-2}	33 cd m^{-2}	51 cd m^{-2}	98 cd m^{-2}	110 cd m^{-2}	120 cd m^{-2}
TFT under 30% strain	0 cd m^{-2}	0 cd m^{-2}	7.5 cd m^{-2}	33 cd m^{-2}	48 cd m^{-2}	57 cd m^{-2}	63 cd m^{-2}

Figure 11. Stretchable CNT transistors. a) Schematic and image of intrinsically stretchable CNT-based transistors fabricated using inkjet printing process. Reproduced with permission.[119] Copyright 2016, American Chemical Society. b) Stretchable CNT transistors with high resolution achieved by photolithography. Reproduced with permission.[120] Copyright 2020, Royal Society of Chemistry. c) OLED operation with various bias and strain conditions. Interconnections are LM-based electrodes. Reproduced with permission.[121] Copyright 2015, Springer Nature. d) Schematic of a thermochromic wearable display fabricated using CNT transistors. Reproduced with permission.[122] Copyright 2019, Wiley-VCH.

channels, the TFTs showed stretchability beyond 50% of strain along direction of length or channel width, and exhibited no significant degradation of electrical performance during tensile stretching cycles.

To fabricate high performance stretchable CNT TFTs with high mobility, low voltage, and high integration density, Huang et al. combined the advantages of solution process and conventional photolithography methods (Figure 11b).[120] They used poly(urea-urethane) (PUU) elastomer as stretchable dielectric material because it has a higher permittivity compared to other elastomeric dielectrics. However, the PUU is easily damaged from photolithographic processes such as plasma etching. To overcome this limitation, removal-transfer-photolithography method was proposed. As a sacrificial layer, indium gallium zinc oxide (IGZO) was used to enhance wettability of PDMS substrate and PUU dielectric, and etching damage of the PUU dielectric was minimized with the appropriate use of sacrificial layers. Since CNT networks have superior carrier mobility and the charge transportation was significantly improved by controlling dielectric capability, the stretchable CNT TFTs showed high mobility (≈221 cm^2 V^{-1} s^{-1}) and maintained their characteristics after 2000 stretching cycles with 50% strain.

Another advantage of CNT to expand the scope of device applications is transparency, which can increase aperture ratio of display pixels or be used for fully transparent wearable devices. Liang et al. fabricated the intrinsically stretchable and transparent CNT TFTs (Figure 11c).[121] AgNWs and PU-co-polyethylene glycol were used for electrodes and elastomeric dielectric for intrinsically stretchable and transparent devices. The fabricated TFT could be stretched up to 50% strain with maintaining its electrical performance and exhibited optical transmittance over 90% in the 450–1100 nm wavelength range, driving OLED in the full brightness range. These results implied the feasibility of a CNT-based backplane for display devices with high transparency.

Furthermore, CNT TFTs could be integrated with stretchable sensors for various wearable devices. Hong et al. fabricated a skin-attachable and intrinsically stretchable CNT TFT array with highly sensitive temperature sensors.[122] By using thermos-responsive film, CNT TFT arrays with a thermochromic property in the range of human body temperature were implemented (Figure 11d). The fabricated devices were easily attached to the human skin with stable operation under skin movement such as wrist bending. As a practical healthcare application, thermochromic display devices with CNT TFTs were demonstrated with showing a possibility of advanced wearable display application.

With the aforementioned unique characteristics, CNTs showed the great possibility to be applied in stretchable driving devices. However, in the chemical manufacturing process of CNTs, both metallic and semiconducting CNTs are grown at once. Therefore, additional purifying processes are needed to improve the semiconducting property of the active channels.

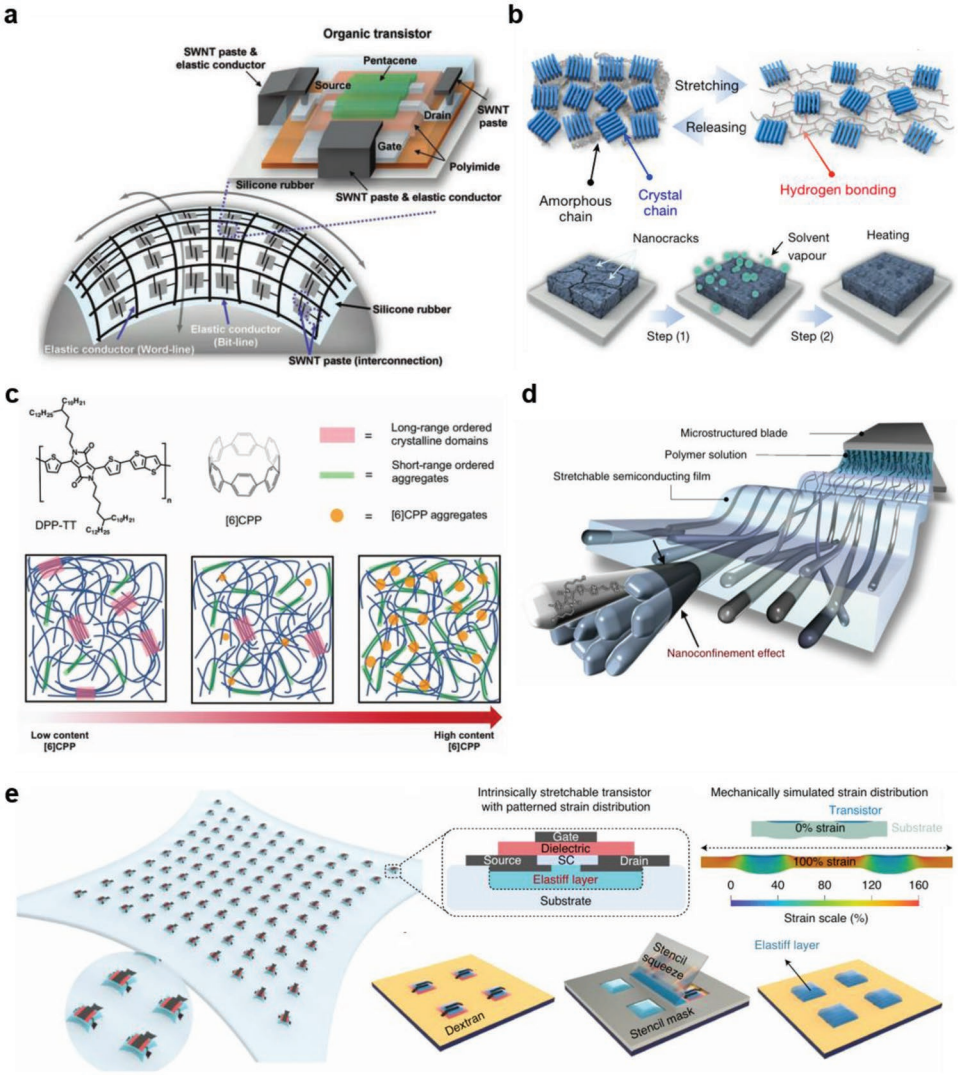

Figure 12. Stretchable organic transistors. a) Schematic of stretchable organic transistor array utilizing PI as rigid islands and images of fabricated devices under stretched states. Reproduced with permission.[123] Copyright 2008, American Association for the Advancement of Science. b) Schematic of polymer dynamics of block copolymer with amorphous and crystal chains and a self-healing process with solvent vapor treatment. Reproduced with permission.[125] Copyright 2016, Springer Nature. c) Changing the crystallinity of conjugated polymers by addition of a conjugated carbon nanoring. Reproduced with permission.[132] Copyright 2019, Wiley-VCH. d) Schematic of solution-shearing process for a composite of elastomer and unidirectional-ordered conjugated polymer induced by nanoconfinement effect. Reproduced with permission.[134] Copyright 2019, Springer Nature. e) Schematic of stretchable organic transistor array with composite-based stretchable semiconductor and elastiff layer for redistribution of applied strain. Reproduced with permission.[135] Copyright 2021, Springer Nature.

Because the remaining metallic CNTs form leakage paths in the channel even after purification, the off-current level can be increased. In addition, the random network structure of CNT channels reduce the uniformity of TFT array. Therefore, development of purification methods with high yield and studies of advanced passivation and percolation structure are required to achieve CNT TFT array with high stability and uniformity.

4.3. Organic TFTs

Organic semiconductors are also one of the promising candidates for active layers of deformable TFTs based on not only easy processability including vacuum and solution processes, but also easy controllability of mechanical and electrical properties through molecular engineering. Similar to the inorganic TFTs, the island-bridge structures were implemented in the early stages of researches about stretchable organic TFTs due to mechanical brittleness of small molecule organic semiconductors.[61,123] Sekitani et al. demonstrated a stretchable organic TFT array utilizing PI as rigid islands (**Figure 12**a).[123] The brittle channel region was located on strain-free region with PI rigid islands to minimize the mechanical stress when the device was stretched. As a result, the fabricated TFT array with stretchable interconnects could be uniaxially and biaxially stretched up to 70% without any mechanical or electrical failures. However,

as mentioned in the section of inorganic and CNT transistors, this approach utilizing rigid islands has still limitations about process complexity due to additional processes for fabrication of rigid regions in the elastomeric substrate and concentrated mechanical stress at the interface.

To overcome aforementioned limitations, molecular engineering methods for the implementation of intrinsically stretchable organic semiconducting materials have been developed. There are three main strategies to develop intrinsically stretchable organic semiconductors: copolymerization or side chain engineering to control crystallinity,[124–130] blending additives to induce phase separation or change in crystallinity,[131,132] and making composite of organic semiconductor and elastomer.[66,69,133–135] In the first case, Oh et al. demonstrated intrinsically stretchable and healable block copolymer-based organic TFTs with conjugated repeating units and non-conjugated moieties as hydrogen bonding units.[125] When strain was applied to the polymer films, energy dissipation occurred through the breakage of hydrogen bonds between amorphous chains (Figure 12b). As a consequence of this energy dissipation, the polymer semiconductor could retain high charge transport abilities in stretched states. Furthermore, the mechanically damaged polymer film could be healed through solvent vapor treatment and thermal annealing, recovering its morphology and field-effect mobility to those of an undamaged film. Stretchable organic TFTs fabricated with CNT electrodes and PDMS dielectric layer could operate stably under 100% strain and even after the 500 stretching cycles at 25% strain.

In the second case, as a strategy of additive to control the crystallinity of polymers, Mun et al. blended a conjugated carbon nanoring, cycloparaphenylenes (CPP), to the conjugated polymer semiconductor to tune the dynamic behaviors of the polymer.[132] As CPP was added to the polymer, long-range crystalline order was reduced, thereby enhancing polymer dynamic motion (Figure 12c). In addition, CPP improved the device performance by lowering the contact resistance and increasing charge transportation. Subsequently fabricated stretchable TFTs with CNT electrodes and PDMS dielectric layer could operate without any dramatic degradation under 100% strain and 1000 stretching cycles with 25% strain.

Although the two main strategies mentioned above enable the realization of intrinsically stretchable organic TFTs, there are some limitations on fine-tuning of stretchability and electrical characteristics of organic semiconductors simultaneously due to constraints of molecular engineering. To overcome those limitations, researchers utilize conjugated polymer and elastomer composites to give stretchability to the semiconductors. Xu et al. reported a composite-based stretchable organic semiconductor that conjugated polymers in composite was unidirectionally ordered by a solution-shearing process (Figure 12d).[134] A nanofiber structure of conjugated polymer in composite was achieved from a nanoconfinement effect induced by a phase separation of elastomer and conjugated polymer. In addition, polymer chains in the composite were aligned and elongated by the solution-shearing process with the intensive unidirectional flow generated from microtrenches of the coating blade. Due to the multi-scale ordering and alignment of conjugated polymers in stretchable composite, charge carrier mobility and stretchability of stretchable semiconductors were greatly enhanced. As a result, fabricated stretchable organic TFTs with CNT electrodes and SEBS dielectric layer can operate without any failures under 100% strain and 1000 stretching cycles with 50% strain. Furthermore, Wang et al. introduced patterned elastomer layers with tunable stiffness to protect composite-based organic semiconductors from the applied strain.[135] By locally tuning the cross-linking density of the elastomer, stiff parts of the substrate were utilized as strain-relief regions similar to rigid island structures (Figure 12e). By combining two approaches of strain-relief structures and composite of elastomer/conjugated polymer, the fabricated intrinsically stretchable organic TFTs showed strain-insensitivity with the change of performance less than 5% under 100% strain.

As described above, organic semiconductors have significant advantages of controlling their mechanical and electrical properties by engineering molecular structures or blending several organic materials. These organic TFTs can achieve high stretchability without any complicated approaches such as island-bridge structures or kirigami patterns. On the other hand, organic semiconductors have disadvantages of vulnerability to chemicals, UV irradiation, or plasma treatments. However, these limitations are also becoming overcome by selective molecular crosslinking of organic materials. Recent work reported high-density intrinsically-stretchable transistors and circuits with all-polymer-materials by direct optical microlithography patterning with channel length of 2 μm and a density of 42 000 transistors cm^{-2}.[136] The electrical properties of polymer semiconductors are lower than inorganic- and CNT-based counterparts, but the intrinsically-stretchable polymer transistor array can be a potential candidate for wearable and electronic skin devices.

5. Stretchable Light-Emitting Devices

Stretchable light-emitting devices stably maintain light-emission under various deformations, providing new design form-factors for deformable electronics, wearable electronics, and soft robotics. There are two main strategies to demonstrate stretchable electroluminescent devices: adapting island-bridge configuration to the rigid and flexible electroluminescent devices and developing intrinsically stretchable electroluminescent devices. Based on island-bridge configurations, various light-emitting devices are integrated with stretchable interconnects that can accommodate external stresses. When external strain is applied, the strain is concentrated into stretchable interconnects, while the active devices that are positioned in the strain-free region can be effectively protected, exhibiting improved mechanical stability. In the case of intrinsically stretchable electroluminescent devices, approaches are similar to the development of intrinsically stretchable TFTs, such as blending additives to induce phase separation or making a composite of light-emitting materials with elastomers or low glass transition temperature polymers to give stretchability. Each strategy for structure and material engineering to achieve desired stretchability can be determined based on the target light-emitting materials. In this section, the representative strategies for the development of stretchable light-emitting devices will be presented with the various light-emitting materials and devices,

including 1) inorganic, 2) polymer (organic), and 3) perovskite light-emitting materials and LEDs, and 4) ACEL.

5.1. Inorganic LEDs

Inorganic LEDs (ILEDs) are representative electroluminescent devices that consist of inorganic compounds of 'III-V' or 'II-VI' materials. Combinations of Ga, In, N, and P such as GaN[137] and GaAs[138] work as a p–n junction with radiative recombination energy released in light. ILEDs generally have great light efficiency, long lifetime, and environmental stability compared to other light-emitting devices. However, intrinsic rigidity from inorganic materials is a critical obstacle to morphological change, therefore, proper integration methods with polymeric substrates are highly required to overcome a significant modulus mismatch.

The island-bridge configuration is an early method to integrate ILEDs with stretchable substrates.[139–141] The epitaxially grown ILEDs on wafer inevitably require additional processes to transfer them to other substrates. Park et al. utilized elastomeric stamp with kinetic control of adhesion in order to transfer ILEDs array mesh to a pre-strained PDMS substrate. The Ti/SiO_2 deposited island structures successfully incorporated with the elastomeric substrate. When the external strain was applied to the PDMS, the chemically bonded islands were not deformed, while the serpentine electrodes deformed out-of-plane to accommodate the strain, ensuring a reliable operation of the stretchable ILEDs array under a uniaxial strain up to ≈22%. (**Figure 13**a).[139] Similarly, Byun et al. also systematically fabricated strain-engineered stretchable platforms by adopting inkjet-printed rigid islands (PRIs). PMMA ink was formulated by changing its molecular weight and the number of printing layers was optimized for the robustness of the islands. After printing the PRIs, another top PDMS was covered to increase stability, preventing the PRIs from being fractured under a uniaxial strain of ≈40%. Then, various inorganic chips, including ILEDs, integrated onto strain-free, engineered PRI employing epoxy adhesives, enabling on-skin electronics. Moreover, the inkjet printing modifies island patterns and interconnects freely, enhancing the degree of freedom of stretchable circuit formation. (Figure 13b).[104]

The island-bridge structures effectively suppressed the deformation around ILEDs. However, the abrupt difference of elastic modulus can induce significant strain concentration at the interfaces, which causes delamination of devices and plastic deformation of substrates. To overcome failure issues, Biswas et al. embedded whole circuit into Ecoflex with very low Young's modulus without additional island structure. The whole circuit components including ILEDs array, stretchable electrodes, and VIAs were fabricated on the PI substrates, and then a low melting point solders were coated on the contact pads, where ILEDs array would be transferred by pick-and-place assembly techniques. The ILEDs circuit on the PI substrate was fully embedded by Ecoflex over molding, and then the PI substrate was partially perforated by electron cyclotron resonance plasma etching, enabling the circuits to be stretchable. The embedded circuits could be stretched up to 260% and showed high deformability under various 3D guided shapes (Figure 13c).[100]

The conventional bonding that utilizes metal soldering or rigid adhesive with high elastic modulus ensures robust bonding, but they are simultaneously vulnerable to mechanical deformation. Therefore, Hwang et al. fabricated intrinsically stretchable anisotropic conductive films (S-ACF) that can directly interconnect ILEDs and substrates. The polystyrene-block-poly(ethylene-ran-butylene)-block-polystyrene-graft-maleic anhydride (SEBS-g-MA) was used as a free-standing and stretchable film. The periodically arranged metal particles were embedded in the S-ACF for electrical connection. The boding of ILEDs was acquired by modifying the bottom surface wettability of ILEDs with 3-aminopropyltriethoxysilane (APTES). The MA-NH_2 amide bond with SEBS-g-MA template enabled stretchable ILEDs array with high stretchability of 70% (Figure 13d).[142]

Several integration methods have been proposed to overcome large modulus difference in the heterogeneous interface between rigid ILEDs and soft substrates. Although the integration concept was proved for a few ILEDs, the successiveness and repeatability to integrate a large number of ILEDs and other electronic devices were not identified. Moreover, since the size of the ILEDs has minimized, a systematic integration, including mechanical and electrical connection, applicable to fine-pitch ILEDs should be further investigated.

5.2. Organic Light-Emitting Devices

Organic light-emitting devices composed of organic materials with electroluminescent property are one of reliable candidates for light-emitting components in stretchable electronics due to its intrinsic softness with mechanical robustness[143–148] and processability on deformable substrates with low-temperature process.[149,150] However, the stretchable organic light-emitting devices should simultaneously sustain multiple axial strains. In this regard, various approaches have been reported to achieving stretchable organic light-emitting devices: using wrinkled structure and serpentine electrodes, island-bridge structures, and intrinsically stretchable materials.

Wrinkled structure has been introduced as a representative method for the fabrication of stretchable devices. To implement the wrinkled structure on elastomeric platform, the stretchable OLEDs were fabricated on pre-stretched elastomer such as PDMS or PU. When pre-stretched platform was released, directional wrinkles were implemented depending on the direction of applied prestrain. When external strain was applied along the wrinkle direction, the structure on the display was unfolded without physical damage. Using this structure, Yokota et al. attached ultrathin OLEDs on pre-stretched elastomer (**Figure 14**a).[151] Ultraflexible OLEDs with thin encapsulation layers were fabricated on 1-μm-thick parylene films, showing stable operation under ambient condition. After lamination process on pre-stretched elastomeric substrate, the device could maintain its electroluminescent performance even after 1000 cycles with 60% strain. The encapsulated stretchable display with ultrathin structure with total thickness of 3 μm could be easily laminated on human skin without degradation, thereby applied to wearable device which can visualize data extracted from human body. Yin et al. expanded the

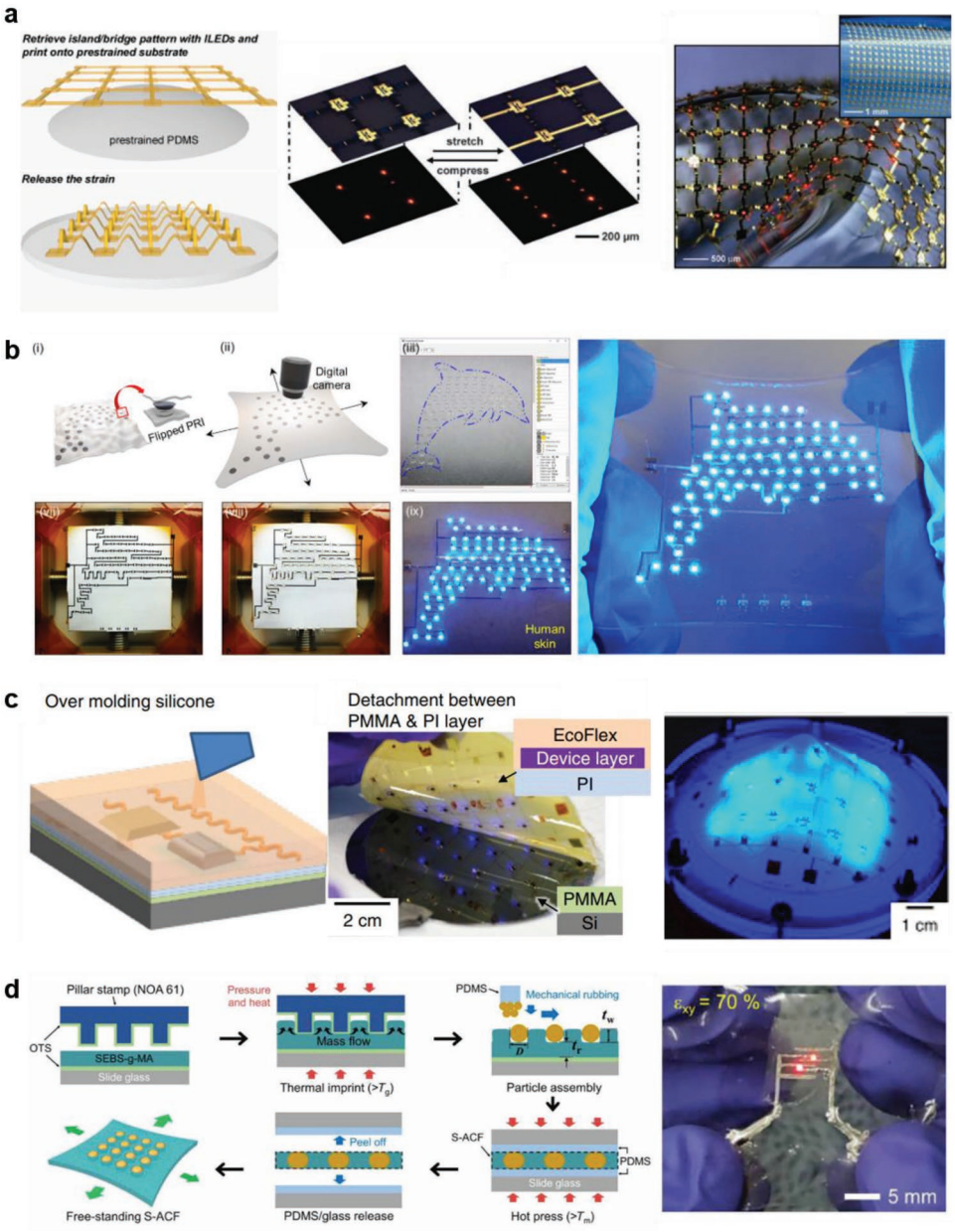

Figure 13. Stretchable ILEDs. a) Island-bridge-based stretchable ILEDs fabricated by transferring an ILED array mesh to a PDMS substrate. Reproduced with permission.[139] Copyright 2009, American Association for the Advancement of Science. b) Customizable stretchable platforms, fabricated by inkjet printing of PRIs and electric circuits, and epoxy bonding of ILEDs. Reproduced with permission.[104] Copyright 2017, Springer Nature. c) Stretchable multilayered circuits fabricated by embedding lithographically fabricated electric circuits into Ecoflex. Reproduced with permission.[100] Copyright 2019, Springer Nature. d) Stretchable ACFs as direct interfaces for the ILEDs and stretchable substrates. Reproduced with permission.[142] Copyright 2021, American Association for the Advancement of Science.

stretchability of devices to 2D direction with random-located buckling networks on the surface of OLEDs (Figure 14b).[152] After attaching ultraflexible OLEDs on 100% pre-stretched elastomer with both 2D directions, the random networks of micro-scale buckling structures were formed after releasing process. Through this approach, OLEDs was operated without degradation even with 50% of 2D strain. On the other side, Jeong et al. focused on the image distortion of stretchable OLEDs with wrinkle structures (Figure 14c).[153] Unlike the other approaches for the stretchable OLEDs with wrinkled structures, the OLEDs were directly fabricated on pre-stretched elastomers without lamination of plastic substrate. After fabrication of OLEDs and releasing process, the mean values of size of wrinkles were all less than 8 μm and those micro-wrinkles demonstrated both distortion-free pixels and high stretchability.

By implementing stretchable OLEDs on strain-engineered platform with serpentine shaped stretchable electrodes, Lim et al. reported another promising approach based on lamination

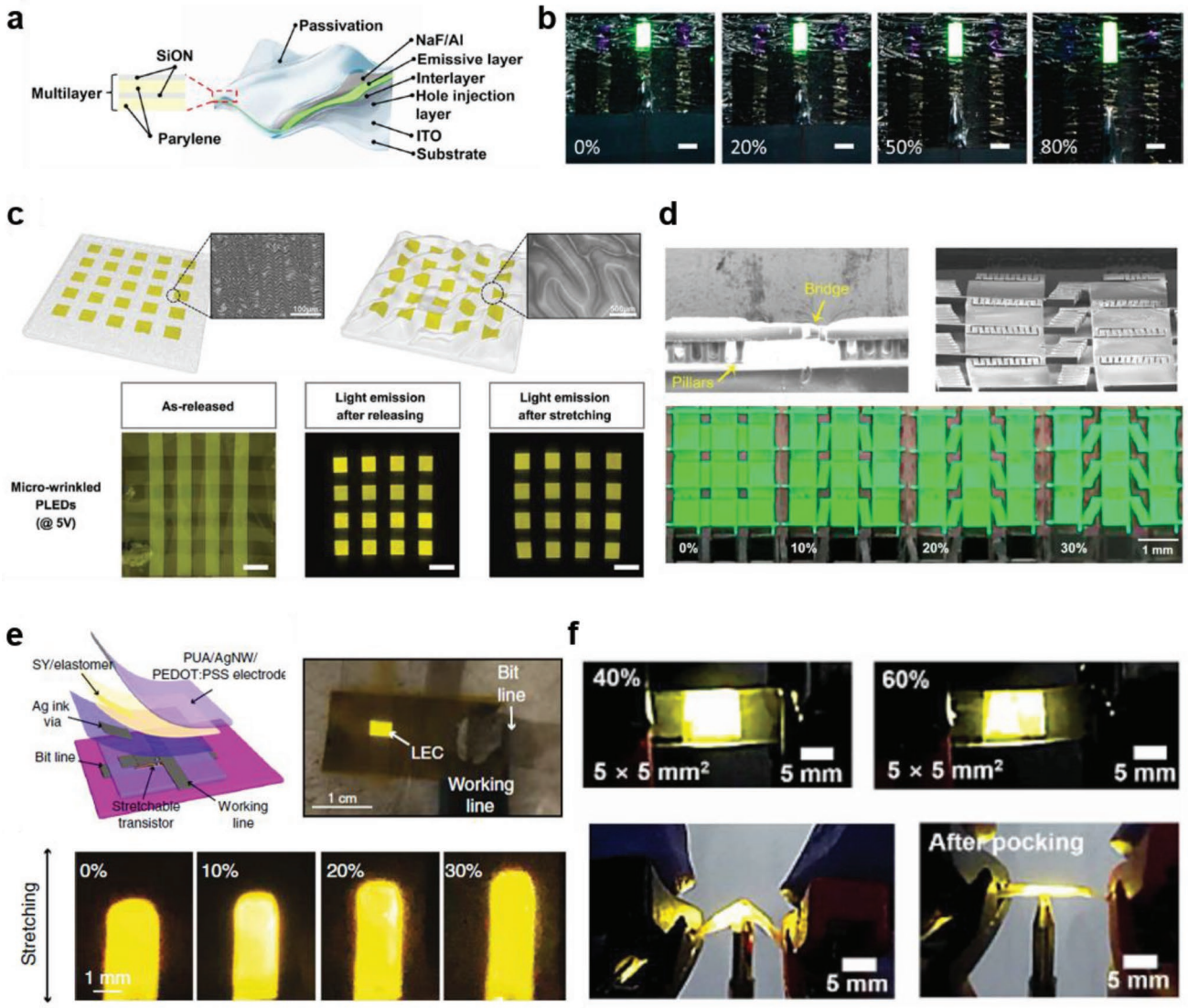

Figure 14. Stretchable organic light-emitting devices. a) Schematic of ultraflexible OLEDs with passivation layers. Reproduced with permission.[151] Copyright 2016, American Association for the Advancement of Science. b) Images of 1D stretchable OLEDs at strains of 0-80%. Reproduced with permission.[152] Copyright 2016, American Chemical Society. c) Schematic of imperceptible/macroscopic wrinkles in stretchable OLEDs, and demonstration of distortion-free pixel arrays. Reproduced with permission.[153] Copyright 2020, Wiley-VCH. d) Cross-sectional and tilted-view SEM image of a stretchable substrate, and images of stretchable OLEDs with strains of 0–30%. Reproduced with permission.[62] Copyright 2020, American Chemical Society. e) Schematic layout and optical image of stretchable OLEC pixels driven by stretchable transistors, and images of a single OLEC pixel with different strains. Reproduced with permission.[70] Copyright 2020, Springer Nature. f) Images of relative luminance change in devices under various 1D strains and 3D-deformed OLEDs. Reproduced with permission.[71] Copyright 2021, American Association for the Advancement of Science.

of 3D island-bridge structures.[62] Micropillar arrays placed on PDMS substrate were laminated with OLEDs on SU-8 substrate, therefore pillars supported the OLED pixels (Figure 14d). In addition, OLED pixels were connected with the bridges with serpentine electrodes. Under the external strain, the serpentine electrodes were stretched while pillars attached with PDMS pixels were maintained its spacing. Because the mechanical strain was dissipated to the serpentine electrodes and PDMS substrate, the OLED arrays were reliably stretched up to 35% without any image distortion.

Although applying island-bridge structures on OLEDs is an efficient method for implementation of reliable stretchable electroluminescent devices, intrinsically stretchable OLEDs with novel material designing have a great deal of attention. Liu et al. suggested intrinsically stretchable AM organic light-emitting electrochemical cell (OLEC) array (Figure 14e).[70] AgNW-coated polyurethane acrylate (AgNW-PUA) was used as anodes and cathodes, and optimized blend of light-emitting materials was adopted for better stretchability. Fabricated OLECs were stable at 30% strain and vertically connected with stretchable polymer semiconductors to fabricate AMOLECs. To further enhance stretchability, Kim et al. blended Triton X-100 surfactant with active layers (Figure 14f).[71] When the surfactant was blended with emissive materials, they interrupted

interchain reactions between emissive materials, thereby making layers stretchable. In addition, when Triton X-100 was mixed with PEDOT:PSS which was used as hole transport layer (HTL), the surfactant hinders the interactions between PEDOT and PSS, so the hole transport can be enhanced and Young's modulus is decreased. The fabricated intrinsically stretchable OLEDs maintained their performance at 40% strain, and showed stable emission even at the strain of 80%.

With promising advantages of OLEDs such as mechanical reliability and possibility of large area process, various approaches were adopted for fabrication of stretchable OLEDs. However, stretchable encapsulation which provides long-term stable operations even under the mechanical strain is a challenge for commercialization. Furthermore, fabrication of large area OLEDs arrays and linkage with stretchable driving circuit should be next steps for stretchable OLED displays.

5.3. Metal-Halide Perovskites LEDs

Metal-halide perovskites (MHP) became promising light-emitting materials since the first development of MHP LEDs in 2014.[154] The narrow emission linewidth (<20 nm) of MHP can achieve ultrahigh color purity with the color gamut ratio >140%. MHP is commonly composed of ABX_3 forming a cubic structure, where A is an organic ammonium or an alkali metal ion, B is a transition metal cation and X is a halide anion.

Controlling dimensionality of MHP from 3D, 2D, 1D to 0D with dimension decreased from micrometer-scale down to nanometer-scale is the most effective approach to confine the charge carriers and to increase the possibility of radiative recombination. Hence, using 0D nanocrystals could achieve highly efficient LEDs on a glass substrate with EQE boosted >23.4%.[155] However, the rigid nature of MHP nanocrystals makes it difficult for stretchable applications.

Introducing the buckling structure to the device with thin substrates will significantly reduce the strain experienced by the device, as the magnitude of the strain was proportional to the thickness of the substrate.[156] The AgNW percolation networks were embedded in the PI substrate (1–2 μm) to form an ultrathin transparent conductive electrode with excellent chemical stability against organic solvents.[157] After multiple successive solution processes and Al electrode deposition, the substrate was conformably attached to pre-strained 3M-VHB tape to create a buckling structure with a small bending radius of 70 μm (**Figure 15**a). The stretchable MHP-based LEDs showed a low turn-on voltage (V_{on}) of 3.2 V (Figure 15b), the maximum luminance of 3187 cd m^{-2} at 9 V, and can retain the device performance with tensile strain up to 50% (Figure 15c).

As an alternative to rigid MHP nanocrystals, methylammonium lead bromide ($MAPbBr_3$) polycrystalline precursors are mixed with an ion-conducting polymer with viscoelastic properties such as poly(ethylene oxide) (PEO) to reduce Young's modulus.[158] By mixing the conducting polymer PEDOT:PSS with 33 wt% of PEO, the highest conductivity of 35600 S m^{-1} was achieved and showed no significant change in conductivity under 20% of strain. The cathode was deposited on the composite emitter using eGaIn (Figure 15d). The stretchable MHP LEDs showed V_{on} = 2.4 V (Figure 15e), and the maximum luminance of 15960 cd m^{-2} at 8.5 V (Figure 15f). A similar approach has been made using $CsPbBr_3$ with the addition of PEO and poly(vinylpyrrolidone) (PVP).[159] The morphological analysis on the failure mechanism of the stretchable MHP LEDs showed that crack initiated at the perovskite layer and prorogated to the bottom electrode.[160] Therefore, improving the stretchability of the perovskite layer is the key for stretchable MHP LEDs.

Alternatively, an air-stable stretchable display has been achieved by the integration of the perovskite stretchable color conversion layer (SCCL) and the stretchable light-emitting devices.[161] Perovskite nanocrystals were dispersed in the elastomer due to the high compatibility between the ligand and the polymer matrix. The SCCL down-converts the blue emission from stretchable light-emitting devices and reemits it as green (Figure 15g). The PL intensity decreased by 29.8% at 100% strain and recovered to the initial state after releasing (Figure 15h). The stretchable light-emitting devices with SCCL show the stretchability of 180% (Figure 15i).

Despite approaches have been made to apply organic-inorganic hybrid perovskites for stretchable applications, more efforts are needed to increase both stretchability and device light-emitting efficiency with innovations in materials aspect.

5.4. ACEL Devices

ACEL devices are normally operated based on hot-electron impact on the light-emitting phosphors under a high electric field across the thick dielectric layer >10 μm. Phosphors are embedded in the stretchable dielectric layer with a high dielectric constant to reduce potential drop, and the dielectric layer is sandwiched between two stretchable electrodes. As there is no direct charge injection from the electrode to the phosphors, the conductivity of the electrode for the ACEL devices is lower than that of other LEDs.

To increase the stretchability of the ACEL devices, an ionic conductive hydrogel is incorporated as a stretchable electrode. With the application of voltage, charges in the electrode are separated at the contact/hydrogel interface over nanometers, which can create large capacitance on the order of 10^{-1} F m^{-2}.[162] Hygroscopic lithium chloride was adopted as the ionic conductor with high conductivity of 10 S m^{-1}, while stretchable polyacrylamide was used as the elastomer matrix.[163] The low elastic modulus of the hydrogel allows the free stretching of the device without delamination at the interface (maximum strain ≈ 480%). The device can be operated at 700 Hz under ≈25 kV cm^{-1} with a luminous efficacy of 43.2 mlm W^{-1}. The matrix with an 8 × 8 array of 4-mm pixels has been fabricated using the replica molding technique, which can also undergo stretching, rolling, folding, and wrapping.

As an alternative to the molding technique, a stretchable multicolor display can be prepared using the transfer printing method. Phosphors mixed with inks can be photopatterned first and then dry transferred to the dielectric layer using a thermal release tape. Multiple cycles of transfer printing allow the assembly of multicolor pixels on the large dielectric.[164]

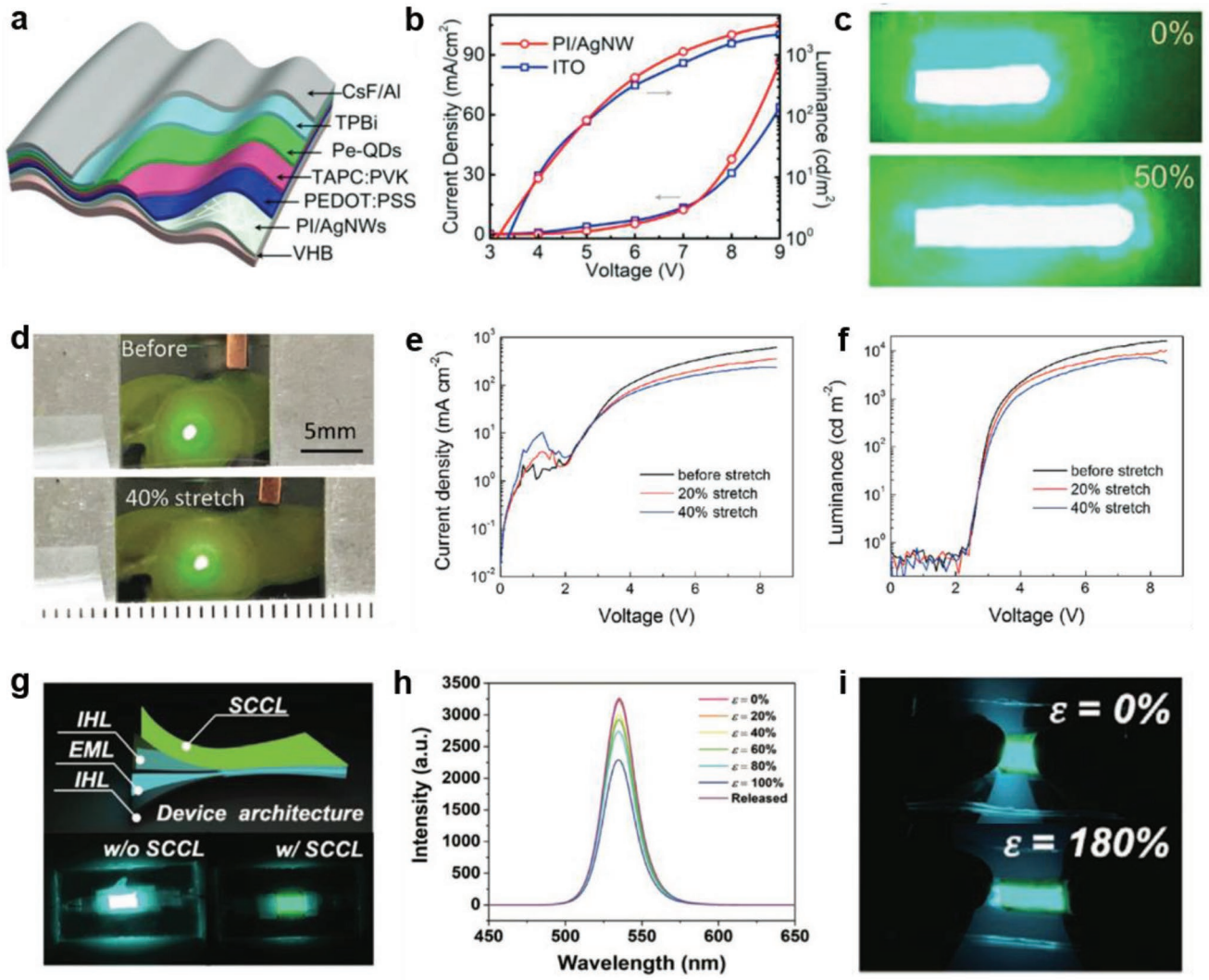

Figure 15. Stretchable perovskite LEDs. a) Device structure, b) current density (*I*)–voltage (*V*)–luminance (*L*), and c) digital images of geometrically stretchable perovskite quantum dot LEDs. Reproduced with permission.[157] Copyright 2019, Wiley-VCH. d) Digital images, and e) *I*–*V* and f) *L*–*V* characteristics, of intrinsically stretchable perovskite LEDs. Reproduced with permission.[158] Copyright 2017, Wiley-VCH. g) Device structure and digital images of stretchable LEDs before and after integration with perovskite stretchable color conversion layer (SCCL). h) PL spectra of the SCCL under uniaxial tensile strain. i) Digital images of the stretchable LED integrated with the SCCL under tensile strains of up to 180%. Reproduced with permission.[161] Copyright 2020, Wiley-VCH.

The ionic conductive hydrogel can also be constructed in the fiber shape to further boost the stretchability up to 800% (**Figure 16**a).[165] Two ellipse-shaped fibers wrapped by ZnS phosphors and elastomer composite to display programmable pattern. The electroluminescent layer also serves as the protecting layer for the hydrogel electrode. The stretchable light-emitting fiber was woven into a stretchable textile display. Also, owing to the high stretchability of hydrogel that can sustain repetitive stretching to 700% for 1000 cycles, another ACEL device can undergo tensile strain up to 700% with maximum luminance = 95 cd m^{-2} (Figure 16b).[166]

Different from the monotonic increase in light emission of ionic conductive hydrogel-based ACEL under stretching, the percolation AgNW-based electrode showed a slight increase in emission intensity of 30% followed by a monotonic decrease in intensity with further stretching (Figure 16c).[167] The electric field concentrated on the AgNW decreased with a larger open area created between AgNWs under stretching, resulting in a decrease in the light intensity.[166] Hence, maintaining the high electric field under large deformation is greatly challenging especially for conventional transparent conductive electrodes based on low-dimensional materials and conducting polymers. Incorporation of dielectric particles such as $BaTiO_3$ can effectively enhance the electric field inside the stretchable light-emitting layer, which substantially increases the electroluminescent intensity (Figure 16d).[168]

In addition, the high operating voltage of stretchable ACEL devices is another issue that limits practical applications; this is caused by the low permittivity of the elastomer. Hence, approaches have been made to increase the permittivity of the

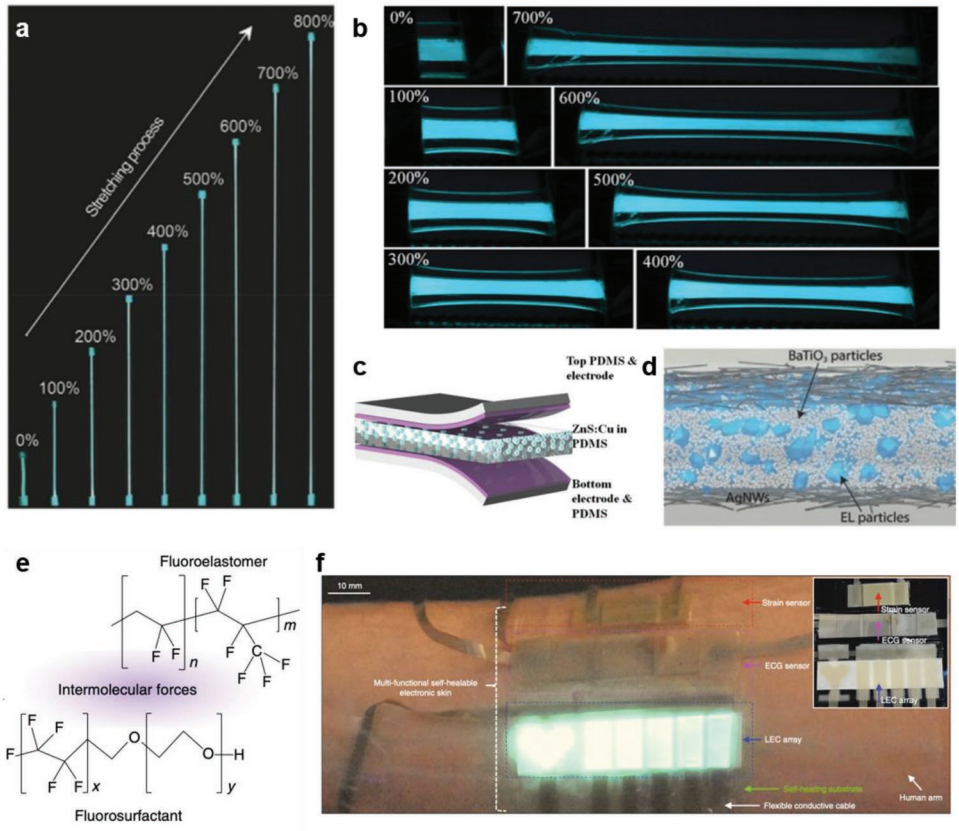

Figure 16. Stretchable ACEL devices. a) Digital images of a stretchable light-emitting fiber being stretched from 0% to 800%. Reproduced with permission.[165] Copyright 2018, Wiley-VCH. b) Digital images of stretchable ACEL devices stretched with different strains. Reproduced with permission.[166] Copyright 2016, Wiley-VCH. c) Device structure of ACEL device using AgNW as the electrode. Reproduced with permission.[167] Copyright 2015, Wiley-VCH. d) Schematic of ACEL device that incorporates $BaTiO_3$ particles. Reproduced with permission.[168] Copyright 2016, Wiley-VCH. e) Molecular structure of a fluoroelastomer with a non-ionic fluorinated surfactant for a healable and low-field illuminating optoelectronic stretchable device. Reproduced with permission.[169] Copyright 2019, Springer Nature. f) Multifunctional self-healable electronic skin device on skin with ACEL devices emitting a blue-green light. Reproduced with permission.[170] Copyright 2019, Springer Nature.

dielectrics. Poly(vinylidene fluoride)-based fluoroelastomer has also been developed as the dielectric materials that can maintain high permittivity and self-healing properties with the addition of non-ionic additives (Figure 16e). The ACEL has achieved a high brightness of 1460 cd m^{-2} at 2.5 V μm^{-1} with a maximum stretchability of 800%.[169] Besides adding $BaTiO_3$ particles into the light-emitting layer will also lead to higher permittivity and brightness (Figure 16f).[170] With above merits, stretchable ACEL devices have been successfully demonstrated for the electronic skin that is composed of strain and electrocardiogram sensors.

Given the fact that the goal of the stretchable ACEL display is the wearable application, both maximum luminance and device efficiency need to be improved to meet the requirement of low power consumption. More innovations in stretchable light-emitting materials are needed to further boost the efficiency.

6. Stretchable LED Matrix Arrays

In the display, multiple LED units that compose a matrix array are driven individually. Stretchable LED arrays in which geometrically or intrinsically stretchable structures, materials, and electronic devices (transistors and LEDs) technologies are integrated are manufactured and driven in PM or AM structures. In this chapter, the structure and characteristics of stretchable displays according to 1) PM and 2) AM operations, and 3) high-resolution full-color displays at the prototype level will be discussed.

6.1. PM Arrays

PM LED array, consisting of driver integrated circuit chip and light-emitting units, is operated by turning on the light-emitting units line by line, where each pixel is defined at the overlapped points of driving electrodes. Thus, PM structure can be obtained by simple manufacturing process without complicated circuit design. However, PM structure has limitations in increasing resolution or panel size due to large power consumption.[171] So, it has been utilized in limited areas, such as low-end and small-sized mobile applications. In this regard, stretchable PM array has been demonstrated to show 1) a novel unit technology for integrated stretchable systems, including stretchable light-emitting units, interconnects, and driving circuit chips,[30,172–175]

or 2) the concept of next-generation wearable displays, such as skin-attachable patch-type display and textile display integrated with health monitoring sensors.[11,104,176–178]

To demonstrate stretchable PM LED array, island-bridge structure with stretchable interconnects is a practical approach. In island-bridge structure, light-emitting units are located at rigid-island region, where the strain is suppressed by structural design, and they are interconnected by stretchable electrodes in bridge region, where the strain is released. Therefore, inherent stretchability of light-emitting unit become less essential in the island-bridge structure, enabling ILED to be utilized in stretchable PM LED array.[30,172–176] Thus, several studies have been implemented ILED-based PM array to demonstrate the feasibility of novel structural designs such as serpentines,[172] helical structures,[174] and intrinsically stretchable materials.[173]

Meanwhile, some research focused on fill factor of stretchable display beyond the stretchability itself.[30,175] Increasing stretchability has trade-off relationship between the fill factor of LEDs, deteriorating the resolution of display. Therefore, a double-layered modular design separating LED unit substrates and stretchable interconnectors (**Figure 17**a)[30] or 3D assembly with hidden pixel structure[175] has been suggested. Meanwhile, Byun et al. demonstrated a PM LED array on inkjet printing-based stretchable platform, including printed rigid island and wrinkled Ag interconnects in a fully-customizable way (Figure 17b).[104] By integrating ILED chips, microcontroller units, and other surface-mount device components on a rigid island-embedded stretchable platform, a 2-bit digital multiplier and temperature monitoring system were demonstrated on skin.

Stretchable PM LED array with island-bridge structures can also be made with thin-film-based LEDs such as OLED and quantum dot LED (QLED) to make them more flexible and conformal.[11,177] Therefore, real-time health monitoring patch that provided biological information on human skin in intuitive way has been reported. Lee et al. demonstrated integrated system of health monitoring patch with stretchable OLED array, photoplethysmography (PPG) heart rate sensor, processing modules, and batteries (Figure 17c).[11] Stretchable OLED array could be realized by modulus-engineered strain relief layer and micro-cracked interconnects, making compatible with lithography processes. Lee et al. also demonstrated a sensor-integrated

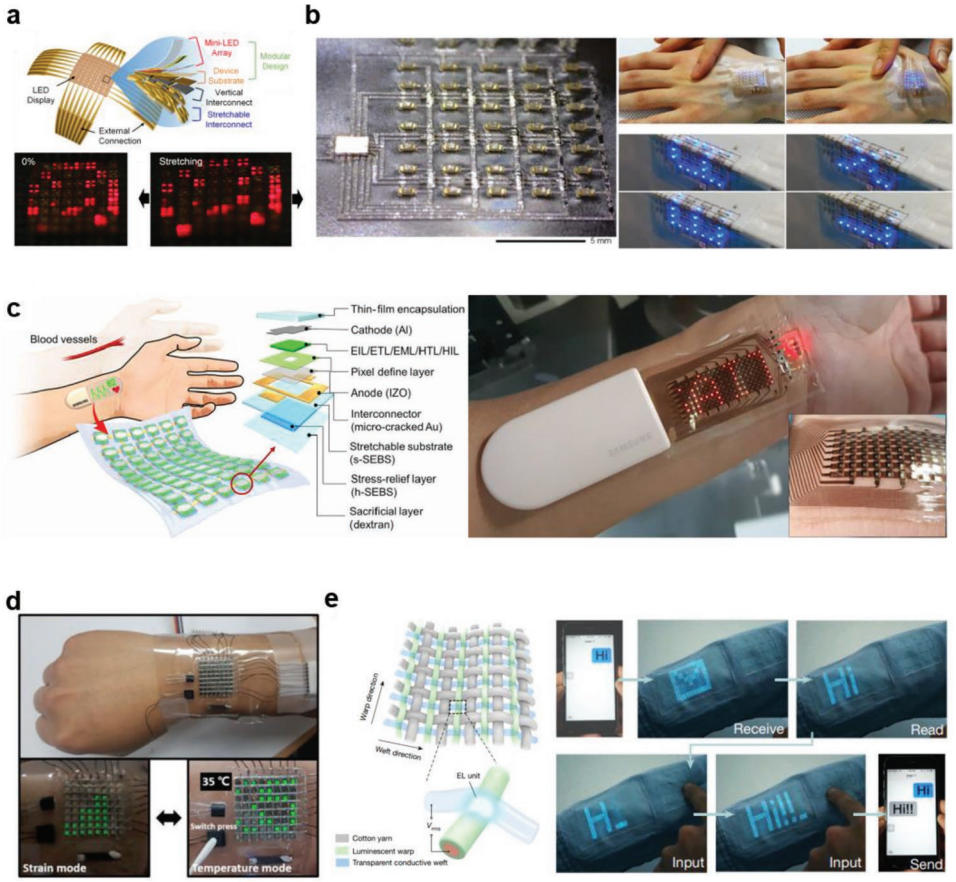

Figure 17. Stretchable PM LED array. a) Stretchable PM ILED array with high fill factor. Reproduced with permission.[30] Copyright 2022, American Chemical Society. b) Customizable inkjet printing-based stretchable PM ILED array. Reproduced with permission.[104] Copyright 2017, Springer Nature. c) Real-time health monitoring patch with stretchable OLED array and PPG sensor. Reproduced with permission.[11] Copyright 2021, American Association for the Advancement of Science. d) Stretchable QLED array for monitoring body movements and temperature. Reproduced with permission.[177] Copyright 2022, Elsevier. e) Textile-based functional systems with intrinsically stretchable ACEL fibers. Reproduced with permission.[178] Copyright 2021, Springer Nature.

stretchable QLED array to monitor body movement and skin temperature (Figure 17d).[177] QLED array deposited on NOA 63 islands were operated by stretchable LM interconnects.

Beyond island-bridge structure, fully stretchable PM array were demonstrated by using intrinsically stretchable ACEL device (Figure 17e).[178] By weaving stretchable conductive fiber and ZnS-coated conductive fiber, each electroluminescent pixel could be defined at contact points. While they require AC operation with high voltage, the feasibility of textile electronics integrated with displays and other electronic components has proven to broaden the applicable areas of stretchable electronics and more intuitive human-machine interfaces. Various next-generation stretchable technologies are expected to continuously be demonstrated through PM driving scheme, suggesting novel concept of wearable display.

6.2. AM Arrays

PM has a simpler structure and more straightforward operation than AM by applying voltage to each data and scan line sequentially to emit light at intersecting pixels. PM divides the scan time by the number of lines and sequentially applies voltage only for a short period of time. During one frame scan, only pixels to which voltages of the scan line and the data line are applied simultaneously emit light. Therefore, a high voltage is required to ensure high brightness during a short light emission time, which shortens the lifespan of the materials. In addition, as the number of lines increases, more time division is required, so there is a limitation in increasing resolution and size.

AM has transistors and storage capacitors in each pixel, so it is possible to store voltage for a certain period of time and maintain light emission for one frame. Also pixels are individually controlled using transistors of the backplane. Therefore, it is suitable for high-resolution large-area displays with advantages such as low-power operation, minimization of line crosstalk and flicker, fast response, and capable of compensation circuit configuration. The AM stretchable display is more challenging than the PM stretchable display because the mechanical stretchability of backplane circuits and their components (e.g., transistors and capacitors) should be improved. The development of AM stretchable display is still in the early stages and many breakthrough studies are required, but it is essential to produce a future high-resolution large-area stretchable display. A few stretchable AM LED arrays have been reported with the extrinsically stretchable geometries and rigid inorganic/organic LEDs or the intrinsically stretchable geometries and polymer LECs. Also, the mature high-mobility silicon transistors or the next-generation transistors that exploit oxide-, CNT-, or polymer–semiconductors have been used for driving AM LED arrays.

A 32 × 32 stretchable AM ILED array (13 ppi) was fabricated on an island-bridge patterned PI substrate with Cu serpentine interconnects.[179] A 2T-1C structure backplane composed of amorphous IGZO TFTs with a mobility ≈10 $cm^2 V^{-1} s^{-1}$ drives rigid ILED pixels. An LED pixel array was connected to a pixelated backplane with isotropic conductive adhesive and pick-and-place technique, then encapsulated with a thin TPU film. The LED chips array had uniform brightness, and showed flexibility and conformability on the complex surfaces without significant loss in the uniformity.

μ-LED refers to an ultrasmall LED with a size of less than 100 μm, and is attracting attention as a next-generation display based on high brightness, low power, high resolution, infinite contrast, fast response, wide color gamut, long lifespan, and stability in air and moisture. Also, fast-response and low-power single crystal Si-TFT with the high field-effect mobility (≈700 $cm^2 V^{-1} s^{-1}$) which is a desirable candidate for large-area and high-resolution display was used to drive μ-LED array. Stretchable AM array composed of 8 × 8 μ-LED and Si-TFT array was fabricated on the PDMS substrate using roll transfer printing (**Figure 18**a).[141] High mobility Si-TFTs and μ-LEDs were fabricated separately and sequentially transferred to a temporary glass substrate with a high yield and precise alignment. Then the Si-TFTs and μ-LEDs are connected by serpentine interconnects and transferred on a rubber substrate to demonstrate stretchable AM μ-LED array. The operation of μ-LED by Si TFT was controlled with high on-off current ratio (≈10^7). The rigid island part was firmly fixed on the PDMS substrate, and the serpentine interconnect at the neutral mechanical plane composed of metal layer sandwiched by polymer was slid on the PDMS surface to maintain the light emitting properties without deterioration even at 40% tensile strain (Figure 18b,c). Especially, the strain applied to the rigid island area was less than 0.1%, so the active components maintained the stable characteristics even after 200 stretching cycles at 40% strain.[141]

An island-bridge structure using intrinsically stretchable and straight interconnects instead of the serpentine interconnects can minimize the space occupied by the interconnects and thereby potentially increase the pixel density and aperture ratio. LM that exhibits small resistance change under strain can be a possible candidate instead of serpentine patterned flexible metal interconnects. SWCNT transistors and μ-LED arrays were fabricated on rigid polyethylene terephthalate (PET) islands embedded in Ecoflex substrates, and each island was connected by intrinsically stretchable and straight LM interconnects (Figure 18d).[180] In bending or stretching, the strain was concentrated in the Ecoflex region with low modulus (69 kPa), and the negligible strain was applied in the rigid PET island region with high modulus (2.0–2.7 GPa). For example, at a biaxial strain of 30%, Ecoflex is subjected to 240% strain, while PET is subjected to near 0% strain. Therefore, the 5 × 5 array SWCNT TFTs fabricated in the PET region shows a drain current change less than 4% at 30% biaxial strain. As a result, 5 × 5 AM μ-LED array fabricated with 10 μ-LEDs on each PET island did not show any deterioration in brightness under 30% biaxial strain and even after 1000 bending cycles (Figure 18e).

Compared to the geometrical strain engineering approaches, intrinsically stretchable electronic components can increase stretchability of AM LED array by reducing the portion of nonstretchable area and might be better for the electronic skin devices with smaller mechanical constraints on the skin. AMOLEC array integrated with intrinsically stretchable organic TFTs and intrinsically stretchable OLECs maintained brightness without deterioration at 30% tensile strain (Figure 18f).[70] In stretchable organic TFTs, the high modulus (>2.25 GPa) of the isoindigo moiety-containing polymer

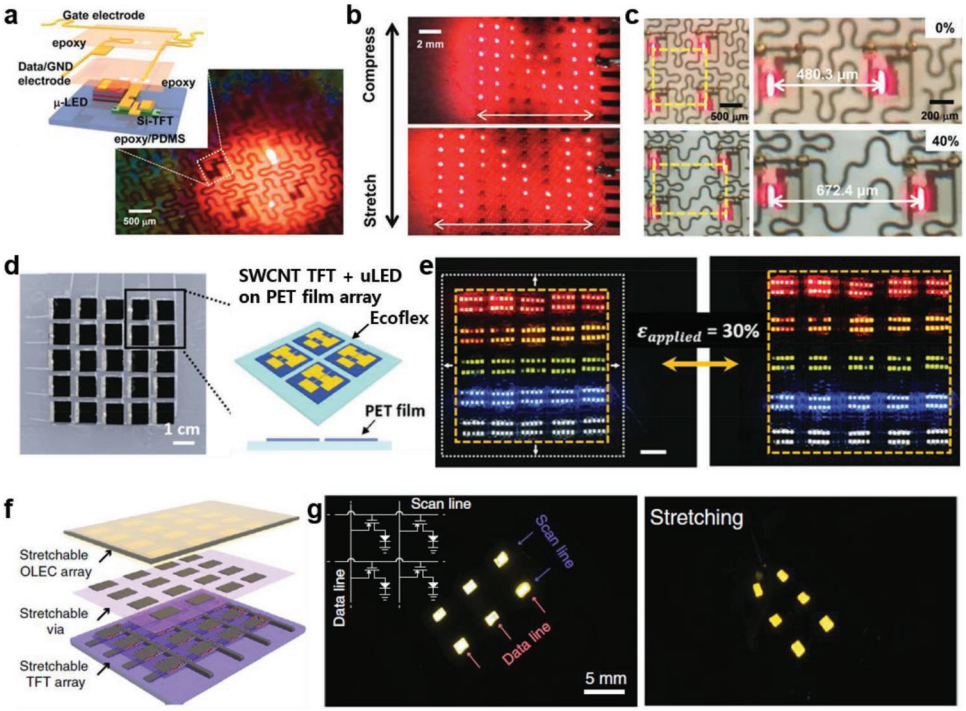

Figure 18. Stretchable AM LED array. a) Schematic and digital image of stretchable AM μ-LED array with single crystal Si-TFT backplane. b) Digital and c) optical images of stretchable AM μ-LED array with serpentine interconnects under strains of 0% and 40%. Reproduced with permission.[141] Copyright 2017, Wiley-VCH. d) Digital image and schematic of AM μ-LED array with SWCNT TFTs. e) Digital images of stretchable AM μ-LED array with intrinsically stretchable straight LM interconnects under strains of 0% and 30%. Reproduced with permission.[180] Copyright 2016, Wiley-VCH. f) Schematic and g) digital images of stretchable AMOLEC array that incorporates intrinsically stretchable OTFT and OLEC arrays. Reproduced with permission.[70] Copyright 2019, Springer Nature.

semiconductor, which cracks at 15% tensile strain was lowered to <0.75 GPa by blending an azide functionalized PDMS crosslinker. The crosslinked semiconductor film did not show cracks even at 100% tensile strain. In addition, crosslinkable stretchable insulators that have the modified hydroxyl groups of perfluoropolyether diols with dimethacrylate groups showed very negligible change in dielectric constant at 100% strain. With CNT stretchable gate, source and drain electrodes, the 5×5 transistor array showed less than one order of magnitude decrease in both the mobility and on-current, and minimal changes in leakage current even after 1000 repeated stretching at 100% strain.

In stretchable OLECs, the AgNWs-PUA electrode and PEDOT:PSS hole injection layer sandwiched the light emission layer that is composed of a blend of a light-emitting polymer (Super Yellow), an ion-conducting polymer (ethoxylated trimethylopropane triacrylate), and lithium trifluoromethane sulfonate, which enables formation of PIN junction in the light emission layer. The stretchable OLECs did not showed delamination, crack formation or degradation of current density under 30% strain. An intrinsically stretchable 2×3 AMOLEC array showed stable operation in bending, twisting, and stretching states (Figure 18g).[70]

Based on such stretchable PM and AM LED arrays introduced in this chapter, a large-area, high-resolution, and full-color stretchable display at a level closer to commercialization will be introduced in the next chapter.

6.3. High-Resolution Full-Color Displays

The development of high-resolution, high-density and full-color stretchable displays is mainly conducted by display industry because of the technological manufacturing maturity and capacity of fabrication facilities. Although many promising intrinsically stretchable light emitting devices introduced in the previous chapters are being actively developed, important factors for manufacturers and users such as processing yield, reliability, uniformity, efficiency, lifespan, and outdoor visibility must be considered to develop commercial products. Therefore, in the current stage, the island-bridge structure with established non-stretchable LEDs and transistors is a viable approach for developing a prototype stretchable displays.

PM stretchable LED array with 10×10 RGB LED package chips and serpentine copper interconnects on the PI substrate was developed in 2015 and demonstrated stable operation at 10% strain.[172] It proved the scalability by demonstrating 80×45 array PM LED display with 8.5 ppi. Also recently, a 2.7 in. and 42 ppi (96×60) stretchable display with 90×150 μm RGB LED chips was reported.[12] The LED chips are transferred by pick-and-place, stamp, and self-assembly techniques on the island-bridge-patterned flexible backplane (**Figure 19**a). Then, assembled backplane was subsequently transferred to and encapsulated by low modulus elastomer that are crosslinkable at low temperature and highly transparent.

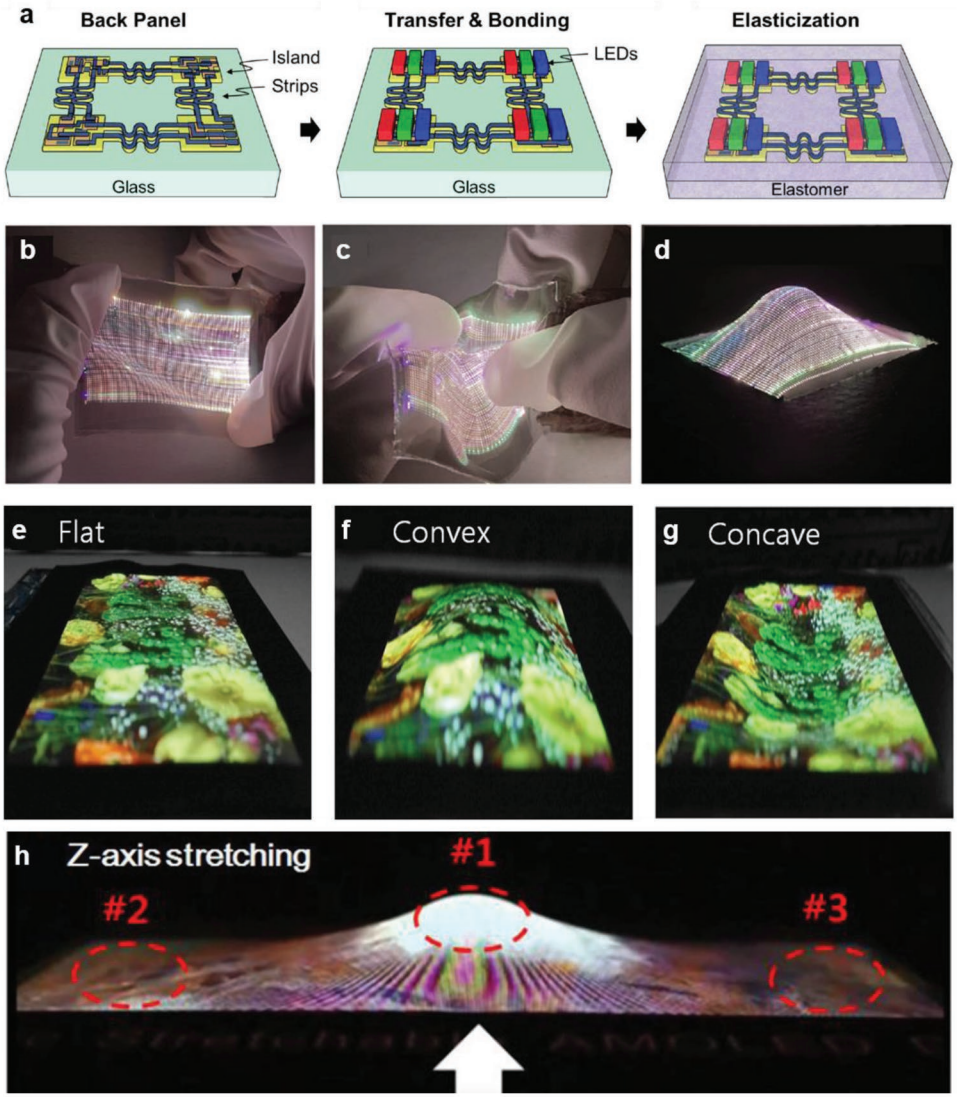

Figure 19. Stretchable high-density full color display. a) Schematics of fabrication process for a stretchable PM ILED display. Digital images of a stretchable PM ILED display under various deformations, including b) biaxial stretching, c) twisting, and d) poking. Reproduced with permission.[12] Copyright 2021, Wiley-VCH. Digital images of a 9.1 in. stretchable AM OLED display e) without deformation and with f) convex and g) concave deformations. Reproduced with permission.[9] Copyright 2017, Wiley-VCH. h) Digital image of a 14.1 in. stretchable AM OLED with selective z-axis stretching marked with a white arrow at #1 and without deformation at #2 and #3. Reproduced with permission.[29] Copyright 2019, Wiley-VCH.

The stretchability of the panel was simulated in terms of the ratio between island and bridge parts, the mechanical modulus of elastomer, and the width of interconnect and flexible substrate. To achieve high stretchability of panel, smaller island/bridge ratio, smaller width of interconnect, and lower modulus elastomer are preferred. The thickness of interconnects and flexible substrate have negligible effects. With 600 μm pixel pitch, the fabricated 42 ppi stretchable display panel demonstrated stable operation with biaxial stretching, free-from twisting, and convex deformation by poking (Figure 19b-d). This approach has a potential to be extended to 120 ppi stretchable display by employing 200 μm pixel pitch and μ-LED with smaller feature size of 20 μm.

AM A 9.1 in. full-color stretchable AMOLED display was demonstrated with island-bridge structure (Figure 19e).[9] The AM display exploits an OLED array which can be directly fabricate on the flexible substrate, and a flexible low-temperature polycrystalline silicon (LTPS) backplane that exhibits excellent properties for the high resolution and high frame rate display with higher carrier mobility (50–100 $cm^2\ V^{-1}\ s^{-1}$) than a-Si (1 $cm^2\ V^{-1}\ s^{-1}$), organic (1 $cm^2\ V^{-1}\ s^{-1}$), and metal oxide semiconductors (10 $cm^2\ V^{-1}\ s^{-1}$). The electrical stability of LTPS TFTs is usually suffered from mechanical deformations because both interface state density and grain boundary state density increase under bending and compression states. The induced instability of leakage current and threshold voltage changes charges stored in the capacitor, resulting in nonuniform brightness of pixel array. The strain applied to the LTPS TFTs was minimized by the geometrical approach of rigid island and serpentine bridge structure under 5% tensile strain. Therefore, the

TFTs maintained stable electrical characteristics of which the threshold voltage shift was lower than 0.1 V and the leakage current was reduced due to aging effect.

The mechanical modulus of the flexible backplane on the patterned PI substrate was 40 MPa which is in the similar range of soft rubber and is much lower than the modulus of PI film (4.2 GPa). Convex and concave shaped displays with 10 mm vertical displacement are demonstrated through thermoforming process by attaching the deformed displays on the patterned mold with thermoplastic sheet and adhesive (Figure 19f,g). Moreover, a 14.1 in. full-color stretchable AMOLED display was developed and it demonstrated no significant degradation under deformation with 45 mm of vertical height and even after 10000 stretching cycles with 5% strain (Figure 19h).[29]

7. Conclusion and Outlook

Stretchable displays, which can be freely bent in any direction and fit on any shape, are almost the end of the form factor innovation beyond flexible displays. Stretchable displays will maximize the portability of users' devices with multidirectional folding, enhance bodily comfort with skin-level moduli and softness, and enhance versatility through multi-curvature deformation. In the case of flexible displays, repeated deformation only occurs in limited bent areas and typically involves unidirectional folding. Moreover, flexible displays with bendable, foldable, and rollable form factors can minimize the actual elongation of active devices by placing them in a mechanically neutral plane. In contrast, stretchable displays involve elongation in length, which leads to the development of stretchable geometries and soft materials with stable electrical and optical properties under elongation to give displays a free-form factor.

This paper reviewed the current state of the research on structural designs and elastic materials with important features, including the conductors for interconnections, semiconductors for TFTs, and light-emitting materials for stretchable displays (**Figure 20**). Furthermore, stretchable display prototypes that have already been demonstrated based on the aforementioned technologies were discussed.

The various approaches that are actively being studied to develop a stretchable display all have their pros and cons. For example, as mentioned above, geometrically stretchable structures such as buckled structures and island-bridge structures, which are close to flexible, have the advantage that the existing semiconductor/display devices and manufacturing processes can be used. However, buckled structures are limited to producing highly integrated arrays with high stretchability, and island-bridge structures, which only increase the gap between pixels, can produce severe image distortion. Intrinsically stretchable structures can control the deformation of the pixel area by adjusting the Young's modulus. Thus, they can produce more natural image deformation and minimize the heterogeneity on the skin, but the development of materials with high performance, long-term stability, and high reliability is required.

For the commercialization of stretchable displays, the required specifications can be varied according to their target applications such as IoT devices, wearables, and automobiles. Nonetheless,

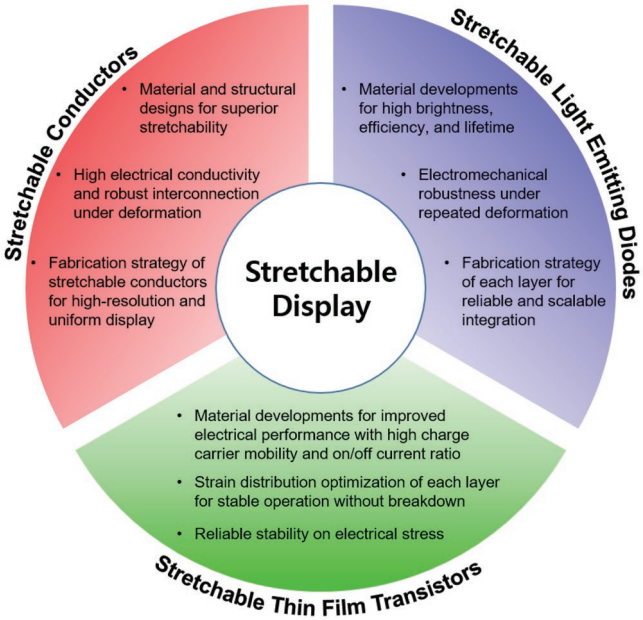

Figure 20. Strategies to develop materials and devices toward realization of stretchable display.

three key design parameters have been identified. First, the stretchability of the display should be higher than 30%, which approximately corresponds to a bending radius of 0.06 mm. Stretchable displays attached to human skin should be mechanically robust and operate stably under at least 30% strain, taking into consideration the strain variation on the skin.[6,11,181,182] Second, the resolution of the display should be higher than 200 ppi, accounting for the viewing distance and size of the display. Third, the display should have a high brightness at low operation voltages for outdoor visibility (e.g., 1000 cd m^{-2} at 5 V).

Consequently, for high-resolution stretchable displays, the conductivity of the stretchable conductor should be higher than 5×10^6 S m^{-1} to prevent a voltage drop across the narrow interconnect lines, which causes nonuniformity of the display. Considering the conductivity and the change in resistance under strain, metal-based stretchable conductors such as LMs, metal thin films, and metal nanomaterials are promising stretchable interconnects. LM has excellent deformability and decent conductivity (≈3.5×10^6 S m^{-1}),[183–185] but it is necessary to completely control the stability and flowability in the subsequent lamination process. In addition, stability must be ensured when the electronic devices are exposed to temperatures below the melting points (e.g., 15.5°C for eGaIn, –19 °C for Galinstan) of LMs.[183–185] For metal thin films, deformability can be achieved by introducing a serpentine structure in addition to having excellent conductivity. However, serpentine interconnects are expected to be much longer and narrower than straight interconnects, and metals with higher conductivities than those of conventional interconnects are required.[186] Metal nanomaterials such as AgNWs are promising next-generation stretchable interconnects because of their excellent conductivity and deformability. However, to apply them to mass production, it is necessary to achieve high uniformity over a large area (e.g., 6th generation mother glass, 1500 × 1850 mm).

For the operation of OLED pixels, driving and switching transistors require high charge carrier mobility >10 cm^2 V^{-1} s^{-1}, low off-current <10 pA, large on/off current ratio (>10^6), and low hysteresis of threshold voltage <0.1 V.[187,188] In addition, it may be necessary to analyze the distribution of strain required in the device in order to optimize the arrangement of the stretchable and rigid parts, so that the stretchable display and the rigid driving circuit and power source can be integrated. For example, the strain on skin near the wrist is approximately 30%, which is much higher than the strain on skin further from the wrist (<7%).[6,11] In addition, rigid parts are required for the protection and handling of devices in daily life, and rigid circuits and batteries can be integrated into hard parts. Flexible and stretchable driving circuits and batteries are also being actively researched.[85,102,194,106,135,136,189–193] This will enable the realization of all-parts-flexible/stretchable electronic devices. Additionally, the user should ideally be able to control the deformation of the devices in the desired situation. For this purpose, controlling the mechanical properties of the substrate using materials such as shape-morphing materials can be a suitable approach.[195–200]

Despite many research achievements, the specific form and applications of stretchable displays are still relatively vague. Recent studies developed deformable displays that could overcome the design constraints and be applied to the A-pillar and dashboard of an automobile, a health monitoring device attached to the skin, and smart fiber-based clothing. Thus, innovation activities to support various user scenarios and overcome technical obstacles are becoming more common. Further work still remains, including work to improve the display resolution, stretchability, and reliability, but it is expected that they will be on the market in the near future as next-generation form-factor displays.

Acknowledgements

Y.L. and H.C. contributed equally to this work. This work was supported by the Industry technology R&D program (20010427) funded By the Ministry of Trade, Industry & Energy (MOTIE, Korea). This work was also supported by the National Research Foundation of Korea (NRF) grant funded by the Korea government (Ministry of Science and ICT) (NRF-2016R1A3B1908431) and the Creative-Pioneering Researchers Program through Seoul National University (SNU). This work was also supported by Basic Science Research Program through the National Research Foundation of Korea (NRF) funded by the Ministry of Education (NRF-2021R1A6A3A03038934).

Conflict of Interest

The authors declare no conflict of interest.

Keywords

flexible displays, stretchable electronics, stretchable LEDs, stretchable materials, stretchable transistors, wearable displays

Received: July 1, 2022
Revised: October 4, 2022
Published online:

[1] M. H. Miraz, M. Ali, P. S. Excell, R. Picking, in *2015 Internet Technologies and Applications*, IEEE, Piscataway, NJ **2015**, pp. 219–224.
[2] S. Nahavandi, *Sustainability* **2019**, *11*, 4371.
[3] A. Shcherbina, C. Mattsson, D. Waggott, H. Salisbury, J. Christle, T. Hastie, M. Wheeler, E. Ashley, *J. Pers. Med.* **2017**, *7*, 3.
[4] B. Bent, B. A. Goldstein, W. A. Kibbe, J. P. Dunn, *npj Digital Med.* **2020**, *3*, 18.
[5] M. Etiwy, Z. Akhrass, L. Gillinov, A. Alashi, R. Wang, G. Blackburn, S. M. Gillinov, D. Phelan, A. M. Gillinov, P. L. Houghtaling, H. Javadikasgari, M. Y. Desai, *Cardiovasc. Diagn. Ther.* **2019**, *9*, 262.
[6] G. H. Lee, H. Kang, J. W. Chung, Y. Lee, H. Yoo, S. Jeong, H. Cho, J.-Y. Kim, S.-G. Kang, J. Y. Jung, S. G. Hahm, J. Lee, I.-J. Jeong, M. Park, G. Park, I. H. Yun, J. Y. Kim, Y. Hong, Y. Yun, S.-H. Kim, B. K. Choi, *Sci. Adv.* **2022**, *8*, eabm3622.
[7] S.-C. Jo, J.-H. Hong, *Dig. Tech. Pap. - Soc. Inf. Disp. Int. Symp.* **2021**, *52*, 741.
[8] J.-Y. Yan, J.-C. Ho, J. Chen, *Inf. Disp.* **2015**, *31*, 12.
[9] J.-H. Hong, J. M. Shin, G. M. Kim, H. Joo, G. S. Park, I. B. Hwang, M. W. Kim, W.-S. Park, H. Y. Chu, S. Kim, *J. Soc. Inf. Disp.* **2017**, *25*, 194.
[10] Q. Yang, P. Wang, F. Cao, L. Liu, Z. Liu, S. Shi, D. Wang, *Dig. Tech. Pap. - Soc. Inf. Disp. Int. Symp.* **2020**, *51*, 1142.
[11] Y. Lee, J. W. Chung, G. H. Lee, H. Kang, J.-Y. Kim, C. Bae, H. Yoo, S. Jeong, H. Cho, S.-G. Kang, J. Y. Jung, D.-W. Lee, S. Gam, S. G. Hahm, Y. Kuzumoto, S. J. Kim, Z. Bao, Y. Hong, Y. Yun, S. Kim, *Sci. Adv.* **2021**, *7*, eabg9180.
[12] J. Kang, H. Luo, W. Tang, J. Zhao, Y.-M. Wang, T. Tsong, P. Lu, A. Gupta, L. Zeng, Z. Zhang, J. Zhou, S. Wang, R. Ma, X. Chen, B.-G. Lee, Z. Yuan, P. Wei, X. Yu, *Dig. Tech. Pap. - Soc. Inf. Disp. Int. Symp.* **2021**, *52*, 1056.
[13] N. Matsuhisa, X. Chen, Z. Bao, T. Someya, *Chem. Soc. Rev.* **2019**, *48*, 2946.
[14] L. Yin, J. Lv, J. Wang, *Adv. Mater. Technol.* **2020**, *5*, 2000694.
[15] X. Hu, Y. Dou, J. Li, Z. Liu, *Small* **2019**, *15*, 1804805.
[16] D.-Y. Khang, H. Jiang, Y. Huang, J. A. Rogers, *Science* **2006**, *311*, 208.
[17] D.-H. Kim, J.-H. Ahn, W. M. Choi, H.-S. Kim, T.-H. Kim, J. Song, Y. Y. Huang, Z. Liu, C. Lu, J. A. Rogers, *Science* **2008**, *320*, 507.
[18] Y. Sun, W. M. Choi, H. Jiang, Y. Y. Huang, J. A. Rogers, *Nat. Nanotechnol.* **2006**, *1*, 201.
[19] M. Drack, I. Graz, T. Sekitani, T. Someya, M. Kaltenbrunner, S. Bauer, *Adv. Mater.* **2015**, *27*, 34.
[20] M. Kaltenbrunner, T. Sekitani, J. Reeder, T. Yokota, K. Kuribara, T. Tokuhara, M. Drack, R. Schwödiauer, I. Graz, S. Bauer-Gogonea, S. Bauer, T. Someya, *Nature* **2013**, *499*, 458.
[21] M. Kaltenbrunner, M. S. White, E. D. Głowacki, T. Sekitani, T. Someya, N. S. Sariciftci, S. Bauer, *Nat. Commun.* **2012**, *3*, 770.
[22] D. W. Kim, M. Kong, U. Jeong, *Adv. Sci.* **2021**, *8*, 2004170.
[23] B. Wang, S. Bao, S. Vinnikova, P. Ghanta, S. Wang, *npj Flexible Electron.* **2017**, *1*, 5.
[24] H. Li, Y. Cao, Z. Wang, X. Feng, *Opt. Mater. Express* **2019**, *9*, 4023.
[25] H. Jiang, D.-Y. Khang, J. Song, Y. Sun, Y. Huang, J. A. Rogers, *Proc. Natl. Acad. Sci. USA* **2007**, *104*, 15607.
[26] J. Song, H. Jiang, Z. J. Liu, D. Y. Khang, Y. Huang, J. A. Rogers, C. Lu, C. G. Koh, *Int. J. Solids Struct.* **2008**, *45*, 3107.
[27] S. Wang, J. Song, D.-H. Kim, Y. Huang, J. A. Rogers, *Appl. Phys. Lett.* **2008**, *93*, 023126.
[28] Y. Ma, K.-I. Jang, L. Wang, H. N. Jung, J. W. Kwak, Y. Xue, H. Chen, Y. Yang, D. Shi, X. Feng, J. A. Rogers, Y. Huang, *Adv. Funct. Mater.* **2016**, *26*, 5345.
[29] S. Kim, J. M. Shin, J.-H. Hong, G. S. Park, H. Joo, J. H. Park, G. Lee, J. Yoon, H. Shin, S.-C. Jo, C. Lee, J. Kwag, *Dig. Tech. Pap. - Soc. Inf. Disp. Int. Symp.* **2019**, *50*, 1194.

[30] N. Kim, J. Kim, J. Seo, C. Hong, J. Lee, *ACS Appl. Mater. Interfaces* **2022**, *14*, 4344.
[31] S. P. Lacour, S. Wagner, R. J. Narayan, T. Li, Z. Suo, *J. Appl. Phys.* **2006**, *100*, 014913.
[32] T. C. Shyu, P. F. Damasceno, P. M. Dodd, A. Lamoureux, L. Xu, M. Shlian, M. Shtein, S. C. Glotzer, N. A. Kotov, *Nat. Mater.* **2015**, *14*, 785.
[33] J. C. Yang, S. Lee, B. S. Ma, J. Kim, M. Song, S. Y. Kim, D. W. Kim, T.-S. Kim, S. Park, *Sci. Adv.* **2022**, *8*, eabn3863.
[34] Y. Zhang, S. Xu, H. Fu, J. Lee, J. Su, K.-C. Hwang, J. A. Rogers, Y. Huang, *Soft Matter* **2013**, *9*, 8062.
[35] R. Xu, Y. Zhang, K. Komvopoulos, *Mater. Res. Lett.* **2019**, *7*, 110.
[36] Y. Su, S. Wang, Y. Huang, H. Luan, W. Dong, J. A. Fan, Q. Yang, J. A. Rogers, Y. Huang, *Small* **2015**, *11*, 367.
[37] K. Sim, Y. Li, J. Song, C. Yu, *Adv. Mater. Technol.* **2019**, *4*, 1800489.
[38] K. Sim, S. Chen, Z. Li, Z. Rao, J. Liu, Y. Lu, S. Jang, F. Ershad, J. Chen, J. Xiao, C. Yu, *Nat. Electron.* **2019**, *2*, 471.
[39] Q. Hua, J. Sun, H. Liu, R. Bao, R. Yu, J. Zhai, C. Pan, Z. L. Wang, *Nat. Commun.* **2018**, *9*, 244.
[40] M. Jablonski, R. Lucchini, F. Bossuyt, T. Vervust, J. Vanfleteren, J. W. C. De Vries, P. Vena, M. Gonzalez, *Microelectron. Reliab.* **2015**, *55*, 143.
[41] K. Zhang, S. Kong, Y. Li, M. Lu, D. Kong, *Lab Chip* **2019**, *19*, 2709.
[42] T. Widlund, S. Yang, Y.-Y. Hsu, N. Lu, *Int. J. Solids Struct.* **2014**, *51*, 4026.
[43] S. Yang, E. Ng, N. Lu, *Extreme Mech. Lett.* **2015**, *2*, 37.
[44] M. Gonzalez, F. Axisa, M. Vanden Bulcke, D. Brosteaux, B. Vandevelde, J. Vanfleteren, *Microelectron. Reliab.* **2008**, *48*, 825.
[45] A. A. Norhidayah, A. A. Saad, M. F. M. Sharif, F. C. Ani, M. Y. T. Ali, M. S. Ibrahim, Z. Ahmad, *Procedia Eng.* **2017**, *184*, 625.
[46] J. Zhao, H. Hu, W. Fang, Z. Bai, W. Zhang, M. Wu, *J. Mater. Chem. A* **2021**, *9*, 5097.
[47] C. A. Silva, J. Lv, L. Yin, I. Jeerapan, G. Innocenzi, F. Soto, Y. Ha, J. Wang, *Adv. Funct. Mater.* **2020**, *30*, 2002041.
[48] Y. Wang, C. Zhu, R. Pfattner, H. Yan, L. Jin, S. Chen, F. Molina-Lopez, F. Lissel, J. Liu, N. I. Rabiah, Z. Chen, J. W. Chung, C. Linder, M. F. Toney, B. Murmann, Z. Bao, *Sci. Adv.* **2017**, *3*, e1602076.
[49] S. Choi, S. I. Han, D. Jung, H. J. Hwang, C. Lim, S. Bae, O. K. Park, C. M. Tschabrunn, M. Lee, S. Y. Bae, J. W. Yu, J. H. Ryu, S.-W. Lee, K. Park, P. M. Kang, W. B. Lee, R. Nezafat, T. Hyeon, D.-H. Kim, *Nat. Nanotechnol.* **2018**, *13*, 1048.
[50] S. Choi, J. Park, W. Hyun, J. Kim, J. Kim, Y. B. Lee, C. Song, H. J. Hwang, J. H. Kim, T. Hyeon, D.-H. Kim, *ACS Nano* **2015**, *9*, 6626.
[51] A. M. V. Mohan, N. Kim, Y. Gu, A. J. Bandodkar, J. You, R. Kumar, J. F. Kurniawan, S. Xu, J. Wang, *Adv. Mater. Technol.* **2017**, *2*, 1600284.
[52] K. Li, Y. Shuai, X. Cheng, H. Luan, S. Liu, C. Yang, Z. Xue, Y. Huang, Y. Zhang, *Small* **2022**, *18*, 2107879.
[53] R. Li, M. Li, Y. Su, J. Song, X. Ni, *Soft Matter* **2013**, *9*, 8476.
[54] L. Xiao, C. Zhu, W. Xiong, Y. Huang, Z. Yin, *Micromachines* **2018**, *9*, 392.
[55] T. Kim, H. Lee, W. Jo, T. Kim, S. Yoo, *Adv. Mater. Technol.* **2020**, *5*, 2000494.
[56] S. Gandla, H. Gupta, A. R. Pininti, A. Tewari, D. Gupta, *RSC Adv.* **2016**, *6*, 107793.
[57] N. Matsuhisa, M. Kaltenbrunner, T. Yokota, H. Jinno, K. Kuribara, T. Sekitani, T. Someya, *Nat. Commun.* **2015**, *6*, 7461.
[58] D. P. J. Cotton, A. Popel, I. M. Graz, S. P. Lacour, *J. Appl. Phys.* **2011**, *109*, 054905.
[59] R. Libanori, R. M. Erb, A. Reiser, H. Le Ferrand, M. J. Süess, R. Spolenak, A. R. Studart, *Nat. Commun.* **2012**, *3*, 1265.
[60] R. Moser, G. Kettlgruber, C. M. Siket, M. Drack, I. M. Graz, U. Cakmak, Z. Major, M. Kaltenbrunner, S. Bauer, *Adv. Sci.* **2016**, *3*, 1500396.
[61] I. M. Graz, D. P. J. Cotton, A. Robinson, S. P. Lacour, *Appl. Phys. Lett.* **2011**, *98*, 124101.
[62] M. S. Lim, M. Nam, S. Choi, Y. Jeon, Y. H. Son, S.-M. Lee, K. C. Choi, *Nano Lett.* **2020**, *20*, 1526.
[63] B. Jang, S. Won, J. Kim, J. Kim, M. Oh, H. Lee, J. Kim, *Adv. Funct. Mater.* **2022**, *32*, 2113299.
[64] Z. Zhang, W. Wang, Y. Jiang, Y.-X. Wang, Y. Wu, J.-C. Lai, S. Niu, C. Xu, C.-C. Shih, C. Wang, H. Yan, L. Galuska, N. Prine, H.-C. Wu, D. Zhong, G. Chen, N. Matsuhisa, Y. Zheng, Z. Yu, Y. Wang, R. Dauskardt, X. Gu, J. B. H. Tok, Z. Bao, *Nature* **2022**, *603*, 624.
[65] J. Mun, Y. Ochiai, W. Wang, Y. Zheng, Y.-Q. Zheng, H.-C. Wu, N. Matsuhisa, T. Higashihara, J. B. H. Tok, Y. Yun, Z. Bao, *Nat. Commun.* **2021**, *12*, 3572.
[66] S. Wang, J. Xu, W. Wang, G.-J. N. Wang, R. Rastak, F. Molina-Lopez, J. W. Chung, S. Niu, V. R. Feig, J. Lopez, T. Lei, S.-K. Kwon, Y. Kim, A. M. Foudeh, A. Ehrlich, A. Gasperini, Y. Yun, B. Murmann, J. B. H. Tok, Z. Bao, *Nature* **2018**, *555*, 83.
[67] Y. Zheng, S. Zhang, J. B. H. Tok, Z. Bao, *J. Am. Chem. Soc.* **2022**, *144*, 4699.
[68] Q. Zhang, J. Liang, Y. Huang, H. Chen, R. Ma, *Mater. Chem. Front.* **2019**, *3*, 1032.
[69] J. Xu, S. Wang, G.-J. N. Wang, C. Zhu, S. Luo, L. Jin, X. Gu, S. Chen, V. R. Feig, J. W. F. To, S. Rondeau-Gagné, J. Park, B. C. Schroeder, C. Lu, J. Y. Oh, Y. Wang, Y. Kim, H. Yan, R. Sinclair, D. Zhou, G. Xue, B. Murmann, C. Linder, W. Cai, J. B.-H. Tok, J. W. Chung, Z. Bao, *Science* **2017**, *355*, 59.
[70] J. Liu, J. Wang, Z. Zhang, F. Molina-Lopez, G.-J. N. Wang, B. C. Schroeder, X. Yan, Y. Zeng, O. Zhao, H. Tran, T. Lei, Y. Lu, Y.-X. Wang, J. B. H. Tok, R. Dauskardt, J. W. Chung, Y. Yun, Z. Bao, *Nat. Commun.* **2020**, *11*, 3362.
[71] J.-H. Kim, J.-W. Park, *Sci. Adv.* **2021**, *7*, eabd9715.
[72] H. Zhou, S. J. Han, A. K. Harit, D. H. Kim, D. Y. Kim, Y. S. Choi, H. Kwon, K. Kim, G. Go, H. J. Yun, B. H. Hong, M. C. Suh, S. Y. Ryu, H. Y. Woo, T. Lee, *Adv. Mater.* **2022**, *34*, 2203040.
[73] J. Noh, G.-U. Kim, S. Han, S. J. Oh, Y. Jeon, D. Jeong, S. W. Kim, T.-S. Kim, B. J. Kim, J.-Y. Lee, *ACS Energy Lett.* **2021**, *6*, 2512.
[74] N. Matsuhisa, S. Niu, S. J. K. O'Neill, J. Kang, Y. Ochiai, T. Katsumata, H.-C. Wu, M. Ashizawa, G.-J. N. Wang, D. Zhong, X. Wang, X. Gong, R. Ning, H. Gong, I. You, Y. Zheng, Z. Zhang, J. B. H. Tok, X. Chen, Z. Bao, *Nature* **2021**, *600*, 246.
[75] Y. Jiang, Z. Zhang, Y.-X. Wang, D. Li, C.-T. Coen, E. Hwaun, G. Chen, H.-C. Wu, D. Zhong, S. Niu, W. Wang, A. Saberi, J.-C. Lai, Y. Wu, Y. Wang, A. A. Trotsyuk, K. Y. Loh, C.-C. Shih, W. Xu, K. Liang, K. Zhang, Y. Bai, G. Gurusankar, W. Hu, W. Jia, Z. Cheng, R. H. Dauskardt, G. C. Gurtner, J. B. H. Tok, K. Deisseroth, et al., *Science* **2022**, *375*, 1411.
[76] S. Wang, J. Y. Oh, J. Xu, H. Tran, Z. Bao, *Acc. Chem. Res.* **2018**, *51*, 1033.
[77] Y. Lee, H. Zhou, T.-W. Lee, *J. Mater. Chem. C* **2018**, *6*, 3538.
[78] Y. Lee, J. Y. Oh, T. R. Kim, X. Gu, Y. Kim, G. N. Wang, H. Wu, R. Pfattner, J. W. F. To, T. Katsumata, D. Son, J. Kang, J. R. Matthews, W. Niu, M. He, R. Sinclair, Y. Cui, J. B. -H. Tok, T. Lee, Z. Bao, *Adv. Mater.* **2018**, *30*, 1704401.
[79] Y. Zheng, Z. Yu, S. Zhang, X. Kong, W. Michaels, W. Wang, G. Chen, D. Liu, J.-C. Lai, N. Prine, W. Zhang, S. Nikzad, C. B. Cooper, D. Zhong, J. Mun, Z. Zhang, J. Kang, J. B. H. Tok, I. McCulloch, J. Qin, X. Gu, Z. Bao, *Nat. Commun.* **2021**, *12*, 5701.
[80] B. Lee, H. Cho, K. T. Park, J.-S. Kim, M. Park, H. Kim, Y. Hong, S. Chung, *Nat. Commun.* **2020**, *11*, 5948.
[81] M. Yang, S. W. Kim, S. Zhang, D. Y. Park, C.-W. Lee, Y.-H. Ko, H. Yang, Y. Xiao, G. Chen, M. Li, *J. Mater. Chem. C* **2018**, *6*, 7207.

[82] Y. Joo, J. Byun, N. Seong, J. Ha, H. Kim, S. Kim, T. Kim, H. Im, D. Kim, Y. Hong, *Nanoscale* **2015**, *7*, 6208.
[83] H.-S. Liu, B.-C. Pan, G.-S. Liou, *Nanoscale* **2017**, *9*, 2633.
[84] Y. Ko, J. Oh, K. T. Park, S. Kim, W. Huh, B. J. Sung, J. A. Lim, S.-S. Lee, H. Kim, *ACS Appl. Mater. Interfaces* **2019**, *11*, 37043.
[85] S. Y. Hong, S. M. Jee, Y. Ko, J. Cho, K. H. Lee, B. Yeom, H. Kim, J. G. Son, *ACS Nano* **2022**, *16*, 2271.
[86] K.-Y. Chun, Y. Oh, J. Rho, J.-H. Ahn, Y.-J. Kim, H. R. Choi, S. Baik, *Nat. Nanotechnol.* **2010**, *5*, 853.
[87] Y. Yang, N. Sun, Z. Wen, P. Cheng, H. Zheng, H. Shao, Y. Xia, C. Chen, H. Lan, X. Xie, C. Zhou, J. Zhong, X. Sun, S.-T. Lee, *ACS Nano* **2018**, *12*, 2027.
[88] M. D. Bartlett, A. Fassler, N. Kazem, E. J. Markvicka, P. Mandal, C. Majidi, *Adv. Mater.* **2016**, *28*, 3726.
[89] C. Pan, E. J. Markvicka, M. H. Malakooti, J. Yan, L. Hu, K. Matyjaszewski, C. Majidi, *Adv. Mater.* **2019**, *31*, 1900663.
[90] A. F. Silva, H. Paisana, T. Fernandes, J. Góis, A. Serra, J. F. J. Coelho, A. T. Almeida, C. Majidi, M. Tavakoli, *Adv. Mater. Technol.* **2020**, *5*, 2000343.
[91] F. Krisnadi, L. L. Nguyen, Ankit, J. Ma , M. R. Kulkarni, N. Mathews, M. D. Dickey, *Adv. Mater.* **2020**, *32*, 2001642.
[92] H. Wang, Y. Yao, Z. He, W. Rao, L. Hu, S. Chen, J. Lin, J. Gao, P. Zhang, X. Sun, X. Wang, Y. Cui, Q. Wang, S. Dong, G. Chen, J. Liu, *Adv. Mater.* **2019**, *31*, 1901337.
[93] S. Park, G. Thangavel, K. Parida, S. Li, P. S. Lee, *Adv. Mater.* **2019**, *31*, 1805536.
[94] J. Y. Oh, S. Kim, H.-K. Baik, U. Jeong, *Adv. Mater.* **2016**, *28*, 4455.
[95] J. Park, H. Yoon, G. Kim, B. Lee, S. Lee, S. Jeong, T. Kim, J. Seo, S. Chung, Y. Hong, *Adv. Funct. Mater.* **2019**, *29*, 1902412.
[96] J. H. Lee, Y. R. Jeong, G. Lee, S. W. Jin, Y. H. Lee, S. Y. Hong, H. Park, J. W. Kim, S.-S. Lee, J. S. Ha, *ACS Appl. Mater. Interfaces* **2018**, *10*, 28027.
[97] M. Vosgueritchian, D. J. Lipomi, Z. Bao, *Adv. Funct. Mater.* **2012**, *22*, 421.
[98] S. P. Lacour, S. Wagner, Z. Huang, Z. Suo, *Appl. Phys. Lett.* **2003**, *82*, 2404.
[99] X. Huang, Y. Liu, H. Cheng, W.-J. Shin, J. A. Fan, Z. Liu, C.-J. Lu, G.-W. Kong, K. Chen, D. Patnaik, S.-H. Lee, S. Hage-Ali, Y. Huang, J. A. Rogers, *Adv. Funct. Mater.* **2014**, *24*, 3846.
[100] S. Biswas, A. Schoeberl, Y. Hao, J. Reiprich, T. Stauden, J. Pezoldt, H. O. Jacobs, *Nat. Commun.* **2019**, *10*, 4909.
[101] K. Li, X. Cheng, F. Zhu, L. Li, Z. Xie, H. Luan, Z. Wang, Z. Ji, H. Wang, F. Liu, Y. Xue, C. Jiang, X. Feng, L. Li, J. A. Rogers, Y. Huang, Y. Zhang, *Adv. Funct. Mater.* **2019**, *29*, 1806630.
[102] S. Xu, Y. Zhang, J. Cho, J. Lee, X. Huang, L. Jia, J. A. Fan, Y. Su, J. Su, H. Zhang, H. Cheng, B. Lu, C. Yu, C. Chuang, T. Kim, T. Song, K. Shigeta, S. Kang, C. Dagdeviren, I. Petrov, P. V. Braun, Y. Huang, U. Paik, J. A. Rogers, *Nat. Commun.* **2013**, *4*, 1543.
[103] H. Cho, Y. Lee, B. Lee, J. Byun, S. Chung, Y. Hong, *J. Inf. Disp.* **2019**, *21*, 41.
[104] J. Byun, B. Lee, E. Oh, H. Kim, S. Kim, S. Lee, Y. Hong, *Sci. Rep.* **2017**, *7*, 45328.
[105] E. Oh, T. Kim, J. Yoon, S. Lee, D. Kim, B. Lee, J. Byun, H. Cho, J. Ha, Y. Hong, *Adv. Funct. Mater.* **2018**, *28*, 1806014.
[106] Z. Huang, Y. Hao, Y. Li, H. Hu, C. Wang, A. Nomoto, T. Pan, Y. Gu, Y. Chen, T. Zhang, W. Li, Y. Lei, N. Kim, C. Wang, L. Zhang, J. W. Ward, A. Maralani, X. Li, M. F. Durstock, A. Pisano, Y. Lin, S. Xu, *Nat. Electron.* **2018**, *1*, 473.
[107] J. Byun, E. Oh, B. Lee, S. Kim, S. Lee, Y. Hong, *Adv. Funct. Mater.* **2017**, *27*, 1701912.
[108] Q. Jiang, S. Zhang, J. Jiang, W. Fei, Z. Wu, *Adv. Mater. Technol.* **2021**, *6*, 2000966.
[109] K. Park, D.-K. Lee, B.-S. Kim, H. Jeon, N.-E. Lee, D. Whang, H.-J. Lee, Y. J. Kim, J.-H. Ahn, *Adv. Funct. Mater.* **2010**, *20*, 3577.
[110] C. W. Park, J. B. Koo, C.-S. Hwang, H. Park, S. G. Im, S.-Y. Lee, *Appl. Phys. Express* **2018**, *11*, 126501.
[111] G. Cantarella, V. Costanza, A. Ferrero, R. Hopf, C. Vogt, M. Varga, L. Petti, N. Münzenrieder, L. Büthe, G. Salvatore, A. Claville, L. Bonanomi, A. Daus, S. Knobelspies, C. Daraio, G. Tröster, *Adv. Funct. Mater.* **2018**, *28*, 1705132.
[112] X. Li, M. M. Hasan, H.-M. Kim, J. Jang, *IEEE Trans. Electron Devices* **2019**, *66*, 2971.
[113] M. Kim, D. K. Brown, O. Brand, *Nat. Commun.* **2020**, *11*, 1002.
[114] P. L. McEuen, M. S. Fuhrer, Hongkun Park, *IEEE Trans. Nanotechnol.* **2002**, *1*, 78.
[115] D. Sun, M. Y. Timmermans, Y. Tian, A. G. Nasibulin, E. I. Kauppinen, S. Kishimoto, T. Mizutani, Y. Ohno, *Nat. Nanotechnol.* **2011**, *6*, 156.
[116] K. Chen, W. Gao, S. Emaminejad, D. Kiriya, H. Ota, H. Y. Y. Nyein, K. Takei, A. Javey, *Adv. Mater.* **2016**, *28*, 4397.
[117] S. H. Chae, W. J. Yu, J. J. Bae, D. L. Duong, D. Perello, H. Y. Jeong, Q. H. Ta, T. H. Ly, Q. A. Vu, M. Yun, X. Duan, Y. H. Lee, *Nat. Mater.* **2013**, *12*, 403.
[118] A. Chortos, G. I. Koleilat, R. Pfattner, D. Kong, P. Lin, R. Nur, T. Lei, H. Wang, N. Liu, Y.-C. Lai, M.-G. Kim, J. W. Chung, S. Lee, Z. Bao, *Adv. Mater.* **2016**, *28*, 4441.
[119] L. Cai, S. Zhang, J. Miao, Z. Yu, C. Wang, *ACS Nano* **2016**, *10*, 11459.
[120] W. Huang, H. Jiao, Q. Huang, J. Zhang, M. Zhang, *Nanoscale* **2020**, *12*, 23546.
[121] J. Liang, L. Li, D. Chen, T. Hajagos, Z. Ren, S.-Y. Chou, W. Hu, Q. Pei, *Nat. Commun.* **2015**, *6*, 7647.
[122] S. Y. Hong, M. S. Kim, H. Park, S. W. Jin, Y. R. Jeong, J. W. Kim, Y. H. Lee, L. Sun, G. Zi, J. S. Ha, *Adv. Funct. Mater.* **2019**, *29*, 1807679.
[123] T. Sekitani, Y. Noguchi, K. Hata, T. Fukushima, T. Aida, T. Someya, *Science* **2008**, *321*, 1468.
[124] C. Müller, S. Goffri, D. W. Breiby, J. W. Andreasen, H. D. Chanzy, R. A. J. Janssen, M. M. Nielsen, C. P. Radano, H. Sirringhaus, P. Smith, N. Stingelin-Stutzmann, *Adv. Funct. Mater.* **2007**, *17*, 2674.
[125] J. Y. Oh, S. Rondeau-Gagné, Y.-C. Chiu, A. Chortos, F. Lissel, G.-J. N. Wang, B. C. Schroeder, T. Kurosawa, J. Lopez, T. Katsumata, J. Xu, C. Zhu, X. Gu, W.-G. Bae, Y. Kim, L. Jin, J. W. Chung, J. B. H. Tok, Z. Bao, *Nature* **2016**, *539*, 411.
[126] G.-J. N. Wang, L. Shaw, J. Xu, T. Kurosawa, B. C. Schroeder, J. Y. Oh, S. J. Benight, Z. Bao, *Adv. Funct. Mater.* **2016**, *26*, 7254.
[127] C. Lu, W.-Y. Lee, X. Gu, J. Xu, H.-H. Chou, H. Yan, Y.-C. Chiu, M. He, J. R. Matthews, W. Niu, J. B.-H. Tok, M. F. Toney, W.-C. Chen, Z. Bao, *Adv. Electron. Mater.* **2017**, *3*, 1600311.
[128] Z. C. Smith, Z. M. Wright, A. M. Arnold, G. Sauvé, R. D. McCullough, S. A. Sydlik, *Adv. Electron. Mater.* **2017**, *3*, 1600316.
[129] J. Mun, G. N. Wang, J. Y. Oh, T. Katsumata, F. L. Lee, J. Kang, H. Wu, F. Lissel, S. Rondeau-Gagné, J. B. H. Tok, Z. Bao, *Adv. Funct. Mater.* **2018**, *28*, 1804222.
[130] Y.-C. Chiang, H.-C. Wu, H.-F. Wen, C.-C. Hung, C.-W. Hong, C.-C. Kuo, T. Higashihara, W.-C. Chen, *Macromolecules* **2019**, *52*, 4396.
[131] J. I. Scott, X. Xue, M. Wang, R. J. Kline, B. C. Hoffman, D. Dougherty, C. Zhou, G. Bazan, B. T. O'Connor, *ACS Appl. Mater. Interfaces* **2016**, *8*, 14037.
[132] J. Mun, J. Kang, Y. Zheng, S. Luo, H. Wu, N. Matsuhisa, J. Xu, G. N. Wang, Y. Yun, G. Xue, J. B. H. Tok, Z. Bao, *Adv. Mater.* **2019**, *31*, 1903912.
[133] M. Shin, J. Y. Oh, K.-E. Byun, Y.-J. Lee, B. Kim, H.-K. Baik, J.-J. Park, U. Jeong, *Adv. Mater.* **2015**, *27*, 1255.
[134] J. Xu, H.-C. Wu, C. Zhu, A. Ehrlich, L. Shaw, M. Nikolka, S. Wang, F. Molina-Lopez, X. Gu, S. Luo, D. Zhou, Y.-H. Kim, G.-J. N. Wang, K. Gu, V. R. Feig, S. Chen, Y. Kim, T. Katsumata, Y.-Q. Zheng,

H. Yan, J. W. Chung, J. Lopez, B. Murmann, Z. Bao, *Nat. Mater.* **2019**, *18*, 594.
[135] W. Wang, S. Wang, R. Rastak, Y. Ochiai, S. Niu, Y. Jiang, P. K. Arunachala, Y. Zheng, J. Xu, N. Matsuhisa, X. Yan, S.-K. Kwon, M. Miyakawa, Z. Zhang, R. Ning, A. M. Foudeh, Y. Yun, C. Linder, J. B. H. Tok, Z. Bao, *Nat. Electron.* **2021**, *4*, 143.
[136] Y.-Q. Zheng, Y. Liu, D. Zhong, S. Nikzad, S. Liu, Z. Yu, D. Liu, H.-C. Wu, C. Zhu, J. Li, H. Tran, J. B. H. Tok, Z. Bao, *Science* **2021**, *373*, 88.
[137] S. Nakamura, T. Mukai, M. Senoh, *Jpn. J. Appl. Phys.* **1991**, *30*, L1998.
[138] K. Fujita, A. Shinoda, M. Inai, T. Yamamoto, M. Fujii, D. Lovell, T. Takebe, K. Kobayashi, *J. Cryst. Growth* **1993**, *127*, 50.
[139] S. Park, Y. Xiong, R.-H. Kim, P. Elvikis, M. Meitl, D. Kim, J. Wu, J. Yoon, C. Yu, Z. Liu, Y. Huang, K. Hwang, P. Ferreira, X. Li, K. Choquette, J. A. Rogers, *Science* **2009**, *325*, 977.
[140] R.-H. Kim, D.-H. Kim, J. Xiao, B. H. Kim, S.-I. Park, B. Panilaitis, R. Ghaffari, J. Yao, M. Li, Z. Liu, V. Malyarchuk, D. G. Kim, A.-P. Le, R. G. Nuzzo, D. L. Kaplan, F. G. Omenetto, Y. Huang, Z. Kang, J. A. Rogers, *Nat. Mater.* **2010**, *9*, 929.
[141] M. Choi, B. Jang, W. Lee, S. Lee, T. W. Kim, H.-J. Lee, J.-H. Kim, J.-H. Ahn, *Adv. Funct. Mater.* **2017**, *27*, 1606005.
[142] H. Hwang, M. Kong, K. Kim, D. Park, S. Lee, S. Park, H.-J. Song, U. Jeong, *Sci. Adv.* **2021**, *7*, eabh0171.
[143] C. W. Tang, S. A. VanSlyke, *Appl. Phys. Lett.* **1987**, *51*, 913.
[144] B. Geffroy, P. le Roy, C. Prat, *Polym. Int.* **2006**, *55*, 572.
[145] Z. B. Wang, M. G. Helander, J. Qiu, D. P. Puzzo, M. T. Greiner, Z. M. Hudson, S. Wang, Z. W. Liu, Z. H. Lu, *Nat. Photonics* **2011**, *5*, 753.
[146] T.-H. Han, Y. Lee, M.-R. Choi, S.-H. Woo, S.-H. Bae, B. H. Hong, J.-H. Ahn, T.-W. Lee, *Nat. Photonics* **2012**, *6*, 105.
[147] T.-H. Han, S.-H. Jeong, Y. Lee, H.-K. Seo, S.-J. Kwon, M.-H. Park, T.-W. Lee, *J. Inf. Disp.* **2015**, *16*, 71.
[148] M.-H. Park, T.-H. Han, Y.-H. Kim, S.-H. Jeong, Y. Lee, H.-K. Seo, H. Cho, T.-W. Lee, *J. Photonics Energy* **2015**, *5*, 053599.
[149] A. Sugimoto, H. Ochi, S. Fujimura, A. Yoshida, T. Miyadera, M. Tsuchida, *IEEE J. Sel. Top. Quantum Electron.* **2004**, *10*, 107.
[150] D.-Y. Kim, Y. C. Han, H. C. Kim, E. G. Jeong, K. C. Choi, *Adv. Funct. Mater.* **2015**, *25*, 7145.
[151] T. Yokota, P. Zalar, M. Kaltenbrunner, H. Jinno, N. Matsuhisa, H. Kitanosako, Y. Tachibana, W. Yukita, M. Koizumi, T. Someya, *Sci. Adv.* **2016**, *2*, e1501856.
[152] D. Yin, J. Feng, N.-R. Jiang, R. Ma, Y.-F. Liu, H.-B. Sun, *ACS Appl. Mater. Interfaces* **2016**, *8*, 31166.
[153] S. Jeong, H. Yoon, B. Lee, S. Lee, Y. Hong, *Adv. Mater. Technol.* **2020**, *5*, 2000231.
[154] Z.-K. Tan, R. S. Moghaddam, M. L. Lai, P. Docampo, R. Higler, F. Deschler, M. Price, A. Sadhanala, L. M. Pazos, D. Credgington, F. Hanusch, T. Bein, H. J. Snaith, R. H. Friend, *Nat. Nanotechnol.* **2014**, *9*, 687.
[155] Y.-H. Kim, S. Kim, A. Kakekhani, J. Park, J. Park, Y.-H. Lee, H. Xu, S. Nagane, R. B. Wexler, D.-H. Kim, S. H. Jo, L. Martínez-Sarti, P. Tan, A. Sadhanala, G.-S. Park, Y.-W. Kim, B. Hu, H. J. Bolink, S. Yoo, R. H. Friend, A. M. Rappe, T.-W. Lee, *Nat. Photonics* **2021**, *15*, 148.
[156] H. Zhou, J.-W. Park, *Thin Solid Films* **2016**, *619*, 281.
[157] Y. Li, S. Chou, P. Huang, C. Xiao, X. Liu, Y. Xie, F. Zhao, Y. Huang, J. Feng, H. Zhong, H. Sun, Q. Pei, *Adv. Mater.* **2019**, *31*, 1807516.
[158] S. G. R. Bade, X. Shan, P. T. Hoang, J. Li, T. Geske, L. Cai, Q. Pei, C. Wang, Z. Yu, *Adv. Mater.* **2017**, *29*, 1607053.
[159] D.-H. Jiang, Y.-C. Liao, C.-J. Cho, L. Veeramuthu, F.-C. Liang, T.-C. Wang, C.-C. Chueh, T. Satoh, S.-H. Tung, C.-C. Kuo, *ACS Appl. Mater. Interfaces* **2020**, *12*, 14408.
[160] S. Adeniji, O. Oyewole, R. Koech, D. Oyewole, J. Cromwell, R. Ahmed, O. Oyelade, D. Sanni, K. Orisekeh, A. Bello, W. Soboyejo, *Macromol. Mater. Eng.* **2021**, *306*, 2100435.
[161] H. Zhou, J. Park, Y. Lee, J. Park, J. Kim, J. S. Kim, H. Lee, S. H. Jo, X. Cai, L. Li, X. Sheng, H. J. Yun, J. Park, J. Sun, T. Lee, *Adv. Mater.* **2020**, *32*, 2001989.
[162] C. Keplinger, J. Sun, C. C. Foo, P. Rothemund, G. M. Whitesides, Z. Suo, *Science* **2013**, *341*, 984.
[163] C. Larson, B. Peele, S. Li, S. Robinson, M. Totaro, L. Beccai, B. Mazzolai, R. Shepherd, *Science* **2016**, *351*, 1071.
[164] S. Li, B. N. Peele, C. M. Larson, H. Zhao, R. F. Shepherd, *Adv. Mater.* **2016**, *28*, 9770.
[165] Z. Zhang, L. Cui, X. Shi, X. Tian, D. Wang, C. Gu, E. Chen, X. Cheng, Y. Xu, Y. Hu, J. Zhang, L. Zhou, H. H. Fong, P. Ma, G. Jiang, X. Sun, B. Zhang, H. Peng, *Adv. Mater.* **2018**, *30*, 1800323.
[166] J. Wang, C. Yan, G. Cai, M. Cui, A. Lee-Sie Eh, P. See Lee, *Adv. Mater.* **2016**, *28*, 4490.
[167] J. Wang, C. Yan, K. J. Chee, P. S. Lee, *Adv. Mater.* **2015**, *27*, 2876.
[168] F. Stauffer, K. Tybrandt, *Adv. Mater.* **2016**, *28*, 7200.
[169] Y. J. Tan, H. Godaba, G. Chen, S. T. M. Tan, G. Wan, G. Li, P. M. Lee, Y. Cai, S. Li, R. F. Shepherd, J. S. Ho, B. C. K. Tee, *Nat. Mater.* **2020**, *19*, 182.
[170] D. Son, J. Kang, O. Vardoulis, Y. Kim, N. Matsuhisa, J. Y. Oh, J. W. To, J. Mun, T. Katsumata, Y. Liu, A. F. McGuire, M. Krason, F. Molina-Lopez, J. Ham, U. Kraft, Y. Lee, Y. Yun, J. B. H. Tok, Z. Bao, *Nat. Nanotechnol.* **2018**, *13*, 1057.
[171] X. Yan, C. Tian, W. Jiang, W. Xia, X. Wei, *J. Soc. Inf. Disp.* **2014**, *22*, 245.
[172] H. Ohmae, Y. Tomita, M. Kasahara, J. Schram, E. Smits, J. van den Brand, F. Bossuyt, J. Vanfleteren, J. De Baets, *SID Symp. Dig. Tech. Pap.* **2015**, *46*, 102.
[173] K. Tybrandt, J. Vörös, *Small* **2016**, *12*, 180.
[174] J. Woo, H. Lee, C. Yi, J. Lee, C. Won, S. Oh, J. Jekal, C. Kwon, S. Lee, J. Song, B. Choi, K. Jang, T. Lee, *Adv. Funct. Mater.* **2020**, *30*, 1910026.
[175] Y. Lee, B. J. Kim, L. Hu, J. Hong, J.-H. Ahn, *Mater. Today* **2022**, *53*, 51.
[176] T. Someya, *IEEE Spectrum* **2021**, *58*, 38.
[177] Y. Lee, D. S. Kim, S. W. Jin, H. Lee, Y. R. Jeong, I. You, G. Zi, J. S. Ha, *Chem. Eng. J.* **2022**, *427*, 130858.
[178] X. Shi, Y. Zuo, P. Zhai, J. Shen, Y. Yang, Z. Gao, M. Liao, J. Wu, J. Wang, X. Xu, Q. Tong, B. Zhang, B. Wang, X. Sun, L. Zhang, Q. Pei, D. Jin, P. Chen, H. Peng, *Nature* **2021**, *591*, 240.
[179] A. K. Tripathi, E. C. P. Smits, J.-L. Van Der Steen, M. Cauwe, R. Verplancke, K. Myny, J. Maas, R. Kuster, S. Sabik, M. Murata, Y. Tomita, H. Ohmae, J. Van Den Brand, G. Gelinck, in Int. Meeting on Information Displays, Daegu, Korea **2015**.
[180] S. Y. Hong, Y. H. Lee, H. Park, S. W. Jin, Y. R. Jeong, J. Yun, I. You, G. Zi, J. S. Ha, *Adv. Mater.* **2016**, *28*, 930.
[181] J. Kim, M. Lee, H. J. Shim, R. Ghaffari, H. R. Cho, D. Son, Y. H. Jung, M. Soh, C. Choi, S. Jung, K. Chu, D. Jeon, S.-T. Lee, J. H. Kim, S. H. Choi, T. Hyeon, D.-H. Kim, *Nat. Commun.* **2014**, *5*, 5747.
[182] R. Maiti, L.-C. Gerhardt, Z. S. Lee, R. A. Byers, D. Woods, J. A. Sanz-Herrera, S. E. Franklin, R. Lewis, S. J. Matcher, M. J. Carré, *J. Mech. Behav. Biomed. Mater.* **2016**, *62*, 556.
[183] T. Daeneke, K. Khoshmanesh, N. Mahmood, I. A. de Castro, D. Esrafilzadeh, S. J. Barrow, M. D. Dickey, K. Kalantar-zadeh, *Chem. Soc. Rev.* **2018**, *47*, 4073.
[184] H. Zhu, S. Wang, M. Zhang, T. Li, G. Hu, D. Kong, *npj Flexible Electron.* **2021**, *5*, 25.
[185] S. Cheng, Z. Wu, *Lab Chip* **2012**, *12*, 2782.
[186] D. Gall, *J. Appl. Phys.* **2020**, *127*, 050901.
[187] D. Ji, J. Jang, J. H. Park, D. Kim, Y. S. Rim, D. K. Hwang, Y.-Y. Noh, *J. Inf. Disp.* **2021**, *22*, 1.

[188] H. Zhu, E. Shin, A. Liu, D. Ji, Y. Xu, Y. Noh, *Adv. Funct. Mater.* **2020**, *30*, 1904588.
[189] J. Park, S. Heo, K. Park, M. H. Song, J.-Y. Kim, G. Kyung, R. S. Ruoff, J.-U. Park, F. Bien, *npj Flexible Electron* **2017**, *1*, 9.
[190] D. G. Mackanic, T.-H. Chang, Z. Huang, Y. Cui, Z. Bao, *Chem. Soc. Rev.* **2020**, *49*, 4466.
[191] Y. Dai, H. Hu, M. Wang, J. Xu, S. Wang, *Nat. Electron.* **2021**, *4*, 17.
[192] S. Liu, D. S. Shah, R. Kramer-Bottiglio, *Nat. Mater.* **2021**, *20*, 851.
[193] W. Song, M. Kong, S. Cho, S. Lee, J. Kwon, H. Bin Son, J. H. Song, D. Lee, G. Song, S. Lee, S. Jung, S. Park, U. Jeong, *Adv. Funct. Mater.* **2020**, *30*, 2003608.
[194] M. S. Kim, S. Kim, J. Choi, S. Kim, C. Han, Y. Lee, Y. Jung, J. Park, S. Oh, B.-S. Bae, H. Lim, I. Park, *ACS Appl. Mater. Interfaces* **2022**, *14*, 1826.
[195] C. Jiang, F. Rist, H. Wang, J. Wallner, H. Pottmann, *Comput. Des.* **2022**, *143*, 103146.
[196] D. Hwang, E. J. Barron, A. B. M. T. Haque, M. D. Bartlett, *Sci. Rob.* **2022**, *7*, eabg2171.
[197] Y. Bai, H. Wang, Y. Xue, Y. Pan, J.-T. Kim, X. Ni, T.-L. Liu, Y. Yang, M. Han, Y. Huang, J. A. Rogers, X. Ni, *Nature* **2022**, *609*, 701.
[198] S. Wu, W. Hu, Q. Ze, M. Sitti, R. Zhao, *Multifunct. Mater.* **2020**, *3*, 042003.
[199] R. M. Neville, F. Scarpa, A. Pirrera, *Sci. Rep.* **2016**, *6*, 31067.
[200] M. Zhang, H. Shahsavan, Y. Guo, A. Pena-Francesch, Y. Zhang, M. Sitti, *Adv. Mater.* **2021**, *33*, 2008605.

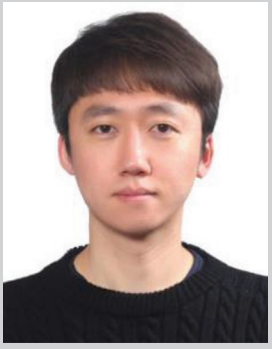

Yeongjun Lee is a postdoctoral researcher in the Department of Chemical Engineering at Stanford University, USA. He received his B.S. in the Department of Materials Science and Engineering (MSE) from Hanyang University, South Korea in 2012. He received his Ph.D. in the MSE from Pohang University of Science and Technology (POSTECH), South Korea in 2018. He joined the MSE at Seoul National University, as a postdoctoral researcher and worked at Organic Material Lab in Samsung Advanced Institute of Technology as a staff researcher (2019-2021). His research interests include printed electronics, stretchable electronics, neuromorphic electronics, and bioelectronics.

Hyeon Cho is a Ph.D. candidate in the Department of Electrical and Computer Engineering, Seoul National University, Republic of Korea. He received his B.S. degree from the Department of Electrical and Computer Engineering, Seoul National University in 2017. His current research interests are stretchable electronic skin and soft energy generators for self-powered wearable electronics.

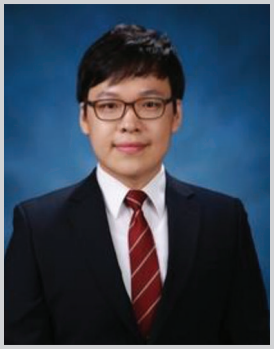

Hyungsoo Yoon is a Ph.D. candidate in the Department of Electrical and Computer Engineering, Seoul National University, Republic of Korea. He received his B.S. degree from the Department of Electrical and Computer Engineering, Seoul National University in 2016. His current research interests are methodologies for the integration of microdevices onto stretchable and flexible platforms for conformable microelectronics.

Hyunbum Kang is currently senior researcher at Samsung Advanced Institute of Technology, Samsung Electronics. He obtained his Ph.D. degree in the Department of Chemical and Biomolecular Engineering at Korea Advanced Institute of Science and Technology, Republic of Korea. His current interests include stretchable electronic materials and devices.

Hyunjun Yoo is a Ph.D. candidate in the Department of Electrical and Computer Engineering, Seoul National University, Republic of Korea. He received his B.S. degree from the Department of Electrical and Computer Engineering, Seoul National University in 2017. His current research interests are various stress mechanisms of carbon nanotube thin film transistors for soft electronics.

Huanyu Zhou is currently a postdoctoral researcher in Materials Science and Engineering at Seoul National University, Korea. He received his B.S. in 2015 and M.S. in 2016 from Yonsei University, and his Ph.D. from Seoul National University in 2022. His current research is mainly focused on flexible and stretchable devices based on organic and organic–inorganic hybrid materials.

Sujin Jeong is a Ph.D. candidate at the Department of Electrical and Computer Engineering, Seoul National University, Republic of Korea. She received her B.S. degree from the Department of Electrical and Computer Engineering, Seoul National University in 2017. Her current research interests are polymer-based optoelectronics and its geometrical engineering for stretchable electronics.

Gae Hwang Lee is currently principal researcher at Samsung Advanced Institute of Technology, Samsung Electronics. He obtained his Ph.D. degree in the Department of Physics from KAIST, South Korea in 2009. He worked for the technologies of organic photodiodes/transistors related to next generation electronics including stacked image sensors, stretchable display. His current interests include stretchable semiconducting materials and wearable sensors for healthcare monitoring.

Geonhee Kim is a Ph.D. candidate in the Department of Electrical and Computer Engineering, Seoul National University, Republic of Korea. He received his B.S. degree from the Department of Electrical and Computer Engineering, Seoul National University in 2016. His current research interests are solution-processed deformable transparent electrodes and electrohydrodynamic printing for high-resolution electronics.

Gyeong-Tak Go is a Ph.D. candidate in the Department of Materials Science and Engineering of Seoul National University, Republic of Korea. He received his B.S. degree from the Department of Materials Science and Engineering, Seoul National University in 2018. His research interests include the stretchable electronics and neuromorphic electronics that exploit artificial synapses.

Jiseok Seo is a Ph.D. candidate in the Department of Electrical and Computer Engineering, Seoul National University, Republic of Korea. He received his B.S. degree from the Department of Electrical and Computer Engineering, Seoul National University in 2016. His current research interests are stretchable electronic skin and solution-processed TFT.

Tae-Woo Lee is a professor in the Department of MSE at Seoul National University, South Korea. He received his Ph.D. in Chemical Engineering from KAIST, South Korea in 2002. He joined Bell Laboratories, USA, as a postdoctoral researcher and worked at Samsung Advanced Institute of Technology as research staff (2003–2008). He was an associate professor in MSE at Pohang University of Science and Technology (POSTECH), South Korea, until August 2016. His research focuses on printed or soft electronics that use organic and organic-inorganic hybrid materials for flexible/stretchable displays, solid-state lighting, solar energy conversion devices, and bioinspired neuromorphic devices.

Yongtaek Hong received B.S. and M.S. in Electronics Engineering, Seoul National University (SNU), Seoul, Korea, and Ph.D. in EE, Univ. Mich., Ann Arbor, MI, USA. He was a senior research scientist at Display Science & Technology Center of Eastman Kodak Company, Rochester, NY, USA (2003~2006). Since 2006, he has worked at ECE, SNU as a professor and now is Head of SNU Entrepreneurship Center, and Vice-Head of SNU R&DB Foundation in Business Affairs. He was a visiting professor at Chem. Eng., Stanford University (2012~2013). His research interests include printed/flexible/stretchable thin-film devices, displays, and sensors for wearable and electronic skin applications.

Youngjun Yun is currently principal researcher at Samsung Advanced Institute of Technology, Samsung Electronics. He obtained his Ph.D. degree in School of Engineering from Durham University, UK in 2011. He worked for the technologies of organic/oxide transistors related to next generation display including reflective color displays, holographic displays, ultra-high-definition displays, and foldable displays. His current interests include flexible and stretchable displays and skin-like sensors for healthcare monitoring.